A thesis entitled

"THE QUANTUM THEORY OF UNIMOLECULAR REACTIONS"

submitted by

Robert Goulston Gilbert

for the degree of Doctor of Philosophy
in The Australian National University

Chemistry Department,
School of General Studies,
Australian National University,
Canberra, A.C.T.

February 1970

The work described in this thesis is the candidate's own work, except as otherwise stated.

R. Gilbert

R.G. Gilbert

TABLE OF CONTENTS

ACKNOWLEDGEMENTS

I wish to express my deepest gratitude to my supervisor, Professor Ian Ross, who has given me so much guidance and aid, as both teacher and friend.

I would also like to thank the following:

Professor A.N. Hambly, Dr. M.F.R. Mulcahy (who suggested that the N_2O problem might be a suitable case for treatment) and Dr. N.J. Daly, for many stimulating discussions on kinetics.

Professors R.S. Berry, D.P. Craig and J. Jortner, for interesting discussions on the quantum mechanics of this problem.

Professor P.-Löwdin and J.-L Calais and the University of Uppsala, and the Australian National University, who helped provide financial assistance to attend the Quantum Chemistry Summer School in Scandinavia in 1968.

The Australian Research Grants Committee, who provided computing funds for this project.

Imperial Chemical Industries of Australia and New Zealand, for the award of a Research Fellowship while at the University of Sydney.

The Australian National University, for the award of a Commonwealth Postgraduate Fellowship.

The staffs of the A.N.U. Computing Centre, and the Basser Computing Department of the University of Sydney, for their patience.

Mrs. T. Clark, for her painstaking typing of this thesis.

INTRODUCTION

When quantum mechanics was formulated in the 1920's, it was realised that the new theory implicitly contained the answer to any chemical problem. However, precise calculation of chemical observables is impossible for most cases of interest; it is the task of the theoretical chemist to develop a theory which must perforce involve approximations, but which furthers our understanding of the problem under investigation. In the first few decades of quantum chemistry, most of the effort was directed towards answering the question, "Why do molecules exist?" Although there is much important work yet to be done in this field, many of the basic problems have now been answered, and with the arsenal of concepts and methods built up by these investigations, an increasing effort is being directed towards the question "Why do molecules react?"

Unimolecular reactions, where the chemical change may in a sense be regarded as occurring in the isolated molecule, comprise the simplest class of chemical reactions. Indeed, these reactions attracted theoretical interest well before the inception of quantum theory. Classical or semi-classical theories, such as the RRKM (Rice and Ramsberger 1927, Kassel 1928) or Slater (Slater 1959) approaches, have been quite successful in describing the reaction and in calculating

rate constants, but they do not have a quantum mechanical basis, and thus give only a partial physical picture of the process. Rigorous quantum theories such as that recently put forward by Levine *et al* (Hall and Levine 1966, Levine 1966, 1968) and Mies (1969) are at present too complex to enable calculations to be carried out on a thermal reaction that can be performed in the laboratory.

The presentation followed here, along lines suggested by Rice (1929), Langer (1929) and Roginsky and Rosenkivitch (1930), attempts the middle road. Since the pioneering work of Lindemann (1922), a unimolecular reaction has been described in terms of the reactant being excited by a collision with an inert gas into an "active" state, which may then be converted to product by an intramolecular process. There are thus two steps in the reaction, collision and excitation. The essence of the model used here is that the conversion step may be described in the same terms as radiationless transitions (internal conversions) of spectroscopy. In other words, we describe the reaction process as excitation by collision with an inert gas to an "active" reactant level which then internally converts into product. A rigorous quantum mechanical justification of this description of a unimolecular reaction is discussed in Chapter I. In Chapter II it is shown how macroscopic unimolecular properties, such as the pressure and temperature

dependence of the rate constant, may be derived from this description. In this chapter we also examine precisely what information is contained in the experimental "activation energy", and show that this parameter is by no means simply related to the height of the barrier between reactant and product. The concept of a transition state is not used in our theory: we show, however, that using certain approximations, our expressions become similar to those appearing in Eyring's (1935) well-known formulae. In Chapters III and IV we calculate the high, low and intermediate pressure rate constants of an actual laboratory reaction, the thermal decomposition of N_2O:

$$N_2O \rightarrow N_2 + O$$

Because of lack of knowledge of the potential surfaces involved, and because of the limited capability of present computers, approximations must be made when calculating these rate constants. The approximations used have a physical basis, and may be justified from the theory of the first two chapters.

As in all "absolute" theories to date which have been used to predict laboratory reaction rates, these approximations involve adjustable parameters which may be used to bring theory into agreement with experiment. Therefore emphasis is laid, not on the unsurprising result that our answers agree moderately well with experiment, but on the

physical insight into the unimolecular process which these calculations provide.

CHAPTER I

THE QUANTUM MECHANICAL DESCRIPTION OF UNIMOLECULAR REACTIONS

Section 1. Classical and Semi-Classical Theories.

In 1922 Lindemann put forward his hypothesis that a unimolecular reaction was characterised by a delay time in the conversion of an energised reactant state to product. By considering collisional activation to an energised state of reactant, and the competing processes of reaction and deactivation in this state, he was able to derive the characteristic pressure and temperature dependence of the reaction rate constant. These basic ideas were extended in the RRK theory (Rice and Ramsberger 1927, Kassel 1928), where it was supposed that Lindemann's delay time was the time required for the energised molecule to acquire a critical energy in a particular vibrational mode (or combination of modes). An alternative to this proposal was put forward by Slater (1959), who postulated that the delay time was the average time that a particular *coordinate* (or set of coordinates) in the collection of oscillators representing the molecule exceeds a critical length. Although these theories are very helpful in understanding the unimolecular process, they suffer from the disadvantage that the phenomenological basis of the theories is classical; the

quantum mechanical extensions of these theories (Slater 1959, Marcus 1968, Hofacker 1965) are really applications of quantum statistics to these classical models. Another important point is that reactant and product are not clearly defined, as the critical energy or length is somewhat arbitrary.

Some of these difficulties are obviated by the application of transition state methods (Marcus 1968, Glasstone, Laidler and Eyring 1941, Eyring, Walter and Kimball 1944, p299). Here the reaction is described in terms of the electronic potential surface of the reacting molecule. Reactant and product are separated by an "activated complex", a set of molecular states situated on top of the potential maximum which lies between the minima corresponding to reactant and product. Eyring's original derivation (Eyring 1935) assumed that reactant and activated complex are in equilibrium, and that one of the degrees of freedom of the latter is a free translation along the reaction coordinate. The delay time corresponds to the rate at which the activated complex passes over the barrier. Although this theory has proved a useful way to describe the reaction process, the definition of the activated complex is not precise. One difficulty is the assumption that is possesses a free translational mode (indeed this is only applicable for a decomposition); another is that the

fundamental step - the conversion of activated complex to product - is still described in classical terms.

An alternative derivation overcomes some of these difficulties (Eyring, Walter and Kimball 1944, p.305), using arguments similar to those in quantum mechanical collision theory. By assuming that the product possesses a free translation, and that there is a definite probability, called the transmission coefficient, of going from reactant to product, a formula for the rate is obtained which is identical to Eyring's earlier expression, without the need to invoke a separate identity for the activated complex. However, a critical assumption here is that the transmission coefficient is a constant (or a slowly-varying function of energy) for energies above the minimum required for reaction: in a detailed analysis this can only be justified by resorting to a classical description of the reactant. Furthermore, in the above theories no provision is made for the breakdown of the Born-Oppenheimer approximation used to define the potential surface. Also the role of the activating and deactivating collision is invariably glossed over. Thus conventional theories do not provide an adequate quantum mechanical description of the unimolecular process.

These kinetic theories envisage a unimolecular reaction as the movement of a point, representing the instantaneous nuclear configuration of the molecule, over a barrier in a multidimensional potential surface. A

spectroscopist, on the other hand, describes photochemical reactions and radiationless transitions (internal conversions) in an isolated molecule as perturbation-induced transitions between the vibrational levels in two electronic states. These two descriptions may be regarded as complementary aspects of a general theory.

Section 2. Qualitative Quantum Mechanical Description of the Unimolecular process.

The suggestion that unimolecular reactions could be treated in the same way as radiationless transitions seems to have first been put forward by Langer (1929), Rice (1929) and Roginsky and Rosenkevitch (1930), and recently has been reconsidered by Mies (Mies and Kraus 1966, Mies 1969). In the following chapter we have not undertaken an historical account of these developments, but rather have attempted to synthesise these concepts into a coherent description of the unimolecular process.

A unimolecular reaction involves an internal change in an isolated molecule brought about by collision with an inert gas. Thus the system under consideration consists of a reactant molecule interacting with an inert gas atom or molecule. This process cannot be properly described without taking into account the interaction between the molecule and the inert gas, just as the phenomenon of internal

conversion apparently violates the laws of quantum mechanics unless the molecule-radiation interaction is considered (Bixon and Jortner 1968). Indeed, theories of radiationless transitions may be converted to thermal unimolecular reaction theories by replacing the interaction of the molecule with the radiation field by the interaction with an inert gas (Mies 1969).

In a thermal unimolecular reaction, all collisions are either elastic or inelastic, meaning that there is no interchange of particles between colliding molecules. The system is only fully described by the complete wave function of the molecule and the inert gas. As no rearrangement collisions occur, and if for convenience we also neglect the possibility of change of internal state of the inert gas,*

---

* This assumption is obviously valid if the inert gas is, say, argon, where no change in electronic state will occur at collision energies which are attainable thermally. If the inert gas is, say, N_2, where changes of vibrational state are possible, the electronic part of the N_2 wave function may still be factored out, and the expansion of the remaining part of the total wave function performed in terms of the products of reactant wave functions and vibrational wave functions of N_2. This would involve only minor changes in the arguments presented in this section.

---

then the internal wave function of the latter may be factored out of the total wave function. Following the standard methods used in calculations involving inelastic collisions (Mott and Massey 1965, p.346), the remaining part of the total wave function may be expanded in terms of the wave functions of the *isolated* molecule, which are eigenfunctions of the complete molecular Hamiltonian H (the expansion coefficients will be functions of the intermolecular coordinates $\{r,\theta,\phi\}$ only). However, *any* set of wavefunctions which spans the space of eigenfunctions of H will serve equally well as a basis. Suppose we divide H into a zero-order Hamiltonian and a perturbation:

$$H = H_0 + V$$

Provided the eigenfunctions of H_0 form a complete set with respect to H, then this basis may also be used to describe the process. As Jortner and Bixon (1969) have pointed out, the descriptions of the reaction in terms of either basis are physically equivalent; the choice of basis is a matter of convenience.

The central point of our development is that H_0 may be chosen such that its eigenfunctions with energy of kinetic significance may be unambiguously designated as belonging either to reactant or product.

Now, the rate constant is determined by measuring either the rate of disappearance of molecules from the

lowest levels of reactant, or the rate of appearance in the lowest levels of product (or appearance of decomposition products if the reaction is dissociative). Therefore an immediate restriction on the choice of H_0 arises when we consider that the experimental observation used to determine the unimolecular rate constant is the time-dependence of the populations of the lowest levels of reactant or product. We therefore wish to consider collision cross sections for all possible channels between these states. Hence H_0 must be chosen so that the wave functions of those states whose populations are being measured are the same in both H and H_0 representations. Restrictions imposed on the choice of H_0 by perturbation convergence criteria will be discussed later in this chapter.

The Reaction Process in Terms of the H ("mixed") Representation.

Consider the eigenfunctions of the complete isolated molecule Hamiltonian H. For purposes of a qualitative description of the reaction process, it is convenient to adopt the adiabatic approximation (Born and Huang 1954, p.402), or its simplification, the Born-Oppenheimer approximation (Kolos and Wolniewicz 1963), although this assumption need not be made in the mathematical development of the succeeding sections. Within this approximation, a set of vibronic states may be associated with a single

electronic potential energy surface, derived from the eigenvalues of the electronic (fixed-nucleus) Hamiltonian. The unimolecular theories discussed in Section 1 of this chapter are all based on the solution of the classical or quantum-mechanical equations of motion of this surface.

If the potential surface of the lowest electronic state of the molecule has two minima, then a thermal unimolecular reaction can take place; if there is one minimum in which at least one bond has infinite length, then the reaction is a decomposition. We feel that such a potential can be associated with almost all observed thermal unimolecular reactions. Using the adiabatic approximation, any two molecular geometries may be joined by a continuous surface, and indeed, in a molecule containing more than three atoms, states of any symmetry may be joined by a potential surface passing through a C_1 configuration.

A description of the reaction in terms of the electronic potential surface corresponding to the H_0 representation will be given in detail in the following part of this section. At this stage, we point out that if the H_0 potential surface consists of two intersecting surfaces, then our requirement that reactant and product states be unambiguously separated will be met.

In the adiabatic approximation, the total isolated molecule wave function may be written as the product of an

electronic and a vibrational wave function, and thus we may differentiate the various eigenstates of the lowest electronic state by their vibrational (and rotational) wave functions. In figures 1a and 1b, we depict typical vibrational wave functions associated with the H and H_o surfaces corresponding to an isomerisation; in figures 2a and 2b, we depict the vibrational wave functions for dissociative potentials. Fig. 1a is based on Kolos and Wolniewicz (1969), and Fig. 2a on Frey and Thiele's (1968) quantitative study of the vibrational wave functions for a highly simplified form of dissociative potential.

It can be seen that for both the dissociative and isomeric double minimum (H) potentials, the wave functions for a state well below the potential maximum may be associated with one or other minimum, and that they are practically identical with the corresponding wave functions for the separated (H_o) potential. Near the potential maximum, the wave functions in the H representation may be described as "mixed": they share the characteristics of wave functions belonging to both minima, and resemble linear combinations of those wave functions with similar energies belonging to the H_o representation.

Reaction occurs when a molecule which is initially in a state associated with reactant is excited by collision through a series of states leading to a state associated

Fig. 1. Wave functions (schematic) for potentials corresponding to a unimolecular isomerization, in (a) the H representation, and (b) the H_o representation.

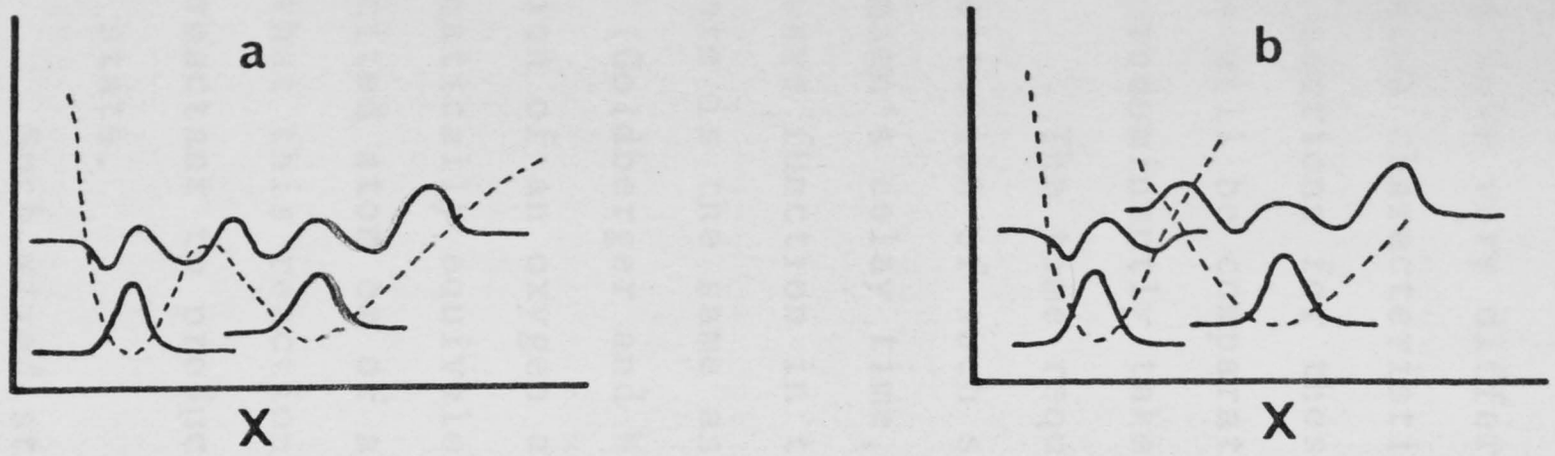

Fig. 2. Wave functions (schematic) for potentials corresponding to a unimolecular decomposition, in (a) the H representation, and (b) the H_o representation.

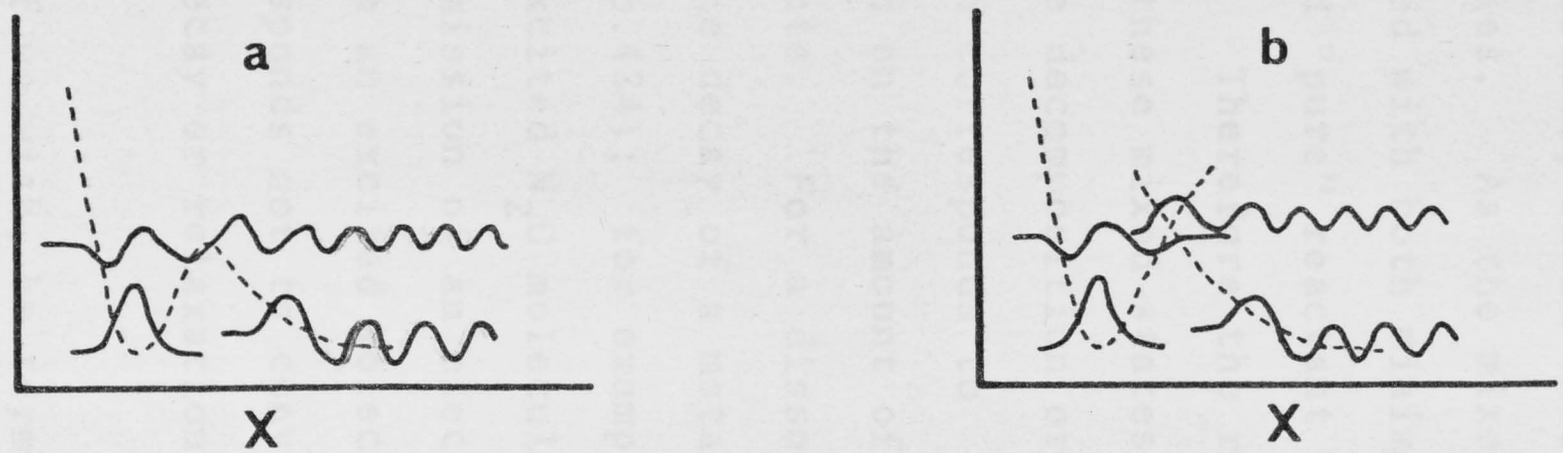

with the product minimum. Direct collisional excitation from a state at the bottom of one minimum to a state at the bottom of the other is highly improbable, since these two states have very different geometries. As the mixed states will have characteristics associated with both minima, the cross sections for these states and "pure" reactant or product states will be comparatively high. Therefore the reaction must predominantly take place via these mixed states.

The time required for the decomposition or de-excitation of such states, which corresponds to Lindemann's delay time, will depend on the amount of product-type wave function in the mixed state. For a dissociation, the rate is the same as that for the decay of a metastable state (Goldberger and Watson 1964 p.424); for example, the emission of an oxygen atom by an excited N_2O molecule is mathematically equivalent to the emission of an electron from an excited atom or of a photon from an excited molecule. Note that this reaction step corresponds not to conversion from reactant to product but the decay or relaxation of a mixed state.

Such mixed states can, if we wish, be termed "activated complexes", but as can be seen from the wave functions displayed in figures 1a and 2a, the wave functions for those mixed states with energies just above and below the potential maximum are similar, and there is a gradation

of this similarity down to the lowest levels of reactant and product. Therefore we cannot assign a definite set of states to the activated complex. A more quantitative comparison with transition state theory will be given in Chapter II; recently Mies (1969) has also examined transition state theory from a similar point of view.

The Reaction Process in Terms of the H_o ("Separated") Representation.

We now turn to what we feel is a more convenient way to describe a unimolecular reaction, using a basis where each eigenstate clearly belongs to either reactant or product: in terms of the adiabatic approximation, we introduce crossing potentials.

There are many advantages in choosing such a basis. Firstly, reaction may be clearly defined as transition from the reactant to the product surface. Secondly, if reactant and product have different symmetry (for example, belong to different point groups or, as is the case with the N_2O decomposition, have different spins) the computation will be simpler if H_o can be defined in such a way that each wave function has the symmetry of either reactant or product. Thirdly, if we choose H_o such that the intramolecular perturbation V is much less than the perturbation induced by collision, then collisions leading to an "active" reactant state effectively involve pure reactant states only,

i.e., reaction and excitation are separate events (Goldberger and Watson 1964, p.479), just as in the theory of internal conversion, excitation by radiation may be considered to involve only pure Born-Oppenheimer states (Bixon and Jortner 1968). The condition for this separability will in fact be automatically satisfied by the requirement, discussed in section 4 of this chapter, that V be sufficiently small for the time dependence of the intra-molecular process to be treated by first-order perturbation theory; the collisional perturbation is so large that the application of first-order theory (the Born approximation, Messiah 1962, p.808) is inadequate for collision energies attainable by a significant proportion of molecules with a thermal distribution of energy.

Note that the condition that V be small compared with the collisional perturbation is equivalent to the condition that the duration of a collision is much less than the time required for conversion from reactant to product.

In terms of the separated basis, therefore, the reaction process consists of initial excitation by collision to a reactant state in the "mixed" region; under the influence of the internal perturbation, this "active" state then converts spontaneously to an energetic product. It is this step that corresponds to Lindemann's delay time; the rate is determined by the perturbation. The energetic product

state is then rapidly deactivated by collision or dissociates. We will later show that, provided certain convergence criteria are satisfied, general unimolecular properties are derivable from this description of the reaction.

As the rate of the reaction step in both the H and H_o representations is determined by the amount of product state in the mixed state, the two descriptions are physically equivalent. The expression for this rate is of course the same in both representations, being given by "Fermi's Golden Rule" (Messiah 1964, p.736). This expression will be discussed in Section 4.

Mixed Levels and the Measurement of Rate Constants.

It is relevant here to examine methods of determining the unimolecular rate constant R, in view of the above discussion on mixed states. R is defined from the time dependence of the total concentration c of reactant:

$$R = - \frac{dc/dt}{c}$$

Now a particular molecular eigenstate may be unambiguously associated with one or other minimum only if the time of interchange between levels associated with the two minima is long compared with the characteristic time of the analytical technique. Techniques of determining the rate constant may be divided into two general categories. The first measures the total concentration of either component, and is typified by the method of sudden cooling of a reaction mixture,

followed by analysis for reactant or product. All the molecules in the cooled mixture will be in the lowest levels of reactant or product; therefore this technique will be a valid method of determining the rate constant if the concentration of molecules in the mixed states is small, and cooling is rapid. The other general technique consists of measuring the populations of individual levels during the course of reaction (for example, monitoring an infra-red emission or absorption band of a reacting gas). This requires firstly that the level being monitored should not be a mixed state, and secondly that the ratio of the population of this level to the total population be constant throughout the course of the reaction (this second point is explored in Chapter II). Both these methods are only valid if the sampling of a mixed state is avoided; a simple example where such states are sampled may be found in the NMR studies of reactions with low activation energies, such as conformational changes: peaks attributable to reactant and product cannot be distinguished at high temperatures.

Section 3. The Nature of the Perturbation.

We now turn to some possible methods of determining the perturbation V, or alternatively the zero-order Hamiltonian H_o, such that the wave functions of reactant and product are unambiguously separated, and the eigenfunctions of H_o corresponding to the lowest levels of reactant and product are as close as possible to the exact eigenfunctions.

We assume immediately that V contains corrections to the Born-Oppenheimer approximation. The eigenstates in the separated representation may then be written as products of electronic and vibrational wave functions, $\phi(X,x)$ and $\psi(X)$, where X and x denote nuclear and electronic space-spin coordinates respectively.

An obvious restriction on the choice of separated wave functions is that reactant and product wave functions belong to the same H_o, i.e. that they are orthogonal. Another restriction is that interactions with higher electronic states do not have to be considered. In summary, the restrictions on H_o are:

(i) The eigenfunctions of H and H_o which correspond to the lowest levels of reactant and product are coincident.

(ii) Higher electronic states do not need to be considered.

(iii) The product eigenfunctions are such that the rate of decomposition or collisional deactivation of an energetic product state is rapid compared with the time required

for conversion from reactant to product; this implies that the reverse reaction can be neglected.

(iv) First-order time-dependent perturbation theory is adequate for the calculation of the rate of conversion (Section 4.)

(v) The separated wave functions are orthogonal.

The electronic wave functions of reactant and product are taken to be eigenfunctions of the separated electronic Hamiltonian, H_o^{el}:

$$H_o^{el}\phi = E(X)\phi$$

The vibrational wave functions ψ are then the solutions of the Schrödinger equation for E(X).

The perturbation matrix element between a reactant vibronic state $|r,i\rangle$ (where r refers to the electronic state of reactant, and i the vibrational state), and a product vibronic state $|p,j\rangle$, is then

$$V_{ri,pj} = \langle ri|V|pj\rangle = \langle ri|H|pj\rangle \qquad (I.1)$$

(as we assume $H|ri\rangle = E_{r,i}|ri\rangle$ and $\langle ri|pj\rangle = 0$). Thus the construction of the separated wave functions is equivalent to the evaluation of the perturbation.

We may further write

$$V_{ri,pj} = \int\int \psi_i(X)\ \phi_r(X,x)\ V\ \phi_p(X,x)\ \psi_j(X)\ dx\ dX$$
$$\equiv \int \psi_i(X)\ V_{rp}(X)\ \psi_j(X)\ dX \qquad (I.2)$$

where V_{rp} is the electronic perturbation matrix element. There are thus two basic methods for determining the perturbation. If H_o is known, its eigenvalues determine $E(X)$ and thus the vibrational wavefunctions, while its eigenvectors are the electronic wave functions, thereby determining V through (1) and (2). Alternatively, we may construct ϕ_r, ϕ_p and the reactant and product potential surfaces, $E_r(X)$ and $E_p(X)$, a procedure which determines V through (1) and (2) without specifying H_o at all. If this second method is adopted, then within the limits imposed by the conditions set out above, the choice of H_o is *arbitrary*.

We now turn to possible methods of determining either H_o or the separated wave functions and potentials.

Born-Oppenheimer Basis

The most precise zero-order eigenfunctions are exact Born-Oppenheimer states. The only non-zero term in (1) is then the matrix element of the nuclear kinetic energy operator Δ_X (Born and Huang 1954, p.402). The calculation of such wave functions is however extremely difficult, and at present has only been carried out for simple diatomics;

strictly speaking, therefore, it is incorrect to refer to the "breakdown of the Born-Oppenheimer approximation" unless such wave functions are available. Some spectroscopic anomalies which are sometimes ascribed to this breakdown can in fact be seen to arise from the use of less accurate wave functions and potential surfaces, as discussed below.

Even if exact Born-Oppenheimer wave functions become available for molecules which actually undergo thermal unimolecular reactions, they might not meet the requirement of unambiguous separability of reactant and product states. To meet this requirement, further restrictions must be imposed on the form of the wave functions; these we now proceed to discuss. Note, however, that the correction to the Born-Oppenheimer approximation, Δ_χ, will always be contained in the perturbation matrix element arising from less accurate wave functions, and may even be the dominating term in the perturbation.

A basis set which satisfies the separability requirement is one involving crossing potential surfaces corresponding to reactant and product, although of course the convergence criteria (ii) and (iv) must still be met.

Crossing Surfaces from Hartree-Fock wave functions.

Probably the most useful method of constructing crossing surfaces is through single determinant Hartree-Fock

wave functions.

One of the best examples of a double-minimum potential surface is the first excited $^1\Sigma_g^+$ state of H_2 (Davidson 1961, Kolos and Wolniewicz 1969); indeed this is at present the only double minimum surface for which accurate wavefunctions are known. If the electronic wave functions are restricted to single Slater determinants, then the Hartree-Fock treatment gives rise to crossing curves, corresponding to (1s2s) and $(2p\sigma_u)^2$ states; these are mixed in a configuration-interaction treatment, and a double-minimum surface is obtained. Such potential crossing has also been studied in NO and N_2 (Felenbok and Lefebvre-Brion 1966, Lefebvre-Brion 1969).

If accurate Hartree-Fock wave functions are used, then for states of like symmetry, the perturbation consists of the nuclear kinetic energy operator together with $1/x_{ij}$, the electron-electron repulsion.

Experimental Determination of the Perturbation.

If the states in the crossing region are observable spectroscopically, then functional forms for the crossing surfaces may be assumed, say Morse curves, and the perturbation evaluated by "deperturbing" the spectrum. To satisfy (i), the assumed functional form for the reactant and product potentials must be an analytic continuation of the potential

function near the reactant or product minimum. This method has been applied to the interaction between the π-π and Δ-Δ states of NO (Lagerqvist and Miescher 1958,1966). Felenbok and Lefebvre-Brion (1966) found that this experimental perturbation is in fair agreement with the value they obtained for the interaction between the corresponding Hartree-Fock states.

Potential Surfaces and Wave Functions from the "Crude Adiabatic Approximation".

This approximation (see, for example, Longuet-Higgins 1961) assumes that the electronic wave function is independent of the internuclear coordinate X:

$$\phi(X) = \phi(X_o) \qquad (I.3)$$

where X_o is usually taken as the equilibrium distance. This crude zero-order wave function may be improved by mixing in higher electronic states through the perturbation $X(\partial H/\partial X)_{X_o}$ (Herzberg-Teller coupling [Herzberg and Teller 1933]). The further assumption is made that the potential function has a simple analytic form (usually a quadratic function of the nuclear coordinates); again this must be an analytic continuation of the potential function near the reactant or product minimum. The application of this method to a unimolecular reaction is less straightforward than it is in spectroscopic contexts. To obtain crossing reactant and

product surfaces which are analytic continuations of the potential functions near the respective minima, different X_o's must be used for the zero-order wave functions of reactant and product, say X_r and X_p (these, incidentally, need not be the equilibrium configurations, but can be chosen close to the crossing point to reduce the size of the perturbation). These wave functions will not in general be orthogonal if $X_r \neq X_p$; therefore two orthogonal wave functions must be constructed from these initial wave functions. There is, however, an infinite number of ways of constructing such an orthogonal set: once one orthogonal set is obtained, we may generate another set by a rotation in function space. The perturbation matrix element between reactant and product will not in general be independent of the angle of this rotation. This apparent inconsistency can be resolved by including interactions with higher electronic states, when the angular dependence will disappear. It might perhaps be possible to make this angular dependence negligibly small by choosing X_r and X_p sufficiently close to the crossing point.

Restriction of the Electronic Hamiltonian.

The simplest example of this method of separating reactant and product is the omission of the spin-orbit coupling term if reactant and product have different spins

(as is the case in the N_2O decomposition). This example illustrates the convenience of the perturbation approach to the theory of unimolecular reactions: it is obviously difficult to work with wave functions which are mixtures of singlets and triplets. Indeed, the perturbation approach is particularly applicable to so-called "non-adiabatic" reactions (Nikitin 1966, p.65) which cause some difficulty in other theories.

Another method of restricting the electronic Hamiltonian is to confine the nuclear geometries for which wave functions and potential surfaces are evaluated. For example, the thermal isomerisation of fulvene to benzene could be treated by restricting the calculation of reactant and product wave functions to fulvene and benzene type geometries respectively, provided the perturbation matrix element could be kept sufficiently small for (iv) to be satisfied. One would then expect those perturbation matrix elements to be largest which involve vibrations distorting the molecule into a geometry intermediate between the two isomers.

In the present work we are not concerned with the actual calculation of the perturbation. It is merely sufficient for the electronic potential to be separable into reactant and product surfaces, and in principle this is always possible. Recently, for example, Hougen and

Lewis (1968) have described a method of achieving this separation if the complete double minimum potential surface is known.

Calculations based on the separated potentials are considerably simplified if the Condon approximation (Condon 1928) can be invoked. Here it is assumed that in equation (2), the electronic perturbation $V_{rp}(X)$ is a slowly-varying function of X, and can be replaced by its value at some central point X_c and taken outside the integral:

$$V_{ri,pj} = V_{rp}(X_c) \int \psi_r \psi_p dX \qquad (I.4)$$

(If one-dimensional curves only are involved in the calculation, then the obvious choice for X_c is the crossing point. If the surfaces are multidimensional, then as those perturbation matrix elements which contribute appreciably to the overall rate constant will usually occur over a comparatively small range of energy, X_c can be given some value in this range).

The validity of the Condon approximation is probably dependent on the nature of the perturbation. For example, in Felenbok and Lefebvre-Brion's NO calculation (1966), where the separated wave functions are single Slater determinants, the variation of $V_{rp}(X)$ near the crossing point is negligible. On the other hand, in Berry and Nielsen's (1969) calculation on predissociation in H_2, where

the zero-order basis consists of exact Born-Oppenheimer states, it is found that $V_{rp}(X)$ can even change sign going through the crossing point.

Section 4. The Time Dependence of the Reaction Step.

We now turn to a more precise discussion of the time dependence of the reaction step, which in the H_o representation is the process of conversion of reactant to product, and in the H representation is the decomposition or deactivation of a metastable state into product. For the moment we will confine our attention to unimolecular decompositions, wherein the states of product belong to a true continuum.

If the internal perturbation V is much less than the collision-induced perturbation, then, in the language of the H_o representation, the active reactant state decays exponentially into the product continuum with time constant Γ(Goldberger and Watson 1964, p.450). First-order perturbation theory may be used to evaluate this time constant, to obtain the rate K_{ii} of internal conversion of level i of reactant into *all* levels of the continuum (Messiah 1964,p.736).

$$K_{ii} = 2\pi V^2_{ri,pE} \rho(E)/\hbar \qquad (I.5)$$

("Fermi's Golden Rule"). Here E is the energy of the level

i, $V_{ri,pE}$ the perturbation matrix element between reactant level i and the continuum level with the same energy, and ρ is the level density. ρ is defined in terms of the normalisation of the continuum wave function; if this is normalised to a δ-function with respect to energy, then $\rho = 1$. The double subscript in (5) is introduced for use in chapter II, where collision-induced transitions between levels i and j are also considered.

If only one level i is involved in the reaction, then the condition for the validity of (5) is simply $E >> \hbar K_{ii}$ (Goldberger and Watson 1964, p.446). However, the decay of neighbouring levels may introduce interference effects, and non-exponential decay will result. Thus a further criterion for the validity of (5) is that the linewidths of neighbouring states should not overlap (Mies and Kraus 1966), i.e. that

$$|E_i - E_j| >> \hbar K_{ii} \qquad (I.6)$$

where i and j refer to neighbouring levels. The derivation of this result (Mies and Kraus 1966, Jortner 1969, Bixon *et al* 1969) requires the introduction of the matrix Γ which is a generalisation of (5):

$$\Gamma_{ij} = \frac{2\pi}{\hbar} \int \langle i|V|E\rangle\langle E|V|j\rangle \rho(E)\,dE$$

where $|i\rangle$ is the i^{th} level of reactant, and $|E\rangle$ a continuum

product state. The time behaviour of the system is then obtained by diagonalising the matrix H - ½iΓ. Therefore the precise condition for non-interference of neighbouring states is that the off-diagonal elements of this matrix are negligible:

$$\Gamma_{ij} \ll |E_i - E_j - \tfrac{1}{2}i(\Gamma_{ii} - \Gamma_{jj})| \qquad (I.7)$$

The above authors have derived the condition (6) by assuming that $\Gamma_{ii} = \Gamma_{jj} = \Gamma_{ij}$. Now it may be seen from our numerical studies in Chapter III that those levels which contribute appreciably to the overall rate constant are confined to a comparatively small energy range, and thus the wave functions of states i and j are similar, as are the wave functions of the corresponding continuum states. Therefore Γ_{ii}, Γ_{jj} and Γ_{ij} will most likely have similar magnitudes, and (6) should be a sufficient condition for (7).

At first sight it would appear that the condition (6) can always be violated simply by adding extra functional groups to the molecule which do not take part directly in the reaction, but decrease the spacing between levels. However, the addition of such functional groups also increases the number of coordinates, which causes the Franck-Condon factor in the perturbation matrix element to contain extra vibrational overlap integrals. This would have the effect of decreasing the perturbation and thereby compensating for

the decrease in spacing between levels.

The time dependence of the internal conversion of a reactant level into a (dense) manifold of *discrete* product levels, i.e., an isomerisation, is less straightforward than that discussed above for a decomposition. At present the theory for this process is in a state of flux (see, for example, Bixon and Jortner 1969, Teller 1969, Schlag and Weyssenhoff 1969, Young 1969, and our remarks in section 3 of this chapter). The main difficulty in the theory is that even if the product states are very closely spaced (a "quasi-continuum"), there is no reason that the perturbation should be a smooth function of energy, which is a necessary prerequisite for the derivation of the Golden Rule. Nevertheless, calculation of rates of internal conversion based on this expression appear to represent experimental results quite adequately (Byrne *et al* 1965). Bixon and Jortner (1968), using the highly simplified assumptions that the product levels are evenly spaced, and that each has the same perturbation matrix element with a given reactant state, have derived an expression for the rate which is formally equivalent to the Golden Rule. In their expression, $\rho(E)$ represents the level density of the discrete states of product. We feel that a more rigorous theory for internal conversion processes involving discrete states will be developed, and that an expression akin to the

Golden Rule is applicable to the calculation of rates of unimolecular isomerisation.

Because of the need to avoid interference effects, expressed in inequality (6), it is clear that in its present form our theory cannot be used to calculate rates for transfer between symmetrical potential surfaces (such as the inversion of ammonia). This is because, for such potentials, the level density in the two wells must be equal. Then, if the level density of product is sufficiently high that the reverse reaction can be ignored (condition [iii]) the inequality (6) cannot be satisfied.

The assumption of the adequacy of first-order theory embodied in the Golden Rule gives rise to exponential decay of the metastable state, and, as we proceed to demonstrate in the following chapter, gives rise to the experimentally observed pressure and temperature dependence of the overall rate constant. If for a unimolecular reaction which exhibits these macroscopic charactistics, first-order theory should prove inadequate for a particular basis set, then as the theory demands a time-independent transition rate, it would be necessary to choose another basis rather than pursue the expansion to higher orders.

CHAPTER II

FORMAL RATE THEORY

Section 1. Introduction

In the previous chapter we considered the quantum mechanical description of thermal unimolecular reactions, and showed that under certain assumptions the reaction may be described in terms of a perturbation-induced transition from reactant levels to product, with a probability proportional to time. We will now show how this gives rise to the experimentally observed pressure and temperature dependence of the overall rate constant.

In a unimolecular reaction taking place in an inert gas heat bath, the rate constant is observed to be independent of pressure at high pressure, and proportional to the pressure of inert gas at low pressure. An approximate Arrhenius behaviour is observed at all pressures. We derive these properties by expressing the overall rate constant as the largest eigenvalue of a matrix whose elements are the rates of collisional transfer between reactant levels and of internal conversion to product. The pressure and temperature dependence follow from the application of eigenvalue theorems, based on the properties of the rates of collision and conversion. The derivation of the Arrhenius behaviour, which

involves no approximations as to the populations of individual levels, gives the surprising result that the low pressure activation energy is largely determined by the deviation of these populations from equilibrium. This is in contrast to the common assumption that the population of "inactive" levels is the same as that in a non-reacting system.

Section 2. The Master Equation and its Solution.

In this section we review the derivation of the reaction rate constant as the largest eigenvalue of the "transport" matrix describing the reacting system.

The reacting system consists of a statistical ensemble of reactant molecules with a set of discrete energy levels i, with energy E_i and population x_i. The population of individual levels varies in time because of two separate processes: collisional exchange between reactant levels and conversion to product (the separation of these processes was discussed in chapter I). In the following we ignore the reverse reaction. (The inclusion of the reverse reaction in this formalism has been discussed by Valance and Schlag [1967]).

The change in population of level i, dx_i is to first order brought about by:

(i) molecules being added to level i from all other levels j by collision, with probability per unit time per

molecule γ_{ji}

(ii) molecules going from level i to all other levels j under the influence of collisions, with rate:

$$\sum_{j \neq i} \gamma_{ij} x_i \equiv -\gamma_{ii} x_i \qquad \text{(II.1)}$$

(iii) molecules being converted to product, with rate $K_{ii} x_i$. Our basic assumption is that K_{ii} can be identified with equation (I.5). We assume that the levels are ordered not by energy but by reactivity, such that all K_{ii} are zero up to a certain level indexed by N, whereafter conversion to product becomes effective. Levels above N are referred as "active".

We then have the master equation describing the system (first written down for unimolecular reactions by Eyring and Zwolinski 1947):

$$\frac{dx_i}{dt} = \sum_j \gamma_{ji} x_j - K_{ii} x_i \qquad \text{(II.2)}$$

or writing

$$\gamma_{ji} = P A_{ij}$$

where P is the pressure of inert gas (we will show below that A_{ij} is pressure-independent) and converting to matrix notation (Berman and Schoenfeld 1956, Montroll and Shuler 1958):

$$\frac{dx}{dt} = (PA-K)\, x \equiv Jx \qquad \text{(II.3)}$$

The matrix K will be diagonal, with zero elements below N+1. From (1), all the diagonal elements of A are negative.

It may be shown (Mirsky 1955, p.347) that the solution to the master equation (3) is

$$x(t) = \exp(Jt)\, x(t=0) \qquad \text{(II.4)}$$

where the matrix exponential is defined as

$$\exp(Jt) = I + Jt + 1/2\, J^2t^2 + \ldots \qquad \text{(II.5)}$$

The matrix exponential is evaluated by expanding J in terms of its Frobenius idempotents (projection operators) $\mathcal{O}_i$ (see, e.g., Perlis 1952, p.175). These are matrices, one corresponding to each eigenvalue λ_i of J, which have the property that for any polynomial f,

$$f(J) = \sum_i f(\lambda_i)\mathcal{O}_i \qquad \text{(II.6)}$$

and so

$$x(t) = \sum_i \mathcal{O}_i e^{\lambda_i t} x(0) \qquad \text{(II.7)}$$

If we denote the largest eigenvalue by λ_o, and assume that

$$\lambda_o >> \lambda_1 > \lambda_2 > \ldots\ldots \qquad \text{(II.8)}$$

then after a sufficiently long time, (Montroll and Shuler 1958)

$$x(t) = e^{\lambda_o t} \mathcal{P}_o x(0) \qquad \text{(II.9)}$$

Hence the total population, $\sum x_i(t)$, is proportional to $\exp(\lambda_o t)$; i.e. we have exponential decay with rate constant $-\lambda_o$, the largest eigenvalue of the matrix $J = (P A - K)$ (Montroll and Shuler 1958).

We may now re-examine assumption (8). By a "sufficiently long time" we mean the time required for the initial population to relax into the "reaction" distribution $\mathcal{P}_o x(0)$, which is the eigenvector of J corresponding to λ_o (Nikitin 1966, p.104). The expansion (7) may therefore be seen as two steps. Firstly the system relaxes to $\mathcal{P}_o x(0)$, under the influence of the $\mathcal{P}_i$'s for $i > 0$. These projection operators then become unimportant as the reaction term $e^{\lambda_o t}\mathcal{P}_o$ begins to dominate the expansion (7). The relaxation part of the process is therefore governed by the smaller eigenvalues $\lambda_1, \lambda_2 \ldots$ Then $-1/\lambda_1$ will approximate to the relaxation time of an unreacting system. Thus the criterion for the validity of (8) is that the relaxation time be very much less than the reciprocal of the reaction rate. This condition is easily met in typical thermal unimolecular reactions. For those reactions where this condition is not met, a quantity called the "mean first passage time", τ, (Montroll

and Shuler 1958, Valance and Schlag 1966) has been proposed as an alternative quantity which may be used to measure the speed of a reaction. This is defined as

$$\tau = \int_0^\infty \sum x_i(t)dt / \sum x_i(t=0) \qquad \text{(II.10)}$$

If the highest eigenvalue approximation is valid, then τ reduces to $-1/\lambda_o$, the reciprocal of the reaction rate constant.

Note that the largest-eigenvalue approximation involves no assumptions as to the populations of reactant levels, such as the "steady state" assumption (Slater 1959, p.16). (It will in fact by shown later that the steady-state approximation can be in serious error in the low pressure region). The largest-eigenvalue approximation merely implies that the ratio of the population of individual levels to the total population is constant throughout the course of the reaction (except during the initial relaxation period). Thus with this assumption the measurement of a unimolecular rate constant requires only the measurement of the concentration of a single reactant level as a function of time, as mentioned in chapter I, section 2.

Section 3. The Properties of the Transport Matrix J.

We now proceed to examine the formal properties of the transport matrix J = PA-K. Although much of this section

is a restatement of earlier work, it has been set out, firstly, to demonstrate precisely the quantum mechanical meanings of the elements of this matrix (this appears not to have been dealt with by previous workers) and secondly as a necessary precursor to the development of the succeeding sections.

From the definition (1), we have the relation

$$A_{ii} = \sum_{j \neq i} A_{ji} \qquad \text{(II.11)}$$

which is a consequence of the conservation of mass in an unreacting system.

We assume that the reactant is dilutely dispersed in an inert gas heat bath, which retains a constant temperature throughout the course of the reaction. Hence only collisions between reactant and inert gas need be considered. (The problem of including reactant-reactant collisions in this formalism has been considered by Schlag and Valance 1968). This assumption is not a severe restriction, as many experimental studies are carried out under conditions such as shock-initiated reactions in inert carrier gases; in fact, unimolecular reactions in condensed media can be considered as the high-pressure limit of these reaction conditions.

The rate of collisional transfer from level j to level i, PA_{ij}, is then the Boltzmann average of the energy-dependent cross section, $Q_{ji}(E)$ (see, for example, Herzfeld and Litovitz 1959, p.264):

$$PA_{ij} = 8\pi\ P\ m^{-\frac{1}{2}}(2\pi kT)^{-3/2} \int_{\Delta E}^{\infty} EQ_{ji}(E)\ e^{-E/kT} dE \qquad (II.12)$$

where T is the temperature, P the pressure of inert gas (in molecules per unit volume), m the mass of the inert gas, and ΔE, the minimum collision energy for the process, is zero if $E_i < E_j$, and $E_i - E_j$ otherwise. For notational convenience, we will assume for the present that the levels i and j are non-degenerate.

The collision matrix PA is often written in the form (Carrington 1962)

$$PA = \omega\ (\tilde{P} - I)$$

where ω is the frequency, and $\tilde{P}_{ij}$ is the "probability of transition per collision". Although this is formally merely an alternative way of writing A, the use of ω and $\tilde{P}$ assumes that $\omega = -A_{ii}$ is independent of i, which cannot be justified quantum mechanically. This objection is removed if ω is treated as a diagonal matrix instead of a scalar (see, for example, Schlag and Valance 1969). However, an individual collision cannot be defined quantum mechanically; rather a cross section is used, which gives rise to a collision rate. Hence the description of $\tilde{P}$ as a probability per collision is also, strictly speaking, invalid. Formal expressions involving ω and $\tilde{P}$ can readily be recast into A- matrix form.

We may prove that microscopic reversibility follows

directly from (12). (A proof similar to that presented below was recently derived independently by Thompson [1968]). From the time-reversal invariance of a collision (Messiah 1964, p.807),

$$v_j^2 \, Q_{ji}(E-E_j+E_i) = v_i^2 \, Q_{ij}(E)$$

where v is the velocity of the colliding particles. Hence

$$[E-E_j+E_i]Q_{ji}(E-E_j+E_i) = E \, Q_{ij}(E) \qquad \text{(II.13)}$$

Substituting (13) into (12) and making a simple change of variable, we have

$$A_{ji} = A_{ij} e^{(E_i-E_j)/kT} \qquad \text{(II.14)}$$

This is the microscopic reversibility condition.

Consider firstly the properties of the A matrix alone. This is equivalent to considering an unreacting system.

(i) It follows directly from (14) and (11) that the Boltzmann vector b:

$$b_i = \exp\,(-E_i/kT) \qquad \text{(II.15)}$$

is an eigenvector of A, with eigenvalue zero. Since it will be shown below that all the eigenvalues of A are less than or equal to zero, it follows that λ_o for A is zero. Hence in an unreacting system, the limit of (7)

becomes

$$\lim_{t\to\infty} x(t) = \mathcal{O}_o x(t=0) = b \qquad \text{(II.16)}$$

since it can be shown directly from the definition of the projection operator $\mathcal{O}_o$ (see, for example, Löwdin 1962) that for an arbitrary vector x, $\mathcal{O}_o$ x=b. Thus an unreacting system reaches equilibrium, and the rate of equilibration is governed by the non-zero eigenvalues, as in section 2.

(ii) The similarity transformation (Montroll and Shuler 1958):

$$B = S\ A\ S^{-1} \qquad \text{(II.17)}$$

where S is diagonal with elements

$$S_{ii} = e^{-E_i/2kT} \qquad \text{(II.18)}$$

$$\text{i.e.} \quad B_{ij} = A_{ij} \exp[(E_i - E_j)/2kT] \qquad \text{(II.19)}$$

converts A to a symmetric matrix,B, which of course has the same eigenvalues as A. Under this transformation, the Boltzmann vector b becomes

$$b_B \equiv Sb = \{e^{-E_i/2kT}\} \qquad \text{(II.20)}$$

As K is diagonal, this transformation also diagonalises J = PA-K. The symmetrised matrix is hermitian; hence all the eigenvalues of J are real (Montroll and Shuler

1958). Thus the rate constant R may be expressed in the forms

$$R = \frac{-c^T(PB-K)c}{c^Tc} = \frac{-g^T(PA-K)g}{g^Tg} \qquad (II.21)$$

where g and c are the unsymmetrised and symmetrised eigenvectors corresponding to R, and g^T and c^T their transposes. The elements of g correspond to the population of the levels of reactant.

(iii) The eigenvalues of A and J are less than or equal to zero. This condition is obviously necessary for the convergence of (7) in the limit of infinite time. Kim (1958) has put forward a proof of this inequality; here we present an alternative proof. We derive the result for the A matrix only; the extension to PA-K is straightforward.

From (11), the sum of the elements in a column of A is zero. Now, if g is an eigenvector of A, then

$$\sum_j A_{ij}g_j = \lambda g_j \qquad (II.22)$$

Summing the set of equations (22) over i, and reversing the order of summation of i and j, we have

$$\sum_i g_i \sum_j A_{ji} = \lambda \sum_j g_j \qquad (II.23)$$

The left hand side of (23) is identically zero, from (11). Therefore either $\lambda=0$ or $\sum_j g_j=0$. If the latter holds

replace g_j in (22) by $-\sum_{j\neq i} g_i$. Now, all $A_{ij}>0$ $(i\neq j)$, and, from (11), $A_{jj}<0$. Let

$$A_{jmax} = \max_i (A_{ji}, i\neq j)$$

Then $A_{jmax}<A_{ji}$. Then (21) can only be satisfied if $\lambda<0$.

(iv) From the eigenvalue relation

$$\sum_j A_{ij}g_j - K_{ii}g_i = Rg_i \qquad \text{(II.24)}$$

we have, summing over i and invoking (11),

$$R = \frac{\sum K_{ii}g_i}{\sum g_i} \qquad \text{(II.25)}$$

which is the familiar equation relating the rate constant to the populations of each level and the microscopic rates of conversion to product.

Section 4. The Pressure Dependence of the Rate Constant.

According to the discussion in chapter I, the formation of product in a unimolecular reaction may be regarded as a purely intramolecular process, i.e., the elements of the K matrix are independent of pressure and temperature. The elements of A are independent of pressure (equation 2). These properties, together with the formal relations of the preceding section, give rise to the experimentally observed pressure

dependence of the rate constant.

High Pressure Limit.

As the elements of A and K are independent of pressure, at high pressures the eigenvalues of J = PA-K may be calculated by treating -K as a perturbation of PA. If the symmetric representation of J is used (equation 17), then conventional perturbation theory for Hermitian matrices may be applied. The unperturbed eigenvector of B corresponding to the largest eigenvalue is b_B, with zero eigenvalue. We then have for the high pressure rate constant, R^{HP},

$$R^{HP} = \frac{b_B^T (PB-K) b_B}{b_B^T b_B} = \frac{b_B^T K b_B}{b_B^T b_B} = \frac{\sum K_{ii} e^{-E_i/kT}}{\sum e^{-E_i/kT}} \qquad (II.26)$$

that is, a Boltzmann average of rates of conversion from reactant to product. This expression (often with $\int$ replacing $\sum$) is well-known. In the high-pressure limit, therefore, the population has its equilibrium value. However, in the low and intermediate pressure regions, significant deviations from equilibrium will occur, as molecules are bled off from the higher inactive levels.

It can be shown that the second-order correction to (26) is proportional to 1/P; this expresses the pressure dependence of the falloff from the high pressure limit.

Low Pressure Limit

At low pressures, consider PB as a perturbation of -K. As -K is a diagonal matrix, with $K_{ii} = 0$ for $i \leq N$, its largest eigenvalue is zero, and this eigenvalue is N-fold degenerate. The corresponding eigenvectors, k_j, are simply unit vectors. From the theory of perturbations of a degenerate eigenvalue, the first-order eigenvalue is the largest eigenvalue of the matrix PB^o, where

$$B^o_{ij} = k_i^T \; B \; k_j \qquad \text{(II.27)}$$

Thus we obtain the result that the low pressure rate constant is proportional to pressure. Furthermore, by considering the form of the unit vectors k_j, it can be seen that B^o is the matrix B truncated at i=N,j=N. Valance and Schlag (1966) have also discussed this result, but their derivation assumed that the population of active levels is zero in the low pressure limit ($g_i = 0, i > N$); this relation is in fact a *consequence* of (27) and (21).

Analogous to (24), we have for the low pressure *second order* rate constant, R^{LP},

$$R^{LP} = \sum_{i \leq N} g_i \, A'_{ii} / \sum g_i \qquad \text{(II.28)}$$

where

$$A'_{ii} = \sum_{\text{all } j} A_{ji} = \sum_{j>N} A_{ji} \qquad \text{(II.29)}$$

These A'_{ii} are the "extra" terms on the diagonal elements of the

truncated collision matrix; they express the rate of reaching active levels ($j>N$) from inactive levels ($j\leq N$). Thus (28) expresses the expected result that, in the low pressure limit, the rate constant is determined by the rate of collisional activation into active levels.

Note that in equation (28), the summation extends only over inactive levels. Those inactive levels for which the A'_{ii} will be greatest will lie just below the first active level. However, it is precisely these levels that one would expect to exhibit the greatest deviation of the actual population, g_i, from equilibrium. Therefore to approximate the populations of these levels by the equilibrium population, b_i, as is implicit in the steady-state approximation, will lead to serious error in the low pressure region. This point is further explored in the following section, and in the calculations of Chapter IV.

The second-order correction to the low pressure rate constant, which expresses the pressure dependence of the approach to the low pressure limit, is proportional to P^2.

We may further prove that the rate constant is a monotonically increasing function of pressure. For, as PB-K is Hermitian, we may apply what has been termed the Hellmen-Feynman theorem (Löwdin 1959) for the differential of an eigenvalue of an Hermitian matrix:

$$\frac{\partial R}{\partial P} = -\frac{c^T (\partial J/\partial P)\, c}{c^T c} = -\frac{c^T B\, c}{c^T c}$$

The denominator is always positive. As B has non-positive eigenvalues, the numerator (being a quadatic form on B) must be negative semi-definite. Hence $\frac{\partial R}{\partial P} > 0$, i.e., the rate constant is monotonically increasing with respect to pressure.

Section 5. The Temperature Dependence of the Rate Constant: the "activation energy" of Unimolecular Reactions.

Although it is recognised that the activation energy of a unimolecular reaction is essentially only a parameter expressing the temperature dependence of the rate constant, this parameter is frequently associated with the height of the potential barrier separating reactant and product. In this section we derive a general expression for the activation energy of a unimolecular reaction at any pressure, in an inert gas heat bath. The expressions obtained, and the calculations of the succeeding chapters, emphasise that the height of the potential barrier is no more than a first approximation to the activation energy.

In the approach followed here - an approach initiated by Tolman (1927, p.260) and further pursued by Slater (1959, p.35) - the populations of reactant molecules in different levels are specifically enumerated, as are the probabilities of transitions between them due to collisions with the inert gas.

Slater made an important assumption concerning the populations of the active levels of the reactant. This assumption, the steady state approximation, postulates that the population of *inactive* levels follows a Boltzmann distribution. The deviation from equilibrium of the populations of these levels is specifically explored here; it is found to lead to an important contribution to the activation energy which goes to zero only in the high pressure limit.

We also take into account the temperature dependence of the thermal averages of the collision cross sections for exchange between reactant levels. Again, this also leads to a significant term in the activation energy in the low and intermediate and low pressure regions. Recently Menzinger and Wolfgang (1969) considered the second of these effects for bimolecular reactions, but in a highly simplified way which amounts to the assumption that the reactants have no internal structure. They also drew attention to the fact that in practical kinetic runs thermalisation of the heat bath may need to be reckoned with; however, this effect can always be minimised if the reactant is sufficiently dilute.

We define the activation energy as

$$E_{act} = -k \frac{\partial R/\partial(1/T)}{R} \qquad \text{(II.30)}$$

Using the symmetric representation of the J matrix (equation 19) and applying the Hellmann-Feynman theorem to equation (21),

we obtain

$$\frac{\partial R}{\partial(1/T)} = - \frac{P\, c^T\, [\partial B/\partial(1/T)]\, c}{c^T c} \qquad \text{(II.31)}$$

From relations (17), (18) and (21),

$$c^T\, [\partial B/\partial(1/T)]\, c = g^T\, S^2\, [\partial A/\partial(1/T)]\, g \qquad \text{(II.32)}$$

From the temperature dependence of A expressed in equations (12) and (14), $\partial A/\partial(1/T)$ can be expressed as the sum of two matrices. One will involve the differential of the Boltzmann average of cross sections, and will be dependent on the energy variation of Q(E). The other will derive solely from microscopic reversibility, and will be independent of the form of Q(E). Because of the form of (12), there will also be a $\frac{3}{2}$ kT term. That is, we have

$$-k\, [\partial A/\partial(1/T)] = \tilde{E}^Q + \tilde{E}^M - \tfrac{3}{2}kTA \qquad \text{(II.33)}$$

where the microscopic reversibility matrix $\tilde{E}^M$ is

$$\tilde{E}^M_{ii} = - \sum_{j>i} (E_i - E_j)\, A_{ji} \qquad \text{(II.34)}$$

$$\begin{aligned} \tilde{E}^M_{ij} &= 0 && \text{for } i<j \\ &= (E_j - E_i)\, A_{ij} && \text{for } i>j \end{aligned} \qquad \text{(II.35)}$$

and the cross-section dependent matrix $\tilde{E}^Q$ is

$$\mathcal{E}^{Q}_{ii} = -\left\{ \sum_{j>i} \mathcal{A}_{ij}\, e^{(E_i - E_j)/kT} + \sum_{j<i} \mathcal{A}_{ji} \right\} \qquad \text{(II.36)}$$

$$\mathcal{E}^{Q} = \mathcal{A}_{ij} \qquad \text{for } i \neq j \qquad \text{(II.37)}$$

where

$$\mathcal{A}_{ij} = 8\pi m^{-\frac{1}{2}} (2\pi kT)^{-3/2} \int_{\Delta E}^{\infty} E^2\, Q_{ji}(E)\, e^{-E/kT}\, dE \qquad \text{(II.38)}$$

Note, incidentally, that the relation of $\mathcal{A}_{ij}$ to its transpose, derived in the same way as equation (14), is

$$\mathcal{A}_{ij} = \mathcal{A}_{ji} e^{(E_j - E_i)/kT} + (E_i - E_j)\, A_{ij}$$

Inserting these values into equation (31), and using the definition of the Boltzmann vector b (equation (15), we find that the right hand side of (32) may be expressed as the sum of three terms. The first is

$$-\tfrac{3}{2} kT\, g^T S^2\, A\, g \qquad \text{(II.39)}$$

the second depends on Q(E):

$$\sum_i \frac{g_i}{b_i} \left\{ \sum_{j>i} \mathcal{A}_{ij} (g_i b_j / b_i - 2g_j) + \sum_{j<i} g_i \mathcal{A}_{ji} \right\} \qquad \text{(II.40)}$$

and the third may be attributed to microscopic reversibility:

$$\sum_i g_i \sum_{j>i} A_{ji} (E_j - E_i) \left\{ \frac{g_i}{b_i} - \frac{g_j}{b_j} \right\} \qquad \text{(II.41)}$$

Separating (41) into two sums involving E_i and E_j, reversing

the order of summation in the E_j term, and using relation (24), the term (41) can be reduced to

$$\frac{1}{P}\sum_i \frac{g_i^2}{b_i} E_i(K_{ii} + R) + \sum_i E_i \sum_{j<i} b_j A_{ij} \left(\frac{g_i}{b_i} - \frac{g_j}{b_j}\right)^2 \qquad \text{(II.42)}$$

Note that the second term in this expression depends on the *difference between the exact and equilibrium populations*. Equations (30), (39), (40) and (42) constitute a general expression for the activation energy at all pressures.

The above general equations for the activation energy at any pressure are carried to the high pressure limit by setting the population vector g equal to the Boltzmann vector b, and to the low pressure limit by setting the population of active levels equal to zero.

Section 6. High and Low Pressure Limits of the Activation Energy.

High Pressure Limit

If g = b, then (39) is identically zero (since Ab = 0), as are (40) and the second term in (42). If the remaining term in (42) is substituted into (30), we obtain

$$E_{act}^{HP} = \frac{\sum E_i K_{ii} e^{-E_i/kT}}{\sum K_{ii} e^{-E_i/kT}} - \frac{\sum E_i e^{-E_i/kT}}{\sum e^{-E_i/kT}} \qquad \text{(II.43)}$$

$$= \frac{\langle EK \rangle}{\langle K \rangle} - \langle E \rangle \qquad \text{(II.44)}$$

This is identical with Tolman's result (1927, p.260) for the high pressure limit, which is obtained by differentiating (26) directly. The terms are the average energy of the active levels, and the average internal energy. The average internal energy (heat capacity) term <E> will be of the order of magnitude of kT per degree of freedom above the zero-point energy. The term <EK>/<K> may be easily shown to be greater than or equal to E_{N+1}, the energy of the lowest active level. Note that this energy need not correspond to either the crossing point of the separated reactant and product potentials, or the maximum of the "mixed" potential; examples in Chapter III will illustrate this point.

If the sums in <EK>/<K> are dominated by a single term, indexed by n (i.e. the microscopic rate K_{nn} is much greater than the microscopic rates of other kinetically accessible levels), then $\langle EK\rangle/\langle K\rangle \simeq E_n$. This term will then be temperature independent. In general, however, the <EK>/<K> will not be independent of temperature, but nevertheless we would expect this term to be approximately the energy of the level where conversion to product first becomes appreciable. Numerical examples in Chapter III show that in many cases <EK>/<K> varies only slowly with temperature, and that the temperature dependence of the activation energy is caused by the <E> term. However, in some cases tunnelling causes E_{act} to have a pronounced temperature dependence. The temperature

dependence of E_{act} has also been studied by Labhardt (1967), who found that it is independent of temperature only for special (and therefore highly improbable) functional forms of K_{ii}.

If the basis chosen for calculating the microscopic rates of conversion to product is such that the Condon approximation is valid, then from equations (I.3), (I.5) and (II.41), the activation energy is *independent of the electronic coupling*, i.e., the splitting induced by the perturbation between the electronic potential surfaces of reactant and product. This is obviously at variance with the assumption that the activation is equal to the barrier height.

Low Pressure Limit

Let N be the index of the highest inactive level. Then in the low pressure limit, $g_i=0$ for $i>N$. As $K_{ii}=0$ for $i\geq N$, from the definition of active levels, the term $\sum g_i^2 E_i K_{ii}/b_i$ in (43) becomes zero. We then find that at low pressure this activation energy is the sum of five terms, from (39), (40) and (42). We obtain

$$E_{act}^{LP} = \langle EA' \rangle / \langle A' \rangle + E^M + E^Q - \langle E_g \rangle - \frac{3}{2}kT \qquad \text{(II.46)}$$

where E^Q arises from the differential of the energy-dependent average cross section:

$$E^Q = \frac{\sum \frac{g_i^2}{b_i} \sum_{j>N} A_{ij} \frac{b_j}{b_i} + \sum \frac{g_i}{b_i} \left\{ \sum_{j=i+1}^{N} A_{ij} (g_i b_j / b_i - 2g_j) + \sum_{j>i} g_i A_{ji} \right\}}{\sum\sum g_i g_j A_{ij} / b_i} \qquad \text{(II.47)}$$

the term <EA'>/<A'> arises from the second term in (43) for i>N, j≤N:

$$<EA'>/<A'> = \frac{\sum_{i>N} E_i \sum_{j\leq N} A_{ij} g_j^2 / b_j}{\sum\sum g_i g_j A_{ij} / b_i} \qquad \text{(II.48)}$$

and E^M is the term containing the difference between the exact and Boltzmann populations:

$$E^M = \frac{\sum E_i \sum_{j<i} b_j A_{ij} \left(\frac{g_i}{b_i} - \frac{g_j}{b_j} \right)^2}{\sum\sum g_i g_j A_{ij} / b_i} \qquad \text{(II.49)}$$

and $<E_g>$ is internal energy, averaged over the actual population.

$$<E_g> = \frac{\sum g_i^2 E_i / b_i}{\sum g_i^2 / b_i} \qquad \text{(II.50)}$$

Equations (46) - (50) constitute an *exact* expression for the low pressure activation energy. The terms <EA'>/<A'> and $<E_g>$ correspond to <EK>/<K> and E in the high pressure activation energy, but as well (46) contains a term E^M which is dependent on the deviation from equilibrium of the

populations of the inactive levels. The term $\langle E_g \rangle$ will have a value very close to that of $\langle E \rangle$ appearing in the high pressure activation energy, because the main contributions to the sums in (50) will come from the lowest inactive levels, where the population differs only slightly from a Boltzmann distribution.

If the levels i have degeneracy d_i, it can be easily shown that (46) - (50) are still valid if we write

$$b_i = d_i \, e^{-E_i/kT}$$

Section 7. Low pressure Activation Energy as a "barrier height."

In this section we will demonstrate that the expression for the low pressure activation energy, (46), is indeed approximately E_N, the energy at which conversion from reactant to product becomes effective.

If we take the steady-state approximation, which implies that the actual population g in an inactive region may be replaced by the equilibrium population b, equations (46) - (50) reduce to

$$E_{act}^{LP} \simeq \sum e^{-E_i/kT} A'_{ii} E_i \; / \; \sum e^{-E_i/kT} A'_{ii} \; - \frac{3}{2}kT - \langle E \rangle + E^Q \qquad (II.50)$$

which apart from the term E^Q is the steady state expression

(Slater 1959, p.38). It is analogous to the high pressure result, with A' replacing K, and it is clear that the first term will have the value of the energy where A'_{ii} is significant, i.e., an energy close to E_N. However, we shall find that the same steady state approximation can lead to serious errors in the frequency factor, and we must therefore examine the exact expression (46).

In an actual unimolecular reaction, thousands of vibrational levels will be involved, and even if one could calculate the cross-sections accurately, manipulation of the complete A matrix is impractical using present techniques. It is therefore customary to introduce a system of condensing the actual levels with a certain range of energy into a single "pseudo-level" with appropriate degeneracy, thereby reducing the size of the collision matrix A (see Chapter IV, and Tardy and Rabinovitch 1966 and references therein). If the A matrix is sufficiently coarsely grained (i.e., if there is a sufficiently large energy gap between the "pseudo-levels") it will be tridiagonal, i.e., only nearest-neighbour transitions need be considered. In this case the activation energy equations (46) - (50) simplify considerably, to

$$E_{act}^{LP} = E_{N+1}\frac{g_N}{b_N} + \sum_{i=2}^{N} E_i \frac{b_{i-1}}{g_N}\left(\frac{g_i}{b_i} - \frac{g_{i-1}}{b_{i-1}}\right)^2 \frac{A_{i,i-1}}{A_{N+1,N}} \qquad (II.51)$$

$$- \langle E_g \rangle - \frac{3}{2}kT + E^Q$$

The last term we are still neglecting. The two terms preceding it are typically only a few kcal/mole, and may also be neglected for the present. The most important terms in the summation will then be those for which i equals or is only slightly less than N. If $g_i=b_i$, the sum in equation (51) is identically zero, and the steady state expression is obtained. If however, the deviation from equilibrium in the upper levels is large ($g_N<<b_N$), then the "difference" term in (51) (i.e. the summation) will become the dominating term. Thus the calculation of the activation energy depends on a knowledge of the deviation from equilibrium of the populations of the inactive levels.

We may further reduce (51) by using the eigenvalue relation for a truncated tridiagonal collision matrix, together with equations (28), (14) and (11). These yield

$$\frac{A_{i,i-1}}{A_{N+1,N}} \frac{b_{i-1}}{g_N} \left[\frac{g_{i-1}}{b_{i-1}} - \frac{g_i}{b_i}\right] = 1 - \sum_{j=i}^{N} g_j \Big/ \sum_{j=1}^{N} g_j \qquad \text{(II.52)}$$

through which equation (51) becomes

$$E_{act}^{LP} = E_{N+1} \frac{g_N}{b_N} + \sum_{i=2}^{N} E_i \left[\frac{g_{i-1}}{b_{i-1}} - \frac{g_i}{b_i}\right]\left[1 - \sum_{j=i}^{N} g_j \Big/ \sum_{j=1}^{N} g_j\right] \qquad \text{(II.53)}$$

$$- \langle E_g \rangle - \frac{3}{2}kT + E^Q$$

Note that this expression depends on the collision rates only through the populations of the inactive levels and E^Q. (This statement holds for the tridiagonal model only).

To force this still complex expression into a form which recognizably relates E_{act}^{LP} to the energy of the first active level (E_{N+1}) we may be tempted to retain only the leading term in the first sum (i=N). Then since $g_N/\sum g_i \ll 1$, and setting $E_N \simeq E_{N+1}$, (53) reduces to

$$E_{act}^{LP} = E_{N+1} \frac{g_{N-1}}{b_{N-1}} - \langle E_g \rangle - \frac{3}{2}kT + E^Q \qquad \text{(II.54)}$$

and if the level spacing is coarse enough, g_{N-1} will not be drastically less than b_{N-1}. Thus E_{act}^{LP} does apparently emerge as closely related to the energy of the first reactive level, if E^Q is ignored. The effect of the neglected terms in the summation in (53) is in fact to make up the difference between b_{N-1}/g_{N-1} and unity. To see this, however, we must turn to specific models for the rates of collision. We undertake a full numerical study of the complete formula (46) in Chapter IV; for the present we turn to a simplified model for the elements of the collision matrix A.

Section 8. Truncated Harmonic Oscillator Model.

We may derive a good approximation for the low pressure population distribution g, and thus the activation

energy, for a simple model: the "harmonic oscillator" collision matrix (Montroll and Shuler 1958, Landau and Teller 1936). This model assumes that the molecule is an harmonic oscillator with dissociation occurring at levels i>N.

For the form of the potential assumed by Landau and Teller, the thermally averaged cross-sections for vibrational transitions induced by collisions are, to a good approximation,

$$\begin{aligned} A_{i,i+m} &= i\chi \qquad (m=1) \\ &= 0 \qquad (m>1) \end{aligned} \tag{II.55}$$

where χ is a constant. Equations (11) and (14) give the remaining elements.

The dissociation truncates this matrix at i=N. The eigenvector problem for this matrix has been studied previously (Montroll and Shuler 1958, Buff and Wilson 1960). The exact solutions are known, but are far too complex to be manageable in equation (53). We have however, come across a simple analytic approximation for the eigenvector, which will be shown to give excellent estimates of the exact value, and which permits the series in equation (53) to be summed. Since the energy levels are equidistant, and non-degenerate, we have

$$e^{(E_1-E_2)/kT} = b_2/b_1 = b_3/b_2 = \ldots = b_N/b_{N-1} = \alpha \tag{II.56}$$

where $\alpha>1$. Our approximation to the eigenvector is

$$g_i \simeq b_i(1-\alpha^{N+1-i}) = \alpha^{i-1}(1-\alpha^{N+1-i}) \qquad \text{(II.57)}$$

(where b has been normalised so that $b_1=1$). We may show analytically that the error involved in this approximation is small by finding the next approximation to the eigenvector in an iterative technique. Form the matrix (Carrington 1962)

$$I + A/Z$$

where

$$Z = \max(-A_{ii}) = A_{NN} = (N-1+N\alpha)\chi \qquad \text{(II.58)}$$

and I is the unit matrix

The eigenvalues of I+A/Z are all less than unity, and it is well known that because g is an eigenvector of A it is also that eigenvector of I+A/Z whose eigenvalue is largest in magnitude, and closest to unity. Thus if $g^{(o)}$ is an approximate eigenvector, then $g^{(1)} = (I+A/Z)\, g^{(o)}$ will be a better estimate (power method of finding the largest eigenvector; see, for example, Perlis 1952, p.208). If we renormalise $g^{(1)}$ so that $g_1{}^{(o)} = g_1{}^{(1)}$, then $g_N{}^{(1)}/g_N{}^{(o)}$ will be the correction to $g_N{}^{(o)}$, which is the most sensitive element of the eigenvector to this procedure. We find in this case that, using expression (57) for g_i,

$$\frac{g_N{}^{(1)}}{g_N{}^{(o)}} = \frac{(N-1)(\alpha+1)}{(N-1+N\alpha)} \qquad \text{(II.59)}$$

If instead, we had used the Boltzmann vector b_i as our initial eigenvector, we would have obtained

$$\frac{g_N^{(1)}}{b_N} = \frac{(N-1)}{(N-1+N\alpha)} \qquad \text{(II.60)}$$

Values of the two functions are given in Table 1 for a representative value of N and α. It can be seen that equation (57) is quite a reliable estimate for the eigenvector, and the Boltzmann vector is not. The deviations from unity of figures in the second half of the table are *minimum* measures of inadequacy of the steady state approximation.

Table 1. First iteration corrections to the populations of the topmost inactive level. Truncated harmonic oscillator model.

N	α 0.01	0.1	0.5	0.75
	Initial vector: $g^{(o)}$, eq. (57)[a]			
10	.999	.99	.96	.96
20	.999	.99	.96	.96
30	.9997	.997	.98	.99
	Initial vector: Boltzmann vector[b]			
10	.99	.90	.64	.55
20	.99	.90	.66	.56
30	.99	.90	.66	.56

a Tabulated entries are values of eq. (59)

b Tabulated entries are values of eq. (60)

If equation (57) for g is substituted into (53) or (46)-(50), we obtain, omitting terms of order α^N,

$$E_{act}^{LP} = \Delta E\,[N + (1-2\alpha)/(1-\alpha)] - \langle E_g \rangle - \tfrac{3}{2}kT + E^Q \qquad (II.61)$$

where ΔE is the energy spacing. The value for α in the computations of Chapter IV for which the collision matrix becomes approximately diagonal is ~ 0.6. Neglecting E^Q, this gives the expected result that the activation energy is approximately E_{N+1}.

At first sight it might seem that (61) becomes unbounded in the limit $\alpha \to 1$, i.e., for small grain size. We can, however, prove that this expression is well-behaved in this limit.

Suppose that the grain size is made finer by dividing ΔE into ℓ sublevels; α will then depend on ℓ. Writing

$$\alpha(\ell) = e^{-\Delta E/\ell kT}$$

the first term in (61) then becomes

$$[\Delta E/\ell]\ \left[\, N + \frac{1 - 2\alpha(\ell)}{1 - \alpha(\ell)}\right]$$

Expanding the expression for α, we find that in the limit of large ℓ,

$$\frac{1 - 2\alpha(\ell)}{1 - \alpha(\ell)} \to \ell kT/\Delta E$$

when (61) becomes

$$N\,\Delta E - \langle E_g \rangle - \tfrac{5}{2}kT + E^Q \qquad \text{(II.62)}$$

If we calculate $\langle E_g \rangle$ from (38), then (61) becomes

$$E_{act}^{LP} = (N+1)\,\Delta E - \tfrac{3}{2}kT + E^Q \qquad \text{(II.63)}$$

which can also be obtained by simply substituting (57) into (28).

We may extend the model by assuming that the levels have degeneracy d_i, when (59) becomes

$$g_N^{(1)}/g_N^{(0)} = (N-1)\,(1+\alpha)/(N-1+N\alpha\,\frac{d_{N+1}}{d_N}) \qquad \text{(II.64)}$$

In such a model it is harder to establish a general connection between the activation energy and E_{N+1}. If we assume that the molecule consists of s degenerate oscillators, then from the well-known combinatorial formula,

$$d_i = (s+i-1)!/i!(s-1)!$$

If we substitute this into (64), and use the representative value of 0.5 for α, then $g_N^{(1)}/g_N^{(0)} > 0.9$ if $s < N/3$. Equation (57) is then still a fairly good approximation for g_i, and (42) is still valid.

This treatment is as far as we have been able to go in establishing a connection between the low pressure activation energy of unimolecular reactions and the energy of the first active level. The general expression for the low

pressure activation energy (46) will be studied numerically in Chapter IV.

Section 9. The High Pressure Rate Constant and Transition State Theory.

The relation between the microscopic rates K_{ii} contained in the expression for the high pressure rate constant (26) and transition state theory has been recently considered in detail by Mies (1969) in terms of his resonant scattering theory of unimolecular reactions. Our purpose in this section is to see under what conditions (26) reduces to the form of the well-known transition state equation (Glasstone, Laidler and Eyring 1941, p.190):

$$R^{HP} = \kappa \, (kT/h) \, (F_{\pm}/F) \, e^{-En/kT} \qquad (II.65)$$

Here κ is the transmission coefficient, $F_{\pm}$ and F are the partition functions of activated complex and reactant:

$$F = \sum_{\substack{\text{all energy} \\ \text{levels}}} e^{-E_i/kT}$$

F is of course the same as the denominator in (26).

Suppose that the wavefunctions of reactant and product are such that the wavefunction corresponding to motion along a special "reaction coordinate" (which is usually taken to be a single bond, but may generally be a combination of

coordinates in a curvilinear coordinate system) may be separated out of the total wavefunction of both reactant and product. The partition function for the remaining coordinates, which then factors out of the numerator in (26), is defined as $F_{\ddagger}$. The high pressure rate constant then becomes:

$$R^{HP} = (F_{\ddagger}/F)\sum K_{ii}\, e^{-E_i/kT} \qquad (II.66)$$

where the summation is over the energy levels of the reaction coordinate only.

If we further suppose that a particular microscopic rate K_{nn} is much greater than the microscopic rates of other kinetically accessible levels, so that the summation reduces to a single term, then (66) becomes (65) if we put

$$\kappa kT/h = K_{nn} \qquad (II.67)$$

Note that this implies a special temperature dependence for κ, as K_{nn} is temperature independent.

In general, however, it will not be the case that one single K_{ii} is much greater than the rest. If the principal terms in the numerator of (66) occur over a comparatively small energy range, than K_{nn} in (67) may be given the value of the average of the microscopic rates in this range; K_{nn} will then be a function of temperature. Under these conditions, the (discrete) reactant levels in this

energy range may formally be associated with an "activated complex", although the meaning of this term will then be rather different from that of the conventional definition (Glasstone, Laidler and Eyring 1941, p.185).

CHAPTER III.

THE HIGH PRESSURE RATE-CONSTANT.

Section 1. Introduction.

In the remaining chapters we have a twofold aim: to show that the theory of Chapters I and II offers a practical route to the calculation of actual laboratory rate constants, and to examine the physical implications produced by these numerical studies. We base our calculations on the thermal decomposition of N_2O, which we examine in some detail. We also apply some of the techniques which we develop to study this reaction to simple models representing other sorts of unimolecular decompositions.

Because of lack of knowledge of potential surfaces and wave functions, and because of computational limitations, we are forced to introduce approximations into our calculations. Like all previous "absolute" reaction rate calculations, some of the difficulties are overcome by introducing adjustable parameters into the calculations and so, not surprisingly, we are able to report results which are in fairly good agreement with experiment. In fact, as we have only one adjustable parameter, this work is rather unusual when compared with previous calculations on the thermal decomposition of nitrous oxide (Stearn and Eyring

1935, Gill and Laidler 1958, Wieder and Marcus 1962, Olschewski *et al* 1966) in that we do not obtain *exact* agreement with experiment; [some workers even obtained a "not unexpected" very good agreement with experiment with incorrect experimental results .(Stearn and Eyring 1935)]. We feel that this shortcoming on our part is made up by the physical insight gained into the unimolecular process.

Our first assumption is the validity of the Condon approximation (Chapter I Section 3). The high pressure rate constant may then be calculated from (I.4), (I.5) and (II.26):

$$K_{ii} = \frac{4\pi^2}{h} V_{rp}(R_c)\ \rho(E) \int \psi_i\ \psi_E\ dX \qquad \text{(III.1)}$$

$$R^{HP} = \sum b_i K_{ii} / \sum b_i \qquad \text{(III.2)}$$

The calculation requires the electronic perturbation V_{rp}, and the vibrational wave functions ψ_i and ψ_E of reactant and product, obtained from the respective electronic surfaces.

We estimated V_{rp} from spectroscopic data. Very little information is available on the product potential surface, and so we calculated ψ_i and ψ_E by assuming various functional forms for reactant and product potentials. The calculation of the Franck-Condon factors in (1) then occupied the bulk of the computation. The information obtained about the high pressure activation energy and its components (which, using the Condon approximation, are independent of the

electronic perturbation V_{rp}), and the behaviour of the microscopic rates K_{ii}, form the principal results of the calculations in this chapter.

Section 2. The Thermal Decomposition of Nitrous Oxide.

The thermal decomposition of N_2O:

$$N_2O \rightarrow N_2 + O\ (^3P) \qquad \text{(III.3)}$$

is particularly suited for our purposes. Together with CO_2 and CS_2, it is the smallest molecule whose rate constant has been studied over the full range from the high to the low pressure limit (Troe and Wagner 1967). The reaction has been investigated in a large excess of argon by a number of workers over a wide temperature range and using a variety of techniques (mainly shock tube methods) (Olschewski *et al* 1966, and references therein to earlier work, Gutman *et al* 1966, Drummond and Hiscock 1967). When side reactions and their exothermicity, and the non-ideality of the carrier gas are taken into account, the results of different workers are in quite good agreement (Troe and Wagner 1967).

The high pressure region (which at 2000°K is reached at about 50 atmospheres of Ar, requiring about 200 atmospheres of driver gas) has been studied only by Olschewski *et al* (1966), but their results with the same apparatus in the low

and intermediate pressure regions are consistent with those obtained by other workers (Troe and Wagner 1967). The low and intermediate pressure decomposition in argon has been studied by various workers between 1200°K and 3000°K, when the rate constant varies over 5 orders of magnitude.

It must however be borne in mind that shock tube measurements are notoriously prone to error. It has even been suggested (Drummond and Hiscock 1967) that because of side reactions, the temperature measurements of previous workers might be in error, which could have the effect of lowering the activation energy by up to 20 kcal/mole: however this claim is based on measurements undertaken with a relatively high - 6% - concentration of N_2O in Ar.

A further uncertainty is that the electronic state of the oxygen atom in the product has not been positively identified, because it immediately undergoes further reaction. It is assumed to be ^3P on energetic considerations alone.

Apart from the extensive experimental investigations, the principal attraction of the N_2O decomposition is the smallness of the molecule. Thus comparatively few coordinates are involved in the calculations; furthermore, *ab initio* calculation of electronic wave functions and potential surfaces is also feasible. Another advantage is that the reaction is spin forbidden, as the reactant is a singlet and the products are thought to be $N_2(^1\Sigma^+)$ and $O(^3P)$.

The perturbation may therefore be immediately identified with spin-orbit coupling.

In connection with the calculation of vibrational collision cross sections (Chapter IV), N_2O is isoelectronic with CO_2, and so the intermolecular potential functions of these molecules with argon are probably similar. We may thus make use of the methods of calculating cross sections which have been developed for CO_2.

The reaction has attracted theoretical interest since Wigner (1931) suggested that the anomolously low frequency factor could be explained if the reaction was spin forbidden. Calculations on the high pressure rate constant using semi-classical theories have been undertaken by Gill and Laidler (1958) and by Wieder and Marcus (1962). Quantum mechanical calculations, based on transition state theory, were undertaken by Stearn and Eyring (1935) and Olschewski *et al* (1966); their approaches will be compared with our own method in later sections.

Section 3. Electronic States of Reactant and Product.

Central to any rate theory is a knowledge of the potential surfaces of reactant and product. The ground state potential of N_2O is fairly well characterised experimentally (Suzuki 1969), but the position with the dissociative product

state is much less satisfactory.

The ground electronic state has symmetry $^1\Sigma^+$. From infra-red data extending 5000 cm^{-1} (14 kcal/mole) above the zero-point level, Suzuki has derived a complete quartic potential which accurately defines the ground state surface. A contour diagram of part of this potential (namely, for linear configurations of the molecule), extended to 90 kcal/mole, is shown in Figure 3. There is only a slight interaction between stretching and bending vibrations.

Very little information, either experimental or theoretical, is available on the dissociative state corresponding to the products. There is in fact experimental information on only two regions of the potential surface. Assuming that the products are N_2 ($^1\Sigma_g^+$) and O (^3P), the thermochemical dissociation energy of 38.6 kcal/mole, corrected for zero-point energies, establishes the limiting value for infinite N-O distance (there is, however, some uncertainty about this figure for the dissociation energy: see Kaufmann 1967). Information on a second point on the surface is obtainable from the ultra-violet spectrum. A very weak continuous absorption with a flat maximum at 35000 cm^{-1} (100 kcal/mole) is observed at a path length of 165 metre-atmospheres (Sponer and Bonner 1940); it is thought to record a transition to the particular dissociative excited state which produces the dissociation products, although the only evidence

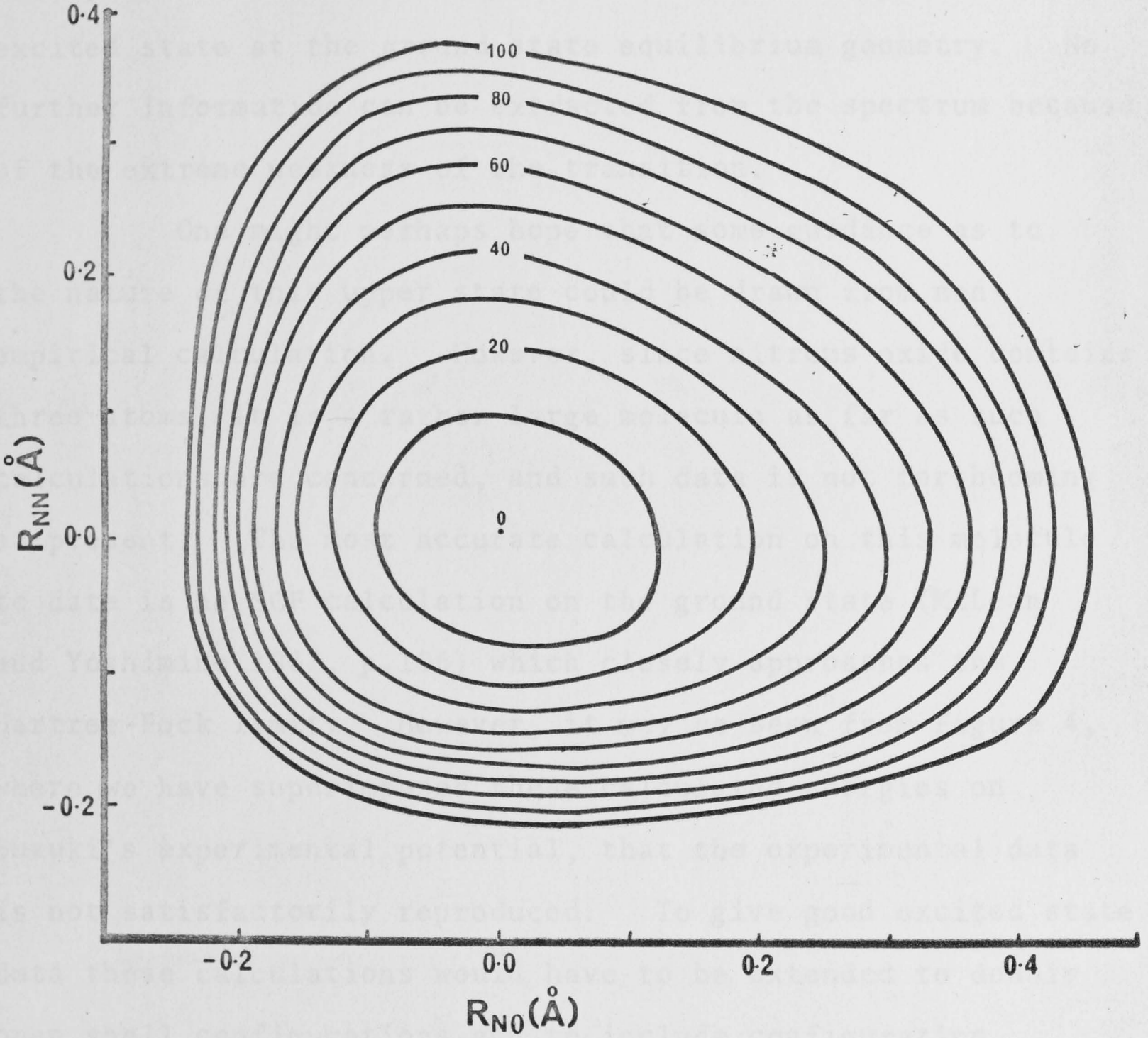

Figure 3.

The potential function for the ground electronic state of N_2O (linear configuration), from Suzuki. The coordinates are displacements from equilibrium; contours are in kcal/mole.

for this is provided by energetic arguments. If these assumptions are valid, this establishes the energy of the excited state at the ground state equilibrium geometry. No further information can be extracted from the spectrum because of the extreme weakness of the transition.

One might perhaps hope that some guidance as to the nature of this upper state could be drawn from non-empirical calculation. However, since nitrous oxide contains three atoms, it is a rather large molecule as far as such calculations are concerned, and such data is not forthcoming at present. The most accurate calculation on this molecule to date is an SCF calculation on the ground state (McLean and Yoshimine 1967, p.196) which closely approaches the Hartree-Fock limit. However, it may be seen from Figure 4, where we have superimposed these calculated energies on Suzuki's experimental potential, that the experimental data is not satisfactorily reproduced. To give good excited state data these calculations would have to be extended to doubly open shell configurations and to include configuration interaction. This inadequacy of accurate single configuration calculations indicates that semi-empirical methods would not reproduce meaningful results.

Peyerimhoff and Buenker (1968) have reported a calculation which includes CI but is restricted in terms of self-consistency and basis set (their calculated equilibrium

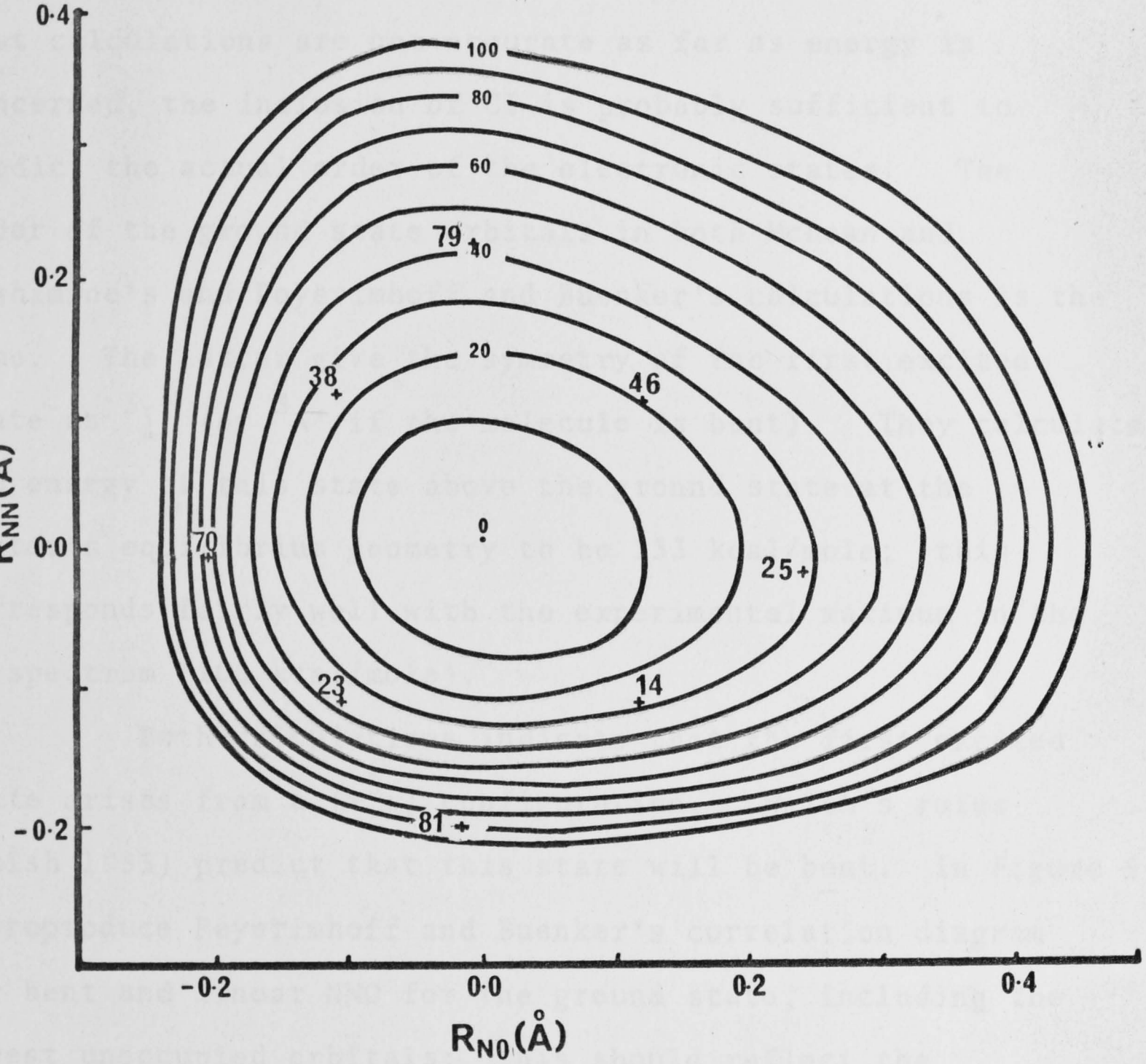

Figure 4.

The experimental NNO ground state potential function of figure 3,with the calculated energies of McLean and Yoshimine superimposed. We take the calculated zero of energy to be at the experimental ground state equilibrium geometry. Energies are in kcal/mole.

ground state energy is 44 kcal/mole greater than McLean and Yoshimine's single configuration energy). Although these last calculations are not accurate as far as energy is concerned, the inclusion of CI is probably sufficient to predict the actual order of the electronic states. The order of the ground state orbitals in both McLean and Yoshimine's and Peyerimhoff and Buenker's calculations is the same. The latter give the symmetry of the first excited state as $^3\Sigma^+$ (or $^3A'$ if the molecule is bent). They calculate the energy of this state above the gronnd state at the latter's equilibrium geometry to be 133 kcal/mole; this corresponds fairly well with the experimental maximum in the UV spectrum (100 kcal/mole).

Both calculations indicate that the first excited state arises from a $(\pi^3\pi)$ configuration. Walsh's rules (Walsh 1953) predict that this state will be bent. In Figure 5 we reproduce Peyerimhoff and Buenker's correlation diagram for bent and linear NNO for the ground state, including the lowest unoccupied orbitals; this should reflect the geometry of the excited state.

The Potential Functions.

Because of the almost total lack of knowledge of the form of the product potential function, we have assumed various analytic forms, based on an inverse exponential function of the NO bond distance. The parameters in these

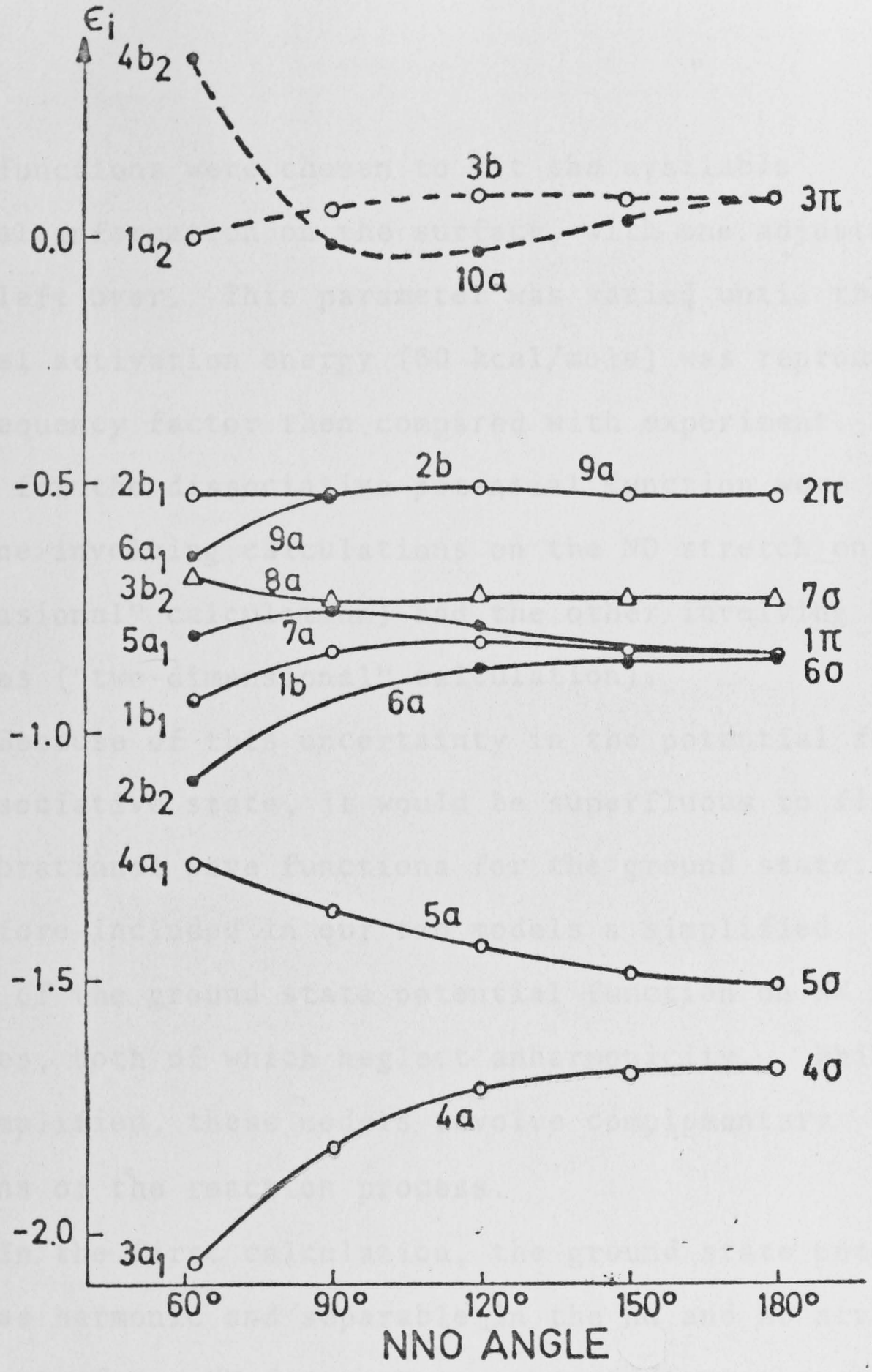

Figure 5.
(From Peyerimhoff and Buenker) : orbital energies ϵ_i in hartrees, for the ground state of NNO, as a function of internuclear angle.
Solid lines: occupied orbitals.
Broken lines: unoccupied orbitals.

potential functions were chosen to fit the available experimental information on the surface, with one adjustable parameter left over. This parameter was varied until the experimental activation energy (60 kcal/mole) was reproduced, and the frequency factor then compared with experiment. Two models for the dissociative potential function were adopted, one involving calculations on the NO stretch only ("one-dimensional" calculation) and the other involving NO and NN stretches ("two-dimensional" calculation).

Because of this uncertainty in the potential function of the dissociative state, it would be superfluous to find precise vibrational wave functions for the ground state. We have therefore included in our two models a simplified dependence of the ground state potential function on NN and NO stretches, both of which neglect anharmonicity. While grossly simplified, these models involve complementary descriptions of the reaction process.

In the first calculation, the ground state potential was taken as harmonic and separable in the NN and NO stretching coordinates, and the NN frequency was assumed not changed in the upper state. In the second calculation, the ground state was taken as harmonic and separable in the linear normal coordinates of the infra-red fundamentals, which are mixtures of the NN and NO stretches. This model can be regarded as a precursor to the theory of reactions in which the reaction

path is not describable in terms of a single coordinate, i.e., reactions in which the classical reaction path goes round a corner. If the upper state is in fact bent, the present reaction would necessarily be of this kind.

We may devise some straightforward extensions of these two basic models, such as the introduction of anharmonicity or the inclusion of bending modes. However, no new principles would be involved in such extensions, and in view of the uncertainty in the upper state potential, they are deemed unnecessary at this stage.

We must admit that our surfaces are in fact less sophisticated than those used by Stearn and Eyring (1935) and Olschewski *et al* (1966). However these authors calculated the transition probability only at the crossing point, using the Landau-Zener WKB expression (Landau 1932, Zener 1932). It is an essential part of our treatment that transitions above and below the crossing point be included, and in the succeeding sections we demonstrate that it is inadequate to assume that reaction occurs only at the crossing point. Furthermore, recent calculations by Murrell and Taylor (1969) show that the simple Landau-Zener formula is quite inaccurate.

In our calculations, we have assumed that the dissociative state is linear. In the high pressure region we neglect bending modes entirely, thereby considerably reducing the computational labor. Although the assumption of linearity

is probably incorrect, we feel that the inclusion of bending would not change the order of magnitude of our results, and in view of the uncertainty in the dependence of the product potential on the NO and NN stretches, its inclusion at this stage does not warrant the large increase in computing time.

If we assume that the dissociative state is linear, then the symmetry of this state is mainly important in determining the magnitude of the spin-orbit coupling, λ. This could be as high as 100 cm^{-1} [cf. 106 cm^{-1} for the coupling between $O(^3P)$ and (^1D) (Condon 1934), which are the oxygen states correlating with $N_2O(^3\Sigma^+)$ and $(^1\Sigma^+)$, or 70 cm^{-1} between $NO(^4\Sigma^-)$ and $(^2\Pi)$ (Lefebvre-Brion and Guerin 1968), which correlate with $N_2O(^1\Sigma^-)$ and $(^3\Sigma^+)$]. If the first excited state were linear $^3\Sigma^+$, then from symmetry considerations a value as low as 1 cm^{-1} for λ would not be impossible. The spin-orbit coupling operator transforms according to the same irreducible representation as a rotation and hence a $^3\Sigma^+$ state cannot couple directly to $^1\Sigma^+$. Coupling can however take place if the molecule is bent, or, if it is linear, by rotation. If, on the other hand, the dissociative state were $^3\Sigma^-$ or $^3\Pi$, as suggested by Sponer and Bonner (1940) and Zelikoff *et al* (1953), then the coupling is directly allowed.

As we assume that λ is independent of configuration (Condon approximation), it is not evaluated here. In our formalism it appears only as a multiplicative factor in the

expression for the rate constant R^{HP}, and the results are therefore reported as R^{HP}/λ; the activation energy is independent of λ.

By assuming that the bending mode is unchanged in going from reactant to product, and is separable from the two stretching vibrations, the partition function for this coordinate cancels out of the numerator and denominator in (1). However, the lowest energy state of the product, i.e., separated N_2 and O, has no bending mode, and thus the product potential must be such that the bending mode disappears at infinite NO distance. This implies the non-separability of bending and stretching modes. Thus in order that we may neglect the bending mode when calculating the Franck-Condon factors in (2), the potential function of the product must be such that the bending mode is independent of the NO stretch in the region where the Franck-Condon factors are appreciable (approximately the region of the crossing point), and it is only beyond this region that the part of the potential dependent on the bending mode goes to zero as the NO distance becomes large.

In calculating the Franck-Condon factors, no allowance was made for rotation. In principle, the potential energy surface should be re-established for each value of the rotational quantum number J, i.e., in the simplest approximation by including a term $\frac{1}{2}\hbar^2 J(J+1)/I$ in the vibrational Schrödinger

equation, where I, the moment of inertia, is a function of the nuclear coordinates, and the rates for each J then compounded as a Boltzmann-weighted average. Predissociation by rotation (i.e., dissociation without change in electronic state, brought about by the $\frac{1}{2}\hbar^2 J(J+1)/I$ term in the vibrational potential function) will not be of concern in the present case, as this would occur at energies near the dissociation energy of the ground state, which is much greater than the experimental activation energy. On the other hand, the effect of including rotational wave functions in the Franck-Condon factor between ground and excited states cannot be easily dismissed. Apart from other considerations, the spin-orbit coupling between $^3\Sigma^+$ and $^1\Sigma^+$ may be effected by rotation. Furthermore the effect of the $J(J+1)/I$ term in the effective potential may be observed experimentally in predissociations akin to that taking place in N_2O (Herzberg 1950, p.430). For the present, we simply hope that such effects are small. If we can agree to ignore them, the only consequence of the inclusion of rotational states will be to introduce into (1) a ratio of rotational partition functions of much the same kind as that appearing in transition state theory. In the latter theory, for rigid rotors this ratio reduces to $I^{\ddagger}/I_o$, the ratio of moments of inertia of the "transition state" and zero-point level respectively. From the discussion in Chapter II, section 9, in the present

formulation this ratio becomes approximately I_a/I_o, where I_a is the moment of inertia averaged over vibrational wave functions for active levels, i.e., levels where K_{ii} is large. For N_2O, even allowing for anharmonicity, this ratio will be quite close to unity, and any attempt to refine this figure would at present be pointless. For a recent transition state treatment of rotation, see Forst (1968); much of his work would be applicable to a treatment of rotation using the present method.

Section 4. One Dimensional Model.

In this model we assume that the ground state potential is harmonic and separable in the NN and NO stretching coordinates. The NN frequency is assumed to be the same in the upper and lower states; as a result the partition function for this coordinate cancels out of (1). Thus the Franck-Condon factors involve only the NO displacement. The ground state potential is given the form:

$$U''(R_{NO}) = \tfrac{1}{2} k_{NO} R_{NO}^2 \qquad \text{(III.4)}$$

where R_{NO} is the displacement from the observed equilibrium bond length. The bond length and the force constant we obtained from the infra-red spectrum assuming a diagonal force field, namely 1.18Å and 13.7 mdyn/Å respectively (Penny and

Sutherland 1938).

The wave functions corrssponding to (4) are simple harmonic oscillator wave functions. For the reduced mass of this vibration, we chose a value of 7.47 amu, corresponding to that of the atom pair NO. This gives a vibrational frequency of 1759 cm^{-1}, approximately halfway between the in-phase and out-of-phase stretching frequencies of N_2O (1285 and 2224 cm^{-1}).

The product potential function was assumed to have an inverse exponential dependence on the NO distance:

$$U'(R_{NO}) = D_e + Be^{-cR_{NO}} \qquad \text{(III.5)}$$

D_e is the thermochemical dissociation energy, D_o, corrected for zero-point energies, and B was chosen to fit the weak maximum ($h\nu_{max}$) of the ultraviolet absorption spectrum when R_{NO} has the ground state equilibrium value. The remaining constant c can then be treated as an adjustable parameter, and varied until the calculated and experimental activation energies are in agreement at a selected temperature; the physical reasonableness of the calculation can then still be checked through a comparison of calculated and observed frequency factors, and of the temperature dependence of the activation energy.

In this model we assume that the NN and the doubly-degenerate stretching frequencies (ν_{NN} and ν_{bend}) are the same

in the ground and excited states. By considering the zero-point energies of reactant and product we have

$$D_e = D_o + 1/2\ h\nu_{NO} + h\nu_{bend} \qquad \text{(III.6)}$$

and similarly

$$B = h\nu_{max} - D_e + 1/2\ h\nu_{NO} \qquad \text{(III.7)}$$

D_o is given the thermochemical value of 38.6 kcal/mole, and $h\nu_{max}$ is 100 kcal/mole. The crossing point occurs at $R_{NO} = R_C$ satisfying

$$1/2\ k_{NO}\ R_C^2 = D_e + B\ e^{-cR_{NO}} \qquad \text{(III.8)}$$

In Figures 6a and b, one and two dimensional representations of the reactant and product surfaces are given, the latter for comparison with Figure 3. The value of c used reproduces the experimental activation energy.

Section 5. The Wave Functions for an Exponential Potential.

The Schrödinger equation for an exponential potential has been solved analytically (Jackson and Mott 1932). The solution is a Bessel function of the second kind of imaginary order, $K_{iq}(z)$, where

Figure 6.

Reactant and product potential functions of N_2O in the one-dimensional model.

(a) 1-dimensional representation
(b) 2-dimensional representation, constructed by assuming an NN force constant of 14.6 mdyne/Å in both reactant and product.

Energies are in kcal/mole, coordinates are displacements from the ground state equilibrium position.

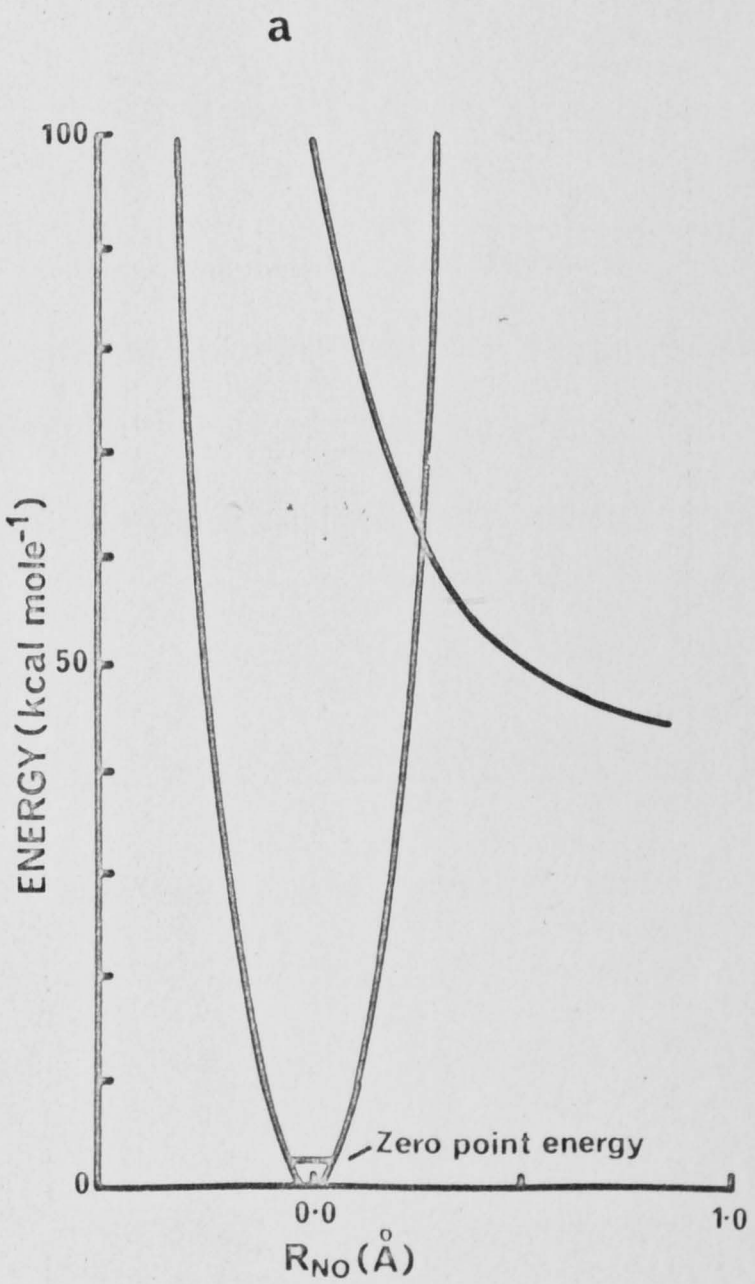

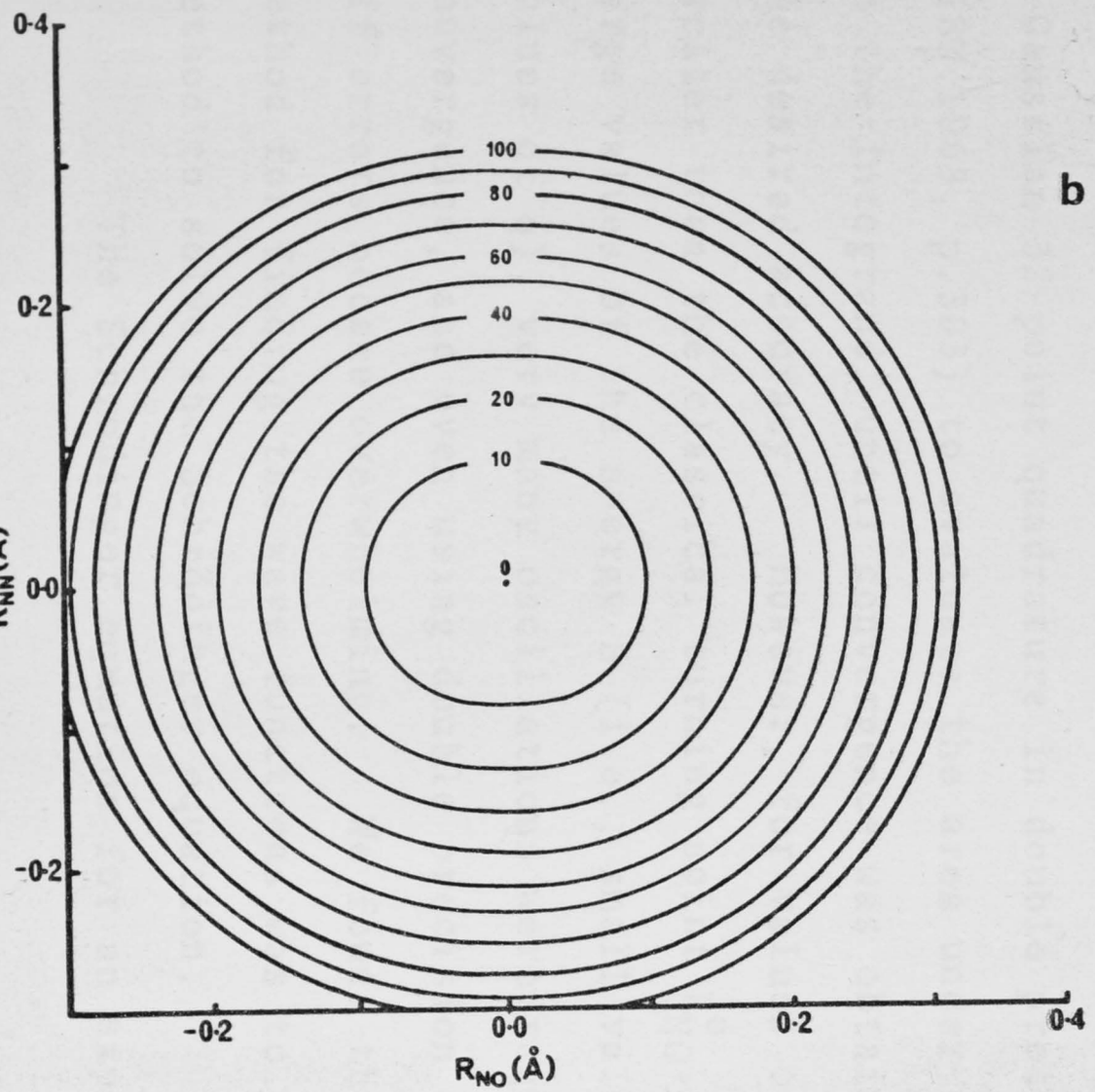
0·4
0·2
0·0
-0·2
R_{NN} (Å)
100
80
60
40
20
10
-0·2
0·0
0·2
0·4
R_{NO} (Å)

b

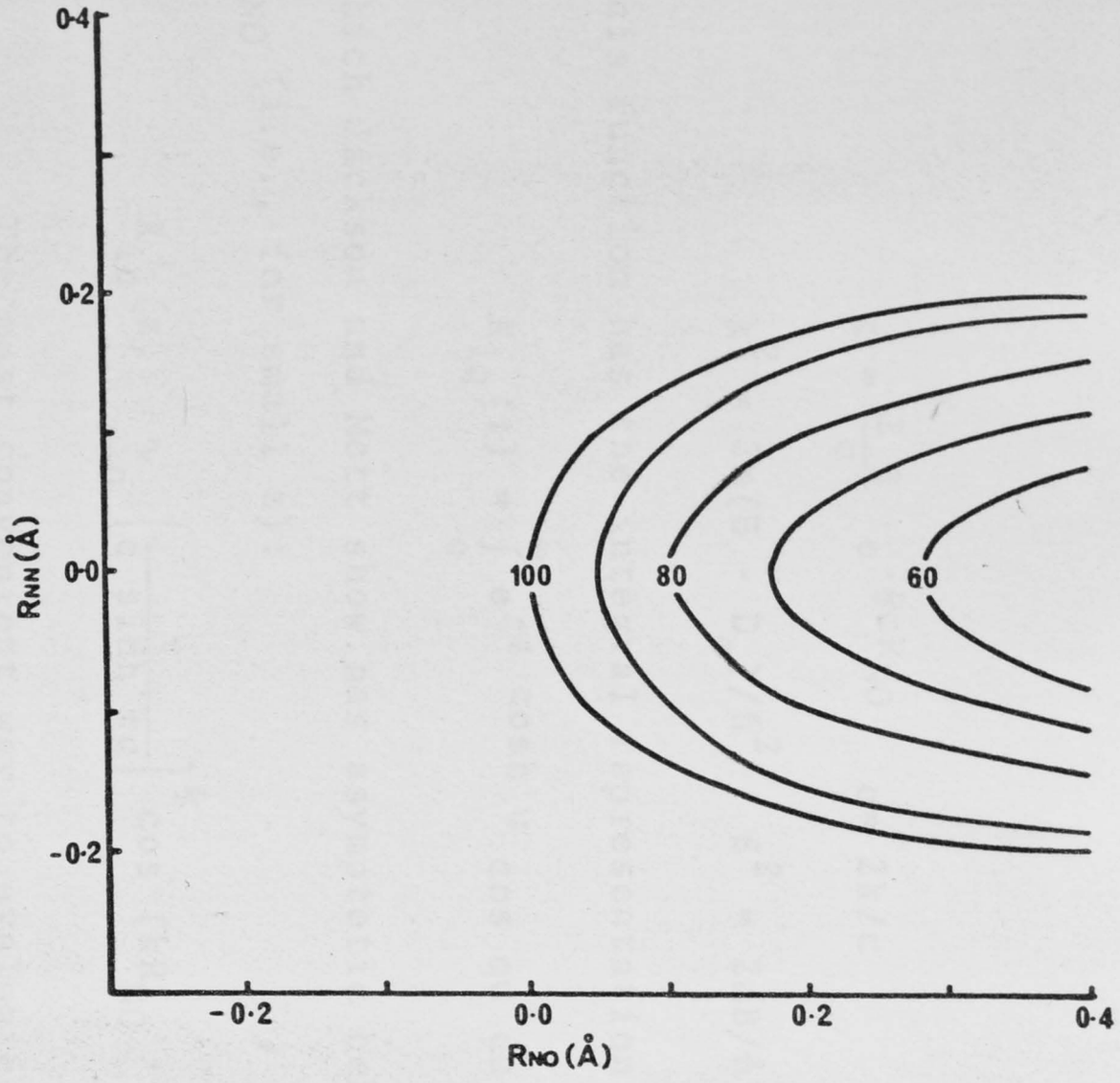
0·4
0·2
0·0
-0·2
R_{NN} (Å)
100
80
60
-0·2
0·0
0·2
0·4
R_{NO} (Å)

$$z = \frac{2\beta}{c} e^{-\frac{1}{2}cR_{NO}} \qquad q = 2k/c$$

$$k^2 = 2m(E - D_e)/\hbar^2 \qquad \beta^2 = 2mB/\hbar^2 \tag{III.9}$$

This function has the integral representation

$$K_{iq}(z) = \int_0^\infty e^{-z \cosh u} \cos qu \, du \tag{III. 10}$$

which Jackson and Mott show has asymptotic behaviour for large R_{NO} (i.e., for small z):

$$K_{iq}(z) \underset{z\to 0}{\sim} \left\{\frac{\pi}{q \sinh \pi q}\right\}^{\frac{1}{2}} \cos (kR_{NO} + \text{const}) \tag{III.11}$$

The most convenient way to evaluate K_{iq} is the integral representation (10). This was done numerically, using a Gaussian 32-point quadrature in double precision arithmetic (IBM 1968, p.303) to evaluate the area under each oscillation in the integrand, until convergence was obtained to within the desired accuracy. However, for values of R_{NO} much greater than the classical turning point R^o_{NO}, and also for large values of the energy E (i.e., small values of z and large values of q), very many oscillations were required for adequate convergence, and even using double precision arithmetic, round-off errors became overwhelming. We found that a preferable method for finding the wave functions was to use a numerical method to solve the Schrödinger equation.

The Schrödinger equation for an exponential potential:

$$\left(\frac{-\hbar^2}{2m}\frac{d^2}{dR_{NO}^2} + D_e + B\, e^{-cR_{NO}} - E\right)\psi = 0 \qquad \text{(III.12)}$$

is converted to two coupled first-order equations by the substitution:

$$\Psi_1 = \psi, \quad \Psi_2 = d\psi/dR_{NO} \qquad \text{(III.13)}$$

when (12) becomes

$$d\Psi_1/dR_{NO} = \Psi_2$$

$$d\Psi_2/dR_{NO} = \frac{2m}{\hbar^2}\left(D_e + B\, e^{-cR_{NO}} - E\right)\Psi_1 \qquad \text{(III.14)}$$

which may be solved using standard methods; the most suitable for this problem is Hamming's predictor-corrector technique (IBM 1968, p.343). This method requires initial values of Ψ_1 and Ψ_2 (the wave function and its slope) as input. These starting values may be found from the analytical solution (10), but again we experience convergence and roundoff difficulties for high energies, even in the classically forbidden region. A more convenient method for determining starting values is from the WKB solution of (12) in the classically forbidden region; this solution will be accurate provided we are sufficiently far from the classical turning point. The WKB solution which goes over to a sine wave of unit amplitude in the classically allowed region is

$$\psi = \tfrac{1}{2}\left[\frac{q^2}{z^2-q^2}\right]^{\frac{1}{4}} \exp -\{(z^2-q^2)^{\frac{1}{2}} + q \tan^{-1}\left[\frac{z^2-q^2}{q^2}\right]^{\frac{1}{2}}\} \qquad \text{(III.15)}$$

$$\frac{d\psi}{dR_{NO}} = \{\frac{1}{4c}\left[\frac{z^2}{z^2-q^2}\right] + (\tfrac{1}{4}z^2c^2 - k^2)^{\frac{1}{2}}\}\ \psi \qquad \text{(III.16)}$$

where the parameters z, q and k are defined in equation (9). The criterion we used for checking the accuracy of the numerical procedure was that the numerical wave function sufficiently far into the classically allowed region should be a sine wave with the amplitude dictated by the starting values of the solution in the classically forbidden region.

In Figure 7, we show some typical wave functions obtained by this method. Note the significant extension of the wave function beyond the classical turning point.

The evaluation of the microscopic rates K_{ii} from these reactant and product wave functions requires that the continuum product wave functions ψ_E be normalised to a delta-function with respect to energy (Chapter I, section 4):

$$\int \psi_E \psi_{E'}\, dR_{NO} = \delta(E-E') \qquad \text{(III.17)}$$

The continuum wave functions which asymptotically approach a sine wave of unit amplitude may be so normalised by multiplying by a factor

$$(\hbar\pi)^{-\frac{1}{2}}\ [\ 2m/E\ ]^{\frac{1}{4}}$$

(Buckingham 1961, p.160)

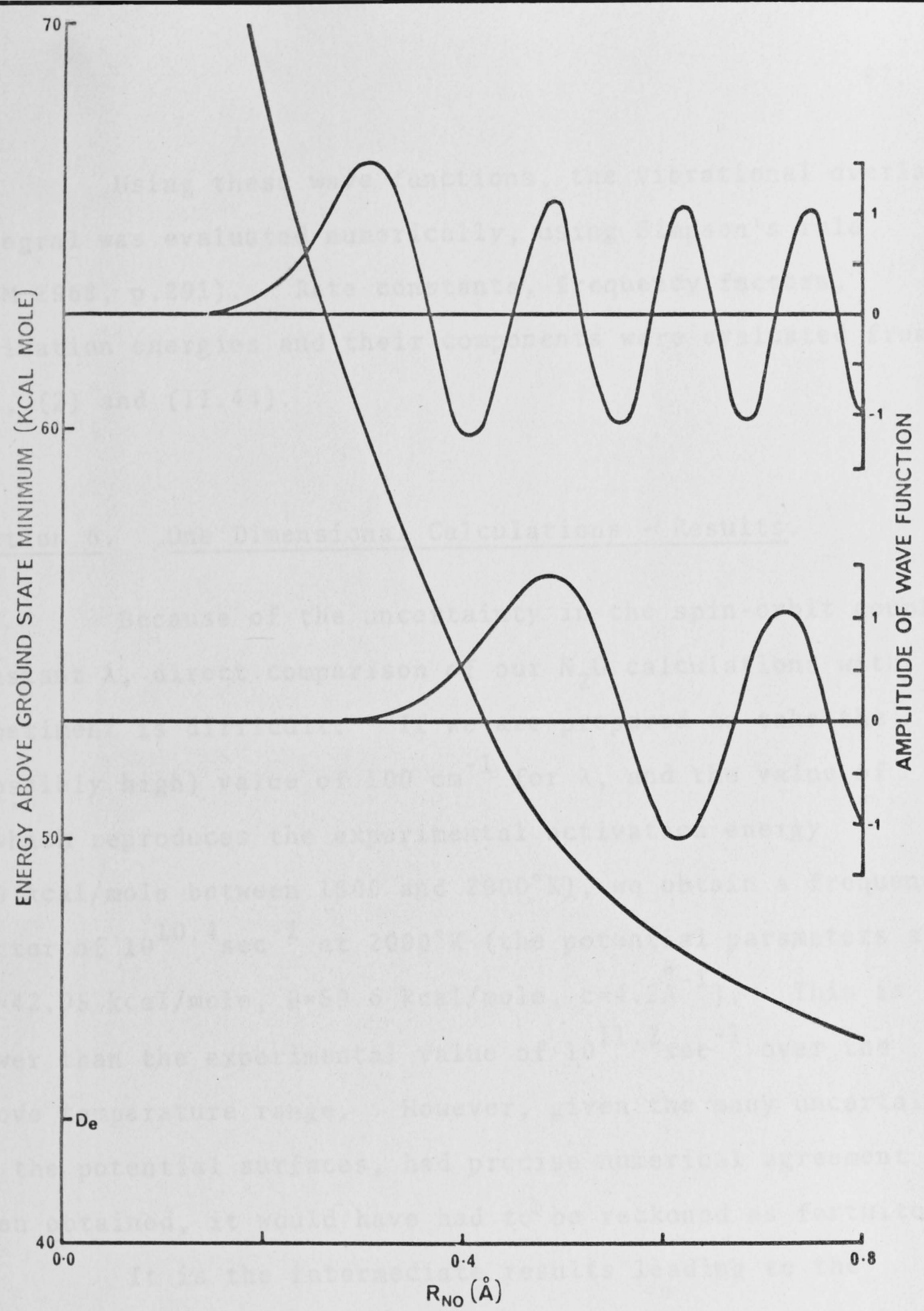

Figure 7.

Wave functions for an exponential potential, normalised to a sine wave of unit amplitude in the asymptotic region. The dissociative potential function is the same as in figure 6. The abscissa is displacement from the NO equilibrium configuration.

Using these wave functions, the vibrational overlap integral was evaluated numerically, using Simpson's rule (IBM 1968, p.291). Rate constants, frequency factors, activation energies and their components were evaluated from (1), (2) and (II.44).

Section 6. One Dimensional Calculations - Results.

Because of the uncertainty in the spin-orbit coupling constant λ, direct comparison of our N_2O calculations with experiment is difficult. If we are prepared to take the (possibly high) value of 100 cm^{-1} for λ, and the value of c which reproduces the experimental activation energy (60 kcal/mole between 1500 and 2000°K), we obtain a frequency factor of $10^{10.4} sec^{-1}$ at 2000°K (the potential parameters are D_e=42.95 kcal/mole, B=59.6 kcal/mole, c=4.2$\mathring{A}^{-1}$). This is lower than the experimental value of $10^{11.2} sec^{-1}$ over the above temperature range. However, given the many uncertainties in the potential surfaces, had precise numerical agreement been obtained, it would have had to be reckoned as fortuitous.

It is the intermediate results leading to the frequency factor which we regard as the useful part of the calculations. In Figure 8 we plot, as functions of energy, the microscopic rates K_{ii} (or rather, the ratio of K_{ii} to the spin-orbit coupling, λ, which is what we actually calculate),

Figure 8. Potential energy surfaces for N_2O (one-dimensional calculation) and derived quantities related to the high pressure rate constant, R^{HP}.

(a) Reactant and product potentials. The dissociative potential goes asymptotically to D_e, and the actual potential function is

$$U'(R_{NO}) \text{ (kcal/mole)} = 42.95 + 59.6 \exp(-4.2\ R_{NO}[\mathring{A}]).$$

This reproduces the experimental activation energy.

(b) Microscopic rates, expressed as K_{ii}/λ, where λ is the spin-orbit coupling in cm^{-1}, plotted on a logarithmic scale.

(c) Franck-Condon integrals between the bound state wave function and the equi-energetic continuum wave function (in atomic units).

(d) Boltzmann-weighted microscopic rates $K_{ii}\exp(-E_i/kT)$ at 2000°K (arbitrary linear scale).

(e) The values of E_{act} and $\langle EK\rangle/\langle K\rangle$ at 2000°K, and D_e.

Calculated rate constants (R^{HP}), activation energies and components ($E_{act} = \langle EK\rangle/\langle K\rangle - \langle E\rangle$) and frequency factors.

T °K	R^{HP}/λ $sec^{-1}cm$	$\langle EK\rangle/\langle K\rangle$	$\langle E\rangle$ kcal/mole	E_{act}	(freq.factor)/λ $sec^{-1}cm$
500	3.1×10^{-18}	58.6	2.5	56.1	1.0×10^{7}
1000	1.5×10^{-5}	62.8	3.0	59.8	1.8×10^{8}
2000	5.9×10^{1}	64.9	4.5	60.4	2.4×10^{8}
4000	1.1×10^{5}	66.1	8.2	57.9	1.5×10^{8}

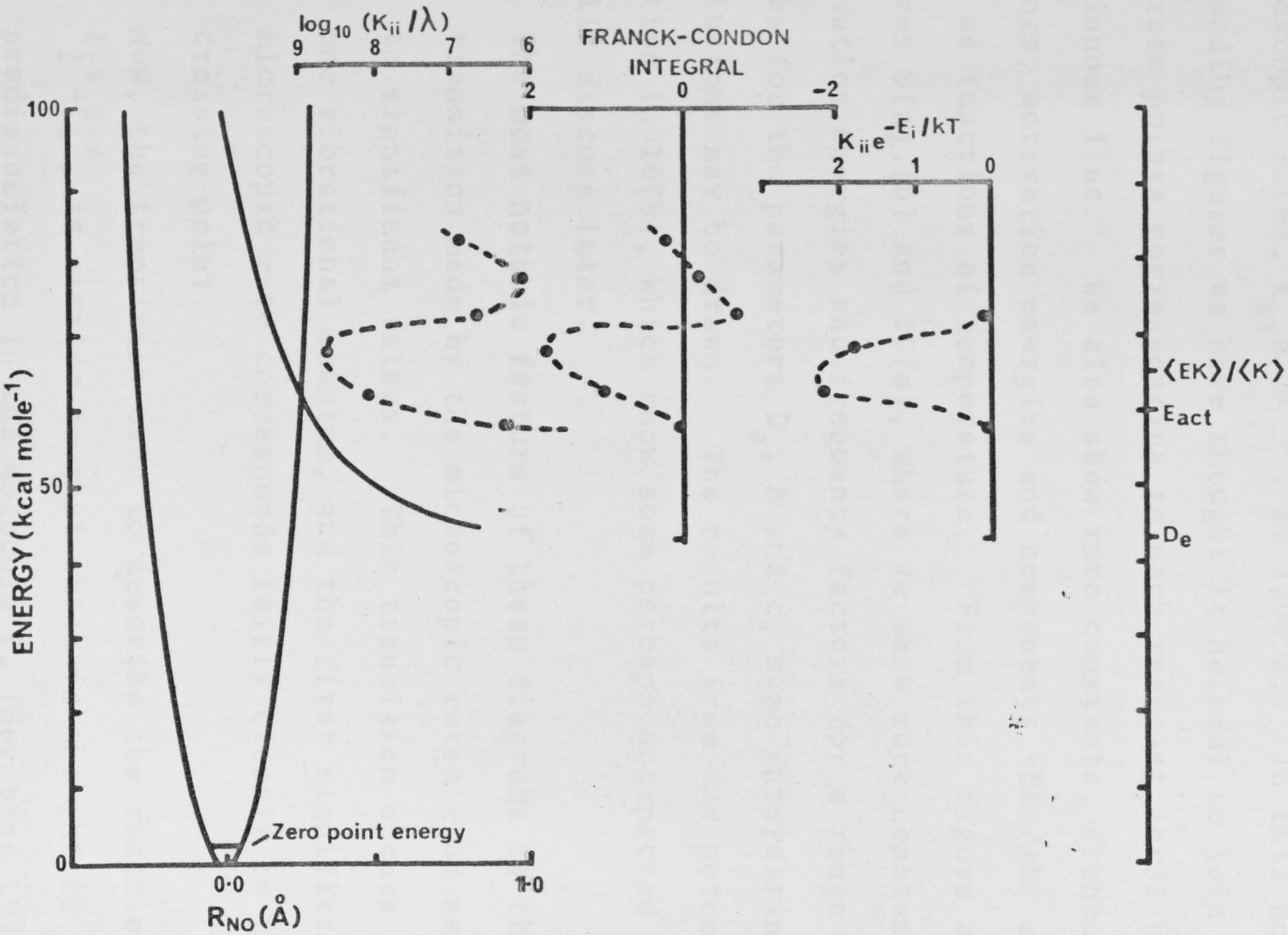
a
b
c
d
e
log10 (Kii /λ)
9
8
7
6
FRANCK-CONDON INTEGRAL
2
0
−2
Kii e−Ei /kT
2
1
0
100
50
0
ENERGY (kcal mole−1)
Zero point energy
0·0
1·0
RNO (Å)
⟨EK⟩/⟨K⟩
Eact
De

the Franck-Condon integral and the Boltzmann-weighted microscopic rates, $K_{ii}e^{-E_i/kT}$, at 2000°K. In this and in the succeeding figures we have thought it helpful to join the discrete points corresponding to each reactant level by a continuous line. We also show rate constants, frequency factors, activation energies and components <EK>/<K> and <E>, as functions of temperature. From this figure and from Figures 9(a),(b) and 10(a), where we show rate constants, activation energies and frequency factors for a range of values for the parameters D_e, B and c, some interesting conclusions may be drawn. The results from the potential function in 10(b), which show some perhaps unexpected features, we will discuss later.

(i) The most notable feature of these diagrams is the sharp transition made by the microscopic rates from negligible to significant values. This transition occurs over one vibrational quantum, and the first significant microscopic rate corresponds fairly closely to the crossing point.

Now, the transition used to describe the reaction, $^1\Sigma^+ \rightarrow {}^3\Sigma^+$, is similar to that which is thought to cause predissociation in the molecule P_2 (Herzberg 1932), namely $^1\Sigma_u^+ \rightarrow {}^3\Sigma_u^+$. Our calculated sudden onset of reaction is consistent with the sharp cutoff observed in the P_2 spectrum at the onset of predissociation.

Figure 9.

Potential functions and microscopic rates (as $\log_{10} K_{ii}/\lambda$) as a function of energy, illustrating unimolecular reactions which are the reverse of recombination reactions with low activation energies. The product potentials are

(a) $U'(R_{NO})$ (kcal/mole) = 42.2+59.6 exp(-10.5 R_{NO}[Å])

(b) $U'(R_{NO})$ (kcal/mole) = 40.0+4.0 exp(-3.36 R_{NO}[Å])

The reactant potentials are the same as in Figure 8. We also indicate <EK>/<K> and the activation energy at 4000°K, and D_e. λ is the spin-orbit coupling in cm^{-1}.

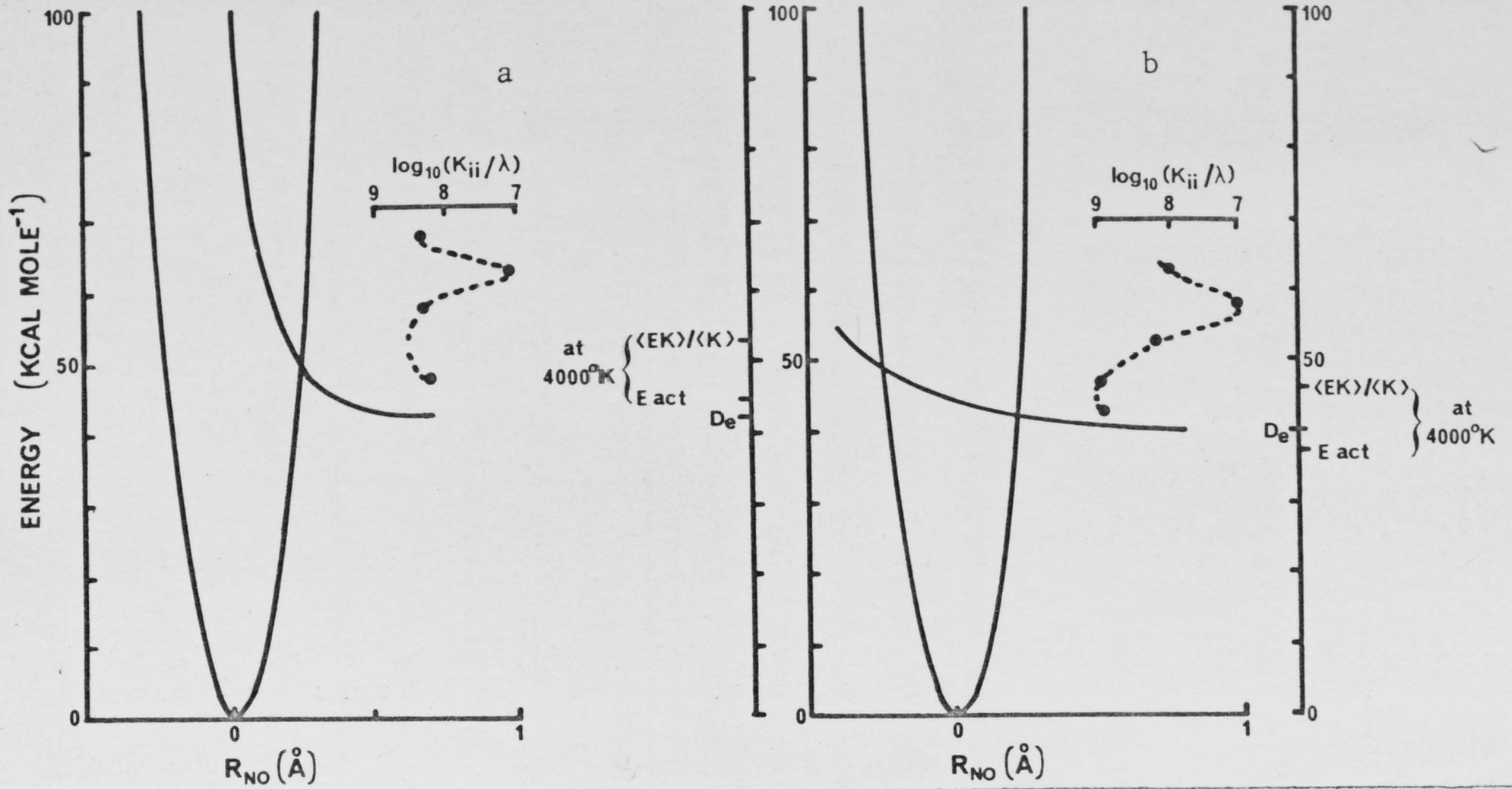

T °K	R^{HP}/λ $sec^{-1}cm$	⟨EK⟩/⟨K⟩ kcal/mole	⟨E⟩ kcal/mole	E_{act} kcal/mole	freq.factor/λ $sec^{-1}cm$
2000	$1x10^{3}$	54.4	4.5	49.9	$3.9x10^{8}$
4000	$7x10^{5}$	55.8	8.2	47.6	$2.6x10^{8}$

T °K	R^{HP}/λ $sec^{-1}cm$	⟨EK⟩/⟨K⟩ kcal/mole	⟨E⟩ kcal/mole	E_{act} kcal/mole	freq.factor/λ $sec^{-1}cm$
2000	$1x10^{4}$	44.2	4.5	39.7	$3.2x10^{8}$
4000	$2x10^{6}$	45.7	8.2	37.5	$2.2x10^{8}$

Figure 10.

Potential functions and microscopic rates (as $\log_{10} K_{ii}/\lambda$) as a function of energy, illustrating unimolecular exothermic decompositions. The product potential functions are:

(a) $U'(R_{NO})$ (kcal/mole) = $-30 + 100 \exp(-0.43\ R_{NO}[\mathring{A}])$

(b) $U'(R_{NO})$ (kcal/mole) = $-30 + 130 \exp(-2.1\ R_{NO}[\mathring{A}])$

The reactant potentials are the same as in Figure 8. The Boltzmann-weighted microscopic rates, $K_{ii} \exp(-E_i/kT)$, are plotted at 500°K and 1000°K; a different (arbitrary) scale is used for each temperature. We also indicate the activation energies at these temperatures, and D_e. λ is the spin-orbit coupling in cm^{-1}.

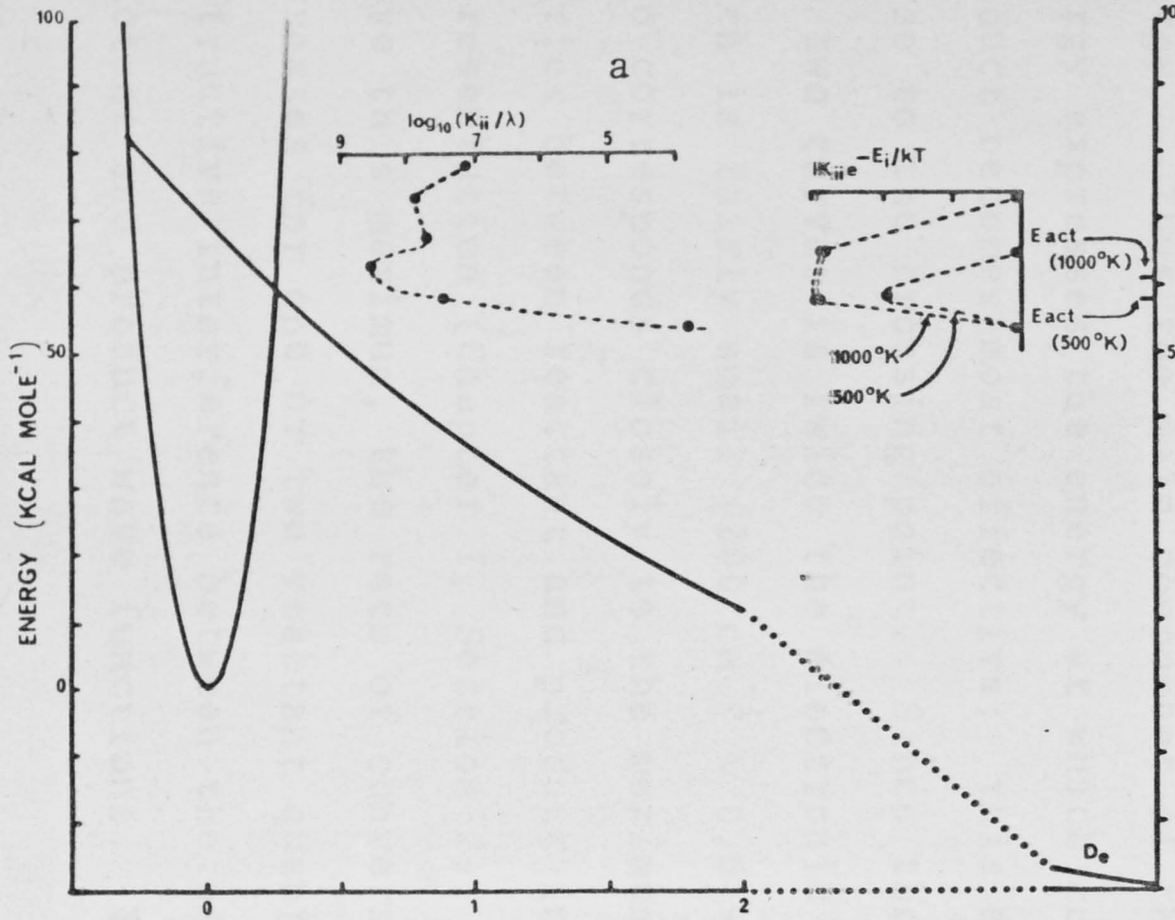

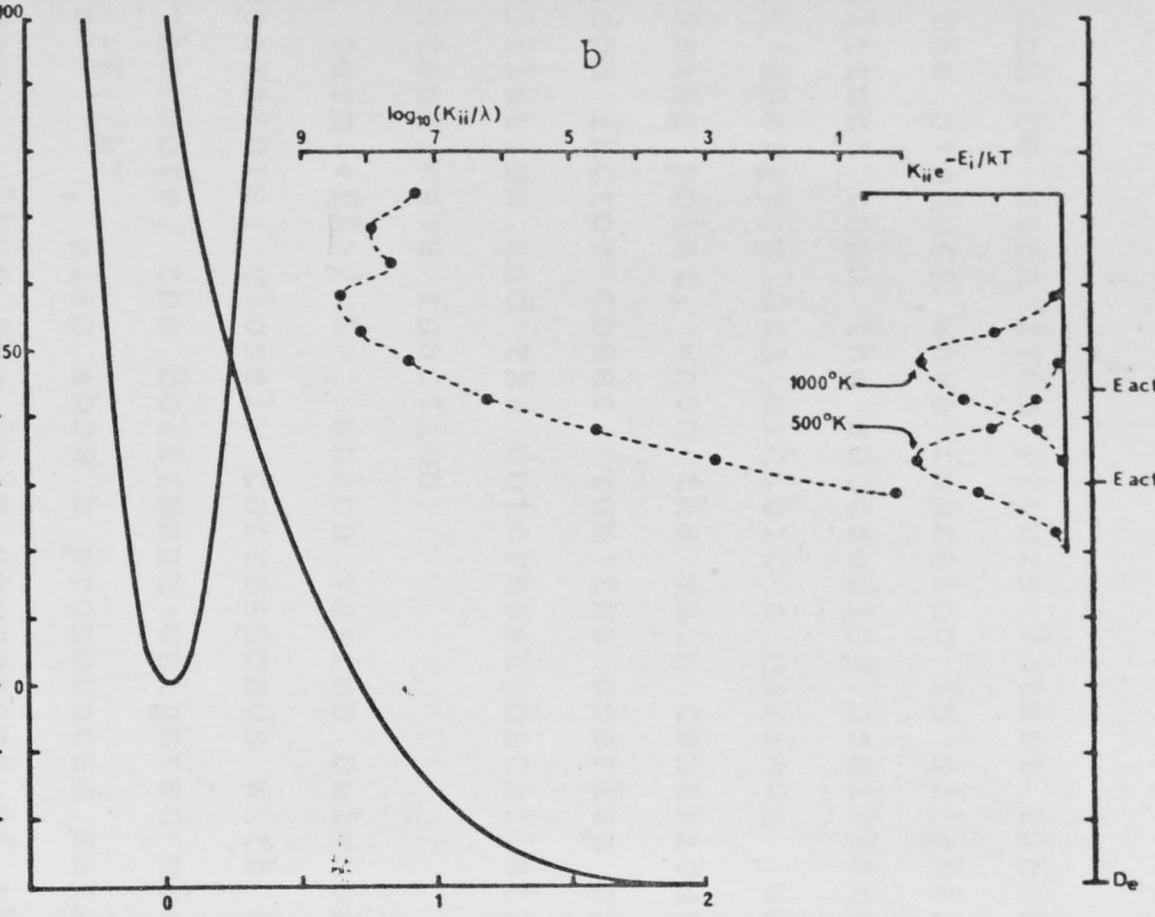

T °K	R^{HP}/λ $sec^{-1}cm$	<EK>/<K> kcal/mole	<E> kcal/mole	E_{act} kcal/mole	freq.factor/λ $sec^{-1}cm$
500	2×10^{-17}	58.0	2.5	55.5	3.7×10^{7}
1000	4×10^{-5}	60.4	3.0	57.4	1.5×10^{8}
2000	9×10^{1}	62.1	4.5	57.6	1.7×10^{8}

T °K	R^{HP}/λ $sec^{-1}cm$	<EK>/<K> kcal/mole	<E> kcal/mole	E_{act} kcal/mole	freq.factor/λ $sec^{-1}cm$
500	7×10^{-11}	32.9	2.5	30.4	1.2×10^{3}
1000	9×10^{-3}	46.5	3.0	43.5	2.9×10^{7}
2000	9×10^{3}	52.2	4.5	47.7	1.5×10^{8}

(ii) It can be seen from Figure 7 that the first oscillation of the product wave function is slightly greater in amplitude than the succeeding oscillations. Thus the rate/energy plots exhibit a maximum just above the crossing point, when the main contribution to the Franck-Condon factor comes from the overlap of this oscillation and the outermost oscillation of the reactant wave function.

(iii) The term <EK>/<K>, which varies only slightly with temperature, closely corresponds with this maximum. Furthermore, the Boltzmann-weighted microscopic rates, $K_{ii}e^{-E_i/kT}$, also show a pronounced maximum at this energy. Thus the main component of the activation energy expresses the energy at which conversion to product becomes most effective; this energy lies fairly close to the crossing point. Since the splitting between the two curves is twice the electronic perturbation, which is fairly small (200 cm^{-1} $\sim$ 0.6 kcal/mole), this also corresponds closely to the maximum of the potential barrier between reactant and product in the mixed representation (Chapter I, Section 2).

(iv) Above this maximum, the rate of conversion to product decreases for one or two reactant quanta, because of destructive interference between the oscillations of reactant and product wave functions. Thereafter the

microscopic rate increases again. Note that the sign of the Franck-Condon factor oscillates after the initial sharp rise. These trends have also been observed by Hougen and Lewis (1968).

(v) Although the term <EK>/<K> is not markedly temperature dependent, over a large temperature range - much greater than that observed experimentally - the activation energy varies significantly with temperature, because of the thermal energy term <E>. This term also causes the activation energy to lie *below* the crossing point.

In Figures 9 and 10 we show rate/energy plots for a variety of product potentials. The reactant potential is in each case the same as in Figure 8.

In 9(a) and (b) we have chosen values of B and c such that the crossing point lies only a few kcal/mole above D_e, the minimum energy for reaction. In 9(a), the dissociative potential rises steeply after the crossing point, while in 9(b), the rise is gradual and the product potential makes a second intersection with the reactant potential a few kcal/mole above the first crossing point. These two potentials are models for unimolecular decompositions which are the reverse of recombination reactions with very low activation energies, such as the recombination of methyl radicals. In (b), we have chosen the potential parameters so that <EK>/<K> is only slightly greater than D_e. At high temperatures, the

activation energy is actually slightly less than the minimum energy for dissociation, because of the <E> term.

In Figures 10(a) and (b) we show potentials where the zero of the product potential lies below that of reactant, corresponding to an exothermic unimolecular decomposition.

The behaviour of the rate/energy plots and the activation energy of the potential of Figure 10(b) is particularly interesting. Here we obtain results which are very different from the predictions of the semiclassical theories of Chapter I, Section 1, where reaction can only occur above the potential maximum separating reactant and product. As in the potentials of Figures 8 and 9, the maximum in the rate-energy plot lies at the crossing point. However, in Figure 10(b) the dissociative potential is such that the product wave functions extend significantly into the classically inaccessible region, and so there is considerable tunnelling to product below the crossing point. Therefore there is no sudden onset of reaction, as in the previous examples. In Figures 10(a) and (b) we have included a plot of the Boltzmann-weighted rates at 500° and 1000°K. In 10(b), where there is no sharp rise in the rate/energy plots, the maximum exhibited by the plot of the Boltzmann-weighted rates is strongly temperature dependent. At high temperatures the conversion to product takes place mainly at the crossing point, but at low temperatures transitions *below* the crossing point

dominate the reaction process. The maximum in the Boltzmann-weighted rate/energy plot at 500°K occurs 15 kcal/mole below that of the 1000°K plot. Thus at 500°K, the <EK>/<K> term, and hence the activation energy, lies considerably below the crossing point, but at higher temperatures the <EK>/<K> corresponds to the crossing point. For potentials exhibiting a sharp onset of reaction, such as the model for the N_2O decomposition (Figure 8) or the exothermic decomposition of Figure 10(a), this effect is not observed.

At low temperatures the reaction occurs principally from levels well below the crossing point, which have low microscopic rates. Hence the frequency factor at low temperatures is orders of magnitude lower than the "normal" frequency factor, observed at high temperatures.

This provides a possible explanation for the extremely low ($10^2 sec^{-1}$) frequency factor observed in the thermal unimolecular decomposition of formyl fluoride at 400°K (Fischer and Buchanan 1964):

$$HCOF \rightarrow CO + HF$$

This reaction is exothermic by 17 kcal/mole. The experimental investigations, however, are insufficient to establish beyond doubt the unimolecularity of the reaction.

Thus if a potential function similar to Figure 10 corresponds to an actual reaction, the activation energy and

frequency factor should show this distinctive temperature dependence. This would perhaps be rather difficult to observe experimentally, as a large temperature range is required, and side reactions might start to interfere at higher temperatures. The abnormally low frequency factor which should be observed at low temperature could possibly be explained by other factors. However, we will show in Chapter IV that the presence of significant microscopic rates below the crossing point is also manifested in a distinctive pressure dependence of the rate constant at a fixed temperature. If such a dependence were experimentally observed, it would furnish important evidence for specific quantum effects in kinetics.

We must, however, add a caveat to this result. The calculations are based on the validity of the Condon approximation: this matter was discussed in Chapter I. To this extent, the validity of our conclusions are still uncertain, though if the breakdown of the Condon approximation is important, there is little likelihood that the result would be to restore the comfortable simplicities of the transition state treatment of this class of reaction.

One of the limitations imposed in Chapter I on our choice of separated basis set was that the time required for dissociation of the energetic product state be much greater than the time constant for conversion from reactant to product

(Chapter I, Section 3, condition [iii]). Some idea of the dissociation time can be obtained by integrating the classical equations of motion for the dissociative potential, taking as initial conditions that the velocity of the particle representing the molecule is zero at the classical turning point, R^o_{NO}. We find that the time, t, required to reach a distance R_{NO} is then

$$t = \frac{1}{c} [m/(E-D_e)] \tanh^{-1}[1-e^{c(R^o_{NO}-R_{NO})}]^{1/2}$$

$$\simeq \frac{\ln 4}{c} [\tfrac{1}{2}m/(E-D_e)]^{1/2} + [\tfrac{1}{2}m/(E-D_e)]^{1/2}(R_{NO}-R^o_{NO}) \text{ for large } R_{NO}.$$

Using the appropriate potential parameters, it is found that, for a level of energy E with an appreciable rate of conversion to product, the time required to reach, say, 10Å is less than 10^{-13} sec. As the conversion rate is about 10^{11} sec^{-1}, the above condition is easily fulfilled.

Section 7. The "square-well" Approximation.

Although the computing time required to produce the data for the preceding section is quite small for a single set of parameters D_e, B and c (about 5 minutes on an IBM 360/50), we carried out many exploratory calculations. The slowest step in the computation is the generation of the continuum wave function, and we therefore searched for a quicker, if

more approximate, method than that used above. Although the WKB solution is quick to compute, it cannot be used near the classical turning point. We found that, for exploratory purposes, a time-saving approximation to the continuum wave function could be obtained by continuing the WKB solution from, say, 0.05Å before the classical turning point with a modification of the wave function for a particle in a one-sided square well. For a given energy E, the square well potential we used was:

$$U_E'(R_{NO}) = D_e \qquad [\ R_{NO} \geq R_{NO}^o(E)\ ]$$
$$= 1.5E \equiv U^{sq}(E) \quad [\ R_{NO} \leq R_{NO}^o(E)\ ] \qquad \text{(III.18)}$$

where R_{NO}^o is the classical turning point corresponding to E. We modify the simple square well wave function by giving the first oscillation a larger amplitude and wavelength than those of the rest of the oscillatory part, in accordance with Figure 7 (the actual figures chosen were 1.5 times the amplitude and 4 times the wavelength). The remaining constants in the approximate wave function were chosen such that this first oscillation joins smoothly onto the rest of the square well solution. The amount 1.5E in the potential function (18) is not critical. The WKB/square-well wave function is then very similar in appearance to the exact (numerical) wave function. The actual form of the approximate wave function,

normalised to a sine wave of unit amplitude, is

$$\left.\begin{aligned} \psi &= \text{WKB solution (eq. 15)} && R' < -0.05\text{Å} \\ &= 1.5 \sin(\theta)\, e^{\chi R'} && -0.05\text{Å} \leq R' < 0 \\ &= 1.5 \sin(\tfrac{1}{4}kR' + \theta) && 0 \leq R' \leq F \\ &= \sin(kR' + 4\theta - 3\pi) && R' > F \end{aligned}\right\} \qquad \text{(III.19)}$$

where $R' = R_{NO} - R_{NO}^{o}$ $\qquad \chi = [2m(U^{sq} - E)]^{\frac{1}{2}}/\hbar$

$\theta = \tan^{-1}(\tfrac{1}{4}k/\chi)$ $\qquad k = [2m(E - D_e)]^{\frac{1}{2}}/\hbar$

$F = 4(\pi - \theta)/k$

(F is where the initial oscillation meets the R' axis).

Using this approximation, the calculation is considerably quicker than using the exact numerical solution. For a wide range of potential parameters, we find that individual Franck-Condon factors are reproduced to within a factor of 2 or better relative to the exact solution, and that the overall rate constant, frequency factor and activation energy are hardly affected. In Table 2 we compare square well and exact microscopic rates, rate constants, frequency factors and activation energies, for the values of the potential parameters which reproduce the experimental activation energy.

Because of the accuracy and rapidity of this approximation, it was used to generate the dissociative wave function in the two-dimensional calculations (below), where the computations are much lengthier than in the one-dimensional

case. We feel that this approximation, or slight variations on it, might also prove useful for other forms of dissociative potential.

Table 2. Comparison of microscopic rates (K_{ii}), high pressure rate constants (R^{HP}), frequency factors and activation energies (E_{act}) calculated from exact (numerical) wave functions and from WKB/square well wave functions, for the potential functions of Fig. 8, at 2000°K (similar agreement is obtained at other temperatures). λ is the spin-orbit coupling (cm^{-1}).

	Exact wave functions	Square well wave functions
Energy of level i (kcal/mole)	K_{ii}/λ (sec^{-1} cm)	
47.8	1.5×10^{-2}	1.6×10^{-2}
52.8	2.6×10^{3}	2.7×10^{3}
57.8	3.1×10^{6}	3.2×10^{6}
62.9	1.7×10^{8}	1.4×10^{8}
67.9	4.7×10^{8}	3.4×10^{8}
72.9	6.9×10^{7}	3.6×10^{8}
77.9	1.3×10^{6}	1.1×10^{6}
83.0	1.0×10^{7}	1.2×10^{7}
	R^{HP}/λ ($sec^{-1}cm$)	
	5.9×10^{1}	5.0×10^{1}
	(frequency factor)/λ ($sec^{-1}cm$)	
	2.4×10^{8}	2.3×10^{8}
	E_{act} (kcal/mole)	
	60.4	61.0

A method commonly used for finding *relative* Franck-Condon factors between discrete levels and continua is the "δ-function" approximation (Coolidge *et al* 1936), which replaces the continuum wave function by a δ-function at the classical turning point. This cannot be used here, since the continuum wave function in this treatment cannot be correctly normalised, as in (17). Another approach, the Landau-Zener WKB formula (Landau 1932, Zener 1932), used by Stearn and Eyring (1935) and Olschewski *et al* (1966), is applicable only for transitions at the crossing point. Our own calculations show that transitions below the crossing can be most important for determining the overall rate constant. Furthermore, Murrell and Taylor (1969) have shown recently that Franck-Condon factors obtained from the Landau-Teller formula are quite inaccurate.

Section 8. The two-dimensional Model.

In this second model we specifically include the NN stretch in the calculations. The ground state potential is taken as harmonic and separable in the linear normal coordinates of the infra-red fundamentals, which are mixtures of the NN and NO stretches. The reactant is described in terms of a different coordinate system: its wave functions are assumed to be separable in the NN and NO stretches. As

we pointed out above, this model can be regarded as a precursor to calculations on reactions where the classical reaction path turns a corner.

The ground state potential is quadratic and separable in the normal coordinates for the out-of-phase and in-phase stretching modes, ξ_1 and ξ_3:

$$U''(\xi_1,\xi_3) = 1/2\ \lambda_1\xi_1^2 + 1/2\ \lambda_3\xi_3^2$$

The values of λ_1 and λ_3 are determined from the frequencies of the corresponding vibrations ($\lambda = 4\pi^2\nu^2$). The relation between (ξ_1,ξ_3) and the displacement coordinates (R_{NN},R_{NO}) is given by the inverse of Wilson's L-matrix (Wilson *et al* 1955, p.309). This matrix may be calculated from the values of the G and F matrices of NNO (Richardson and Wilson 1950). We obtain

$$\begin{pmatrix}\xi_1\\ \xi_3\end{pmatrix} = \begin{pmatrix}-2.71 & 1.13\\ 2.92 & 3.96\end{pmatrix} \times 10^{-12} \begin{pmatrix}R_{NN}\\ R_{NO}\end{pmatrix} \qquad \text{(III.20)}$$

where (ξ_1,ξ_3) are in cm $g^{1/2}$ and (R_{NN},R_{NO}) are in cm.

The potential function we adopt for the dissociative state is similar to that used in the one dimensional model, with the addition of an independent quadratic potential in the NN stretch:

$$U'(R_{NN},R_{NO}) = D_e + B\ e^{-cR_{NO}} + 1/2\ k'_{NN}(R_{NN}-R^o_{NN})^2 \qquad \text{(III.21)}$$

The parameters D_e, B and c were chosen as in the one dimensional calculation. For k'_{NN} we used the force constant of the ground state of the reaction product, N_2. The corresponding frequency we denote by ν_{NN}. R^o_{NN} is the N_2 equilibrium distance.

Contour diagrams for the ground and excited states are shown in Figure 11, for comparison with the experimental potential function (Figure 3) and the one-dimensional potential function (Figure 6).

Internal Conversion into a Degenerate Level.

An important feature of the two-dimensional model, which does not arise in the one-dimensional calculation, is degeneracy of the product states. If a level in the ground state has energy E, then the excited state level with the same energy has degeneracy v + 1, where v is the maximum integer such that

$$h\,\nu_{NN}\,(v + 1/2) < E - D_e$$

That is, a total excess energy of $E-D_e$ in the upper state may contain 0,1,...., v quanta of NN vibrational energy. The rate of conversion from the corresponding reactant state is then the sum of the conversion rates into all degenerate levels. The proof of this statement is an extension of the proof of the Golden Rule for the rate of conversion into a pure continuum state (Messiah 1964, p.732). Our proof is as follows.

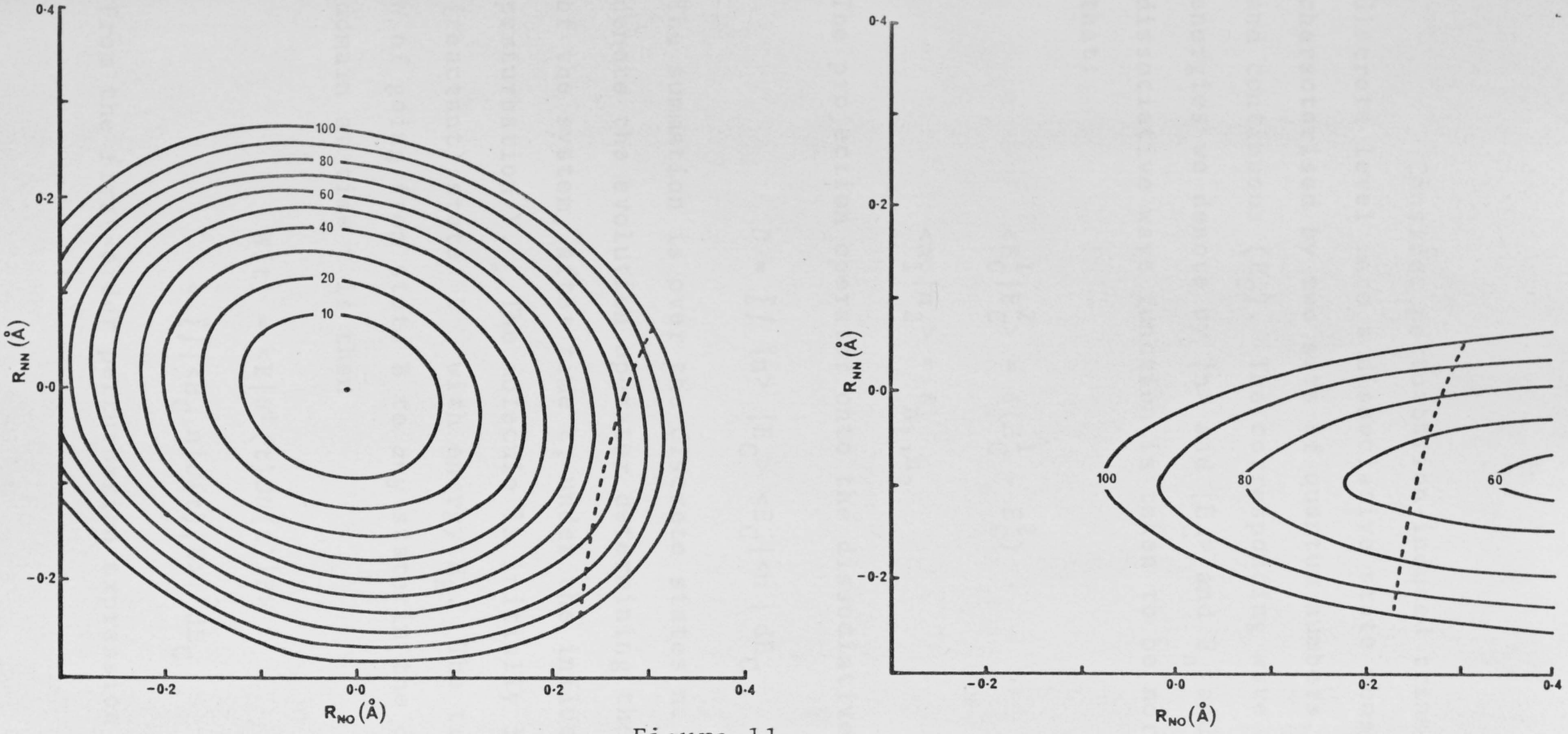

Figure 11.

Reactant and product potential contours for the two-dimensional model.The broken line indicates the line of intersection of the two potential surfaces.Energies are in kcal/mole,the coordinates are displacements from the ground state equilibrium.

Consider perturbation-induced transitions from a discrete level into a dissociative state whose energy is characterised by two sets of quantum numbers, discrete (n) and continuous (E_C). The corresponding wave functions and energies we denote by $|n\rangle$ and $|E_C\rangle$ and E_n and E_C. The dissociative wave function is taken to be normalised such that:

$$\langle E_C^1 | E_C^2 \rangle = \delta(E_C^1 - E_C^2)$$
$$\langle n_1 | n_2 \rangle = \delta_{n_1,n_2} \qquad \text{(III.22)}$$

The projection operator onto the dissociative state is then

$$\mathcal{O} = \sum\int |n\rangle |E_C\rangle \langle E_C| \langle n| \, dE_C \qquad \text{(III.23)}$$

The summation is over the discrete states n. Let U (t) denote the evolution operator determining the wave function of the system, after time t, under the influence of the perturbation V. The molecule is initially in a bound (reactant) state B , with energy E_B. The transition probability W of going from state B to *any* state in the dissociative domain at time t is then

$$W(t) = \langle B | U^\dagger(t) \mathcal{O} U(t) | B \rangle$$
$$= \sum\int |\langle E_C, n | U(t) | B \rangle|^2 dE_C \qquad \text{(III.24)}$$

From the first-order perturbation expression for the evolution

operator (Messiah 1964, p.372), (24) may be rewritten:

$$W(t) = \sum\int V_{B,nE_C} f(\omega)\, dE_C/\hbar^2 \qquad \text{(III.25)}$$

where V_{B,nE_C} is the perturbation matrix element

$$V_{B,nE_C} = \langle B|\ V\ |\ E_C,n\rangle \qquad \text{(III.26)}$$

and where

$$\omega = (E_B - E_n - E_C)/\hbar \qquad \text{(III.27)}$$

$$f(\omega) = 2(1 - \cos\ \omega\ t)/\omega^2 \qquad \text{(III.28)}$$

From (27), $d\omega = dE_C/\hbar$, and so

$$W(t) = V^2_{B,nE_C} f(\omega)\, d\omega/\hbar \qquad \text{(III.29)}$$

As $f(\omega)$ may be replaced by $2\pi t\ \delta(\omega)$ when the limits of the integral are extended to infinity,

$$W(t) = \frac{2\pi t}{\hbar} \sum_n V^2_{B,nE_C}(\omega=0) \qquad \text{(III.30)}$$

The transition probability W is proportional to time, as expected. The perturbation matrix element is evaluated at $\omega = 0$, i.e., when the total energy of the dissociative state is equal to that of the bound (reactant) state. The sum extends over all possible values of the discrete index n, which in our case is 0,1,....,v. This is the required result.

The Integration.

The ground state wave function in our two dimensional model is the product of the harmonic oscillator wave functions of the normal coordinates. Now, as the integration will be over the displacement coordinates (R_{NN},R_{NO}), the ground state wave function must be normalised to unity with respect to these coordinates. Thus these wave functions are conventionally normalised harmonic oscillator wave functions for the normal coordinates, multiplied by the Jacobi determinant for the transformation, i.e., the determinant of equation (20). These wave functions are not separable into a simple product of the type $\psi(R_{NN})\psi(R_{NO})$.

The R_{NN} dependent part of the dissociative wave function is also an harmonic oscillator wave function. The R_{NO} dependent (continuum) part of the dissociative wave function was evaluated using the WKB/square well approximation discussed in the preceding section.

The overall rate constant requires the microscopic rates from all possible initial levels into all equi-energetic levels of the excited state. The calculation of all these different rates considerably complicates the computational labour.

As the Franck-Condon factor is no longer separable into two one-dimensional integrals, we must evaluate two-dimensional integrals. This is a straightforward, although

time-consuming numerical procedure: the integral over (R_{NN}, R_{NO}) is simply the integral over R_{NO} of the set of integrals over R_{NN}. The integration was carried out using Simpson's rule (IBM 1968, p.291). As the integrand contains four oscillating functions, numerical integration is quite slow if carried out over a large area. We found that much time could be saved by the following simple procedure for determining the area in which the integrand assumes significant values.

The energy of the reactant level is the sum of the energies E_1 and E_3, from the normal coordinates ξ_1 and ξ_3. These energies define a rectangle in normal coordinate space, with sides

$$\xi_1 = \pm\sqrt{2E_1/\lambda_1} \qquad \xi_3 = \pm\sqrt{2E_3/\lambda_3}$$

wherein the reactant wave function assumes significant values. Under the transformation (20), this becomes a parallelogram in displacement coordinate space. The product wave function assumes significant values in a rectangle in displacement coordinate space. This rectangle can be found in a similar manner from the components E_n and E_C of the total energy. Because the NO dependent part of the wave function belongs to a continuum, one side of this rectangle is at infinite NO distance. The opposite side will be at the classical turning point corresponding to E_C. To allow for tunnelling, we extend

the reactant parallelogram and the product rectangle by, say, ¼ Å in all directions. The intersection of these two figures then defines the area in which the Franck-Condon integrand assumes significant values. With this procedure, we found that a grid of 25x25 points was sufficient to determine the overlap integral fairly accurately. Once the value of the parameter c which reproduced the experimental activation energy had been determined, the integrations were carried out with a finer grid. Preliminary calculations to determine this value of c required about 15 minutes each on an IBM 360/50. Once c had been determined, the accurate calculation required a total of about 30 minutes computing time.

Results.

For a calculated activation energy of 60 kcal/mole at 2000°K, we obtain a frequency factor of $10^{11.8}\,sec^{-1}$, with a spin-orbit coupling of 100 cm^{-1}. This is in fairly good agreement with the experimental value of $10^{11.2}\,sec^{-1}$. However, because of the unknown nature of the dissociative potential, and the neglect of anharmonicity and bending, this agreement must be regarded as comforting but coincidental. The value of c which gives this result is $2.8\,Å^{-1}$. The components of the activation energy at the above temperature are $\langle EK\rangle/\langle K\rangle$ = 69 kcal/mole, $\langle E\rangle$ = 9 kcal/mole.

As the calculation involves hundreds of levels, direct display of microscopic rates as in Figure 8 is not very informative. A simple picture may be obtained by averaging the rates of all levels whose energies lie within a given range. Figure 12 shows a plot of microscopic rates averaged into 1000 cm^{-1} (2.9 kcal/mole) "blocks", as a function of the average energy of the levels within the block. The similarity between this figure and the equivalent figure from the one-dimensional calculation indicates that the simpler model embodies much of the physical significance of more extensive formulations. Again, we have a sharp transition from negligible to significant microscopic rates over a small energy range, and <EK>/<K> corresponds with the maximum in the rate/energy plot. Here, however, we note that <EK>/<K> now lies significantly (5 kcal/mole) *above* the lowest point on the line of intersection of the reactant and product potential surfaces (64 kcal/mole). The reason for this may be seen from a more detailed examination of the largest microscopic rates.

On constructing the "area of intersection" of reactant and product wave functions (see above), it can be seen that for levels with large microscopic rates, the largest oscillations of all four wave functions involved in the Franck-Condon integrand overlap. There is of course no reason why such levels should correspond with the lowest energy of

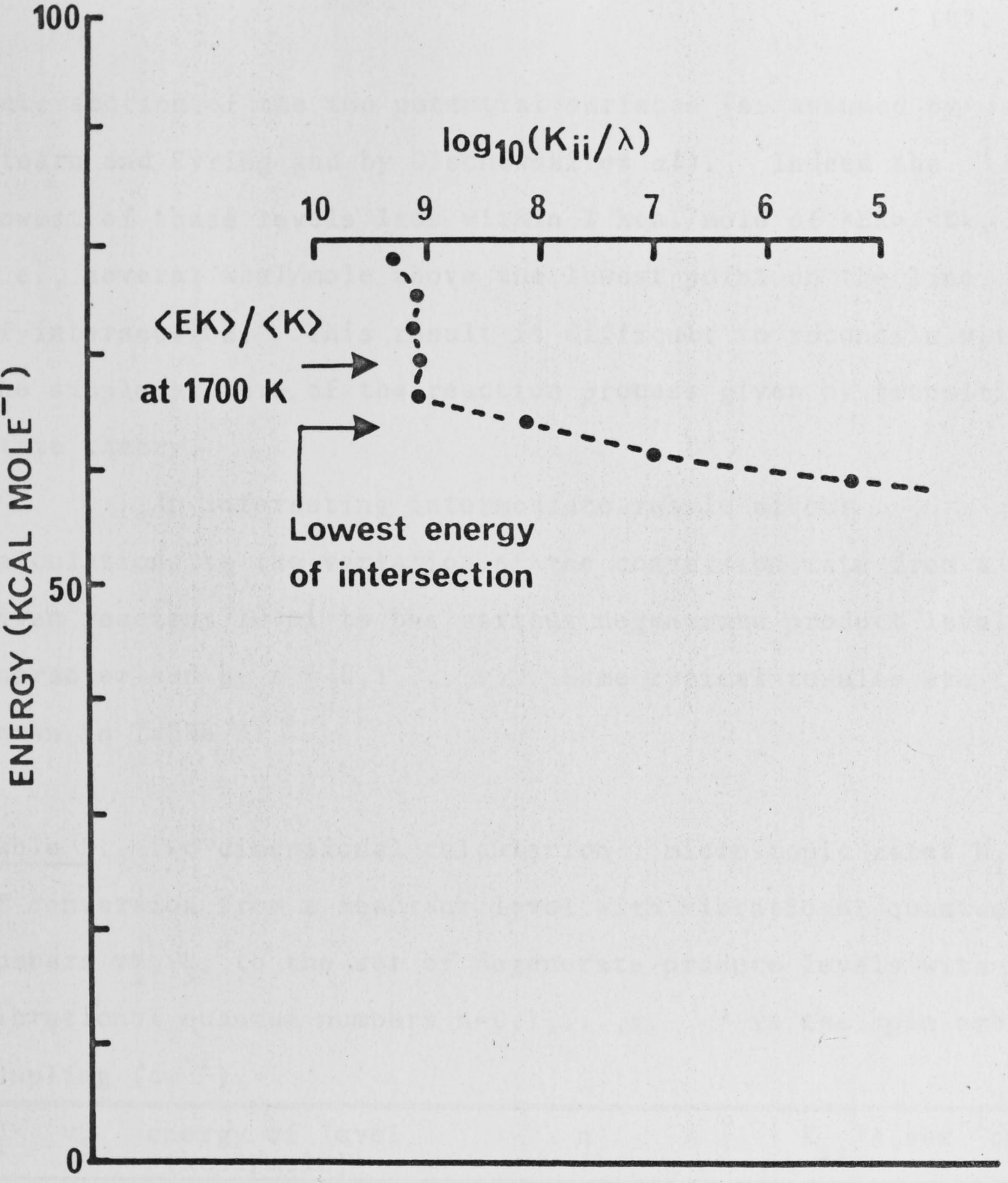

Figure 12.

Microscopic rates as a function of energy from the two-dimensional calculation, averaged into 1000 cm^{-1} (2.9 kcal/mole) "blocks". The format of the diagram is the same as that of the corresponding figure for the one-dimensional calculation (figure 8).

intersection of the two potential surfaces (as assumed by Stearn and Eyring and by Olschewski *et al*). Indeed the lowest of these levels lies within 1 kcal/mole of <EK>/<K>, i.e., several kcal/mole above the lowest point on the line of intersection. This result is difficult to reconcile with the simple picture of the reaction process given by transition state theory.

An interesting intermediate result of our calculations is the variation of the conversion rate from a given reactant level to the various degenerate product levels, characterised by n = 0,1....,v. Some typical results are shown in Table 3.

Table 3. Two dimensional calculation : microscopic rates K_{ii} of conversion from a reactant level with vibrational quantum numbers v_1'', v_3'', to the set of degenerate produce levels with NN vibrational quantum numbers n=0,1,...,v. λ is the spin-orbit coupling (cm^{-1})

v_1''	v_3''	energy of level (kcal/mole)	n	K_{ii}/λ ($sec^{-1}cm$)
5	10	74	0	1.1×10^{9}
			1	1.8×10^{9}
			2	5.2×10^{2}
			3 (v)	2.9×10^{-7}
7	5	68	0	8.7×10^{9}
			1	1.2×10^{6}
			2 (v)	1.6×10^{-4}

It can be seen that the rate of conversion is greatest into those product levels with low values of the N_2 vibrational quantum number, n. This phenomenon can be readily explained. A given total energy in the product is composed of two parts, discrete (E_n) and continuous (E_C). If the product involves a high value of the N_2 vibrational quantum number, then E_n will be large, and E_C correspondingly small. If E_C is small, then the classical turning point of the continuum wave function will occur at large values of R_{NO}. As this classical turning point determines one boundary of the rectangle in which the product wave function is significant, the reactant wave function parallelogram and the product wave function rectangle will be well separated. Hence the rate will be small.

Because of the time involved in these computations, it is clear that if calculations were attempted in more than two dimensions, then brute-force evaluation of multi-dimensional integrals, such as we have used here, would be impractical. An alternative technique to that which we have used would be to express reactant and product wave functions as linear combinations of products of wave functions which were separable in the relevant coordinates, e.g.,

$$\psi(\text{product}) = \sum_{i}\sum_{j} a_{ij}\psi_i(R_{NO})\ \psi_j(R_{NN})$$

The multidimensional integrals may then be expressed as sums of products of one-dimensional integrals.

CHAPTER IV.

THE LOW AND INTERMEDIATE PRESSURE RATE CONSTANT.

Section 1. Introduction.

In Chapter II we showed that the (second-order) low pressure rate constant is the largest eigenvalue of the truncated matrix of rates of collisional exchange between reactant levels; truncation is effected at the highest inactive level, which we index N. The intermediate pressure rate constant is the largest eigenvalue of the complete matrix $J = PA - K$.

The calculation of these rate constants therefore consists of two parts: firstly, the evaluation of the elements of the collision matrix A, which are the thermal averages of the collision cross sections, and secondly, finding the eigenvalue of the truncated matrix. The latter problem is equivalent to determining the population vector g of the reactant energy levels, because of the relations (Chapter II, Section 4):

$$R^{LP} = \sum_{i \leq N} g_i A'_{ii} / \sum g_i \qquad \text{(IV.1)}$$

$$A'_{ii} = \sum_{j > N} A_{ji} \qquad \text{(IV.2)}$$

As in Chapter III, our calculations are based on the thermal

decomposition of N_2O. The complete calculation, involving every thermally accessible reactant level, is at present impossible, because of inadequacies in calculating collision cross sections, and because of computer limitations. As in the high pressure case, we try to reduce the task by means of approximations which retain as much as possible of the physical significance of the problem.

To calculate vibrational collision cross sections, we use an approximate theory due to Schwartz, Slawsky and Herzfeld (SSH) (1952), also Schwartz and Herzfeld (1954). We attempt to specifically include collisional exchange between all vibrational modes; however we again ignore rotation. The complete calculation would involve thousands of vibrational levels, making the solution of the eigenvalue problem intractable. We therefore introduce a system of graining to reduce the size of the collision matrix, by condensing all the vibrational levels over a given energy range into a single "pseudo-level" with appropriate degeneracy.

Our low pressure calculations involve no adjustable parameters, but because of the inaccuracies introduced by the use of the SSH theory and the pseudo-level approximation, we cannot hope to obtain better than order-of-magnitude agreement with experiment. Therefore our aim is again the elucidation of physical processes rather than the reproduction of experimental results. We pay particular attention to the

relative importance of the various components of the low pressure activation energy (Chapter II, equations 46 to 50).

Section 2. Some Alternative Methods of Determining Collision Rates and Reactant Populations.

Probably the simplest and most widely used low pressure rate theory combines the steady state and strong coupling approximations (Slater 1959, p.16). The former assumption implies that the inactive levels have the same population as at equilibrium, and the latter finds A'_{ii} from the assumption that the rate of collisional deactivation is independent of the final state, and that this rate is given by the gas-kinetic collision rate ω. After a slight rearrangement, (1) and (2) become:

$$R^{LP} = \omega \sum_{i>N} e^{-E_i/kT} \Big/ \sum_{i=1}^{\infty} e^{-E_i/kT} \qquad \text{(IV.3)}$$

There are two principal objections to this simple theory, even when ω is treated as an adjustable parameter so that the experimental rate constant is reproduced. Firstly, there is experimental evidence that the strong-coupling approximation is invalid, and that the collision cross section is very small between levels with a large energy gap, as evidenced by the success of theories of vibrational relaxation which predict such a dependence (see, for example, Yardley and Moore 1968).

Secondly, it was pointed out in Chapter II that the assumption of an equilibrium population for the highest inactive levels can lead to serious error in the low pressure rate constant: the calculations in a later section will illustrate this point.

An alternative method of finding the rate constant is the "weak coupling" scheme, which assumes that only collisions leading to nearest neighbours are effective. The starting point of this method for finding A and g is the harmonic oscillator model for diatomic molecule/inert gas collisions, discussed in Chapter II. This method can be used to take into account deviations from equilibrium. However, even when the model is extended by allowing the levels to be degenerate (Buff and Wilson 1960), the basic restriction to a single vibration obscures the effect of collisional exchange between different vibrational modes, which can have a high cross section (see, for example, Yardley and Moore 1967a).

An alternative viewpoint is to differentiate the molecular levels by energy instead of by quantum number. Of particular interest is the approach adopted by Olschewski *et al* (1966). They assumed first of all that the density of vibrational levels in the region of interest is sufficiently high to replace the sums in (1) and (2) by integrals. They then assume that A_{ij} is a smoothly-varying function of the energy difference ΔE between the states i and j, and is other-

wise independent of i and j. If it is assumed that the population has a steady state distribution, and that $A_{ij}(\Delta E)$ has a simple functional form such as

$$A_{ij}(\Delta E) - \omega e^{-\Delta E/\gamma}$$

where ω is the gas kinetic collision number, and γ an adjustable parameter; (1) and (2) may then be integrated. This semi-empirical method avoids the neglect of anharmonicity and of exchange between different vibrational modes, but the use of the steady state approximation is a serious drawback. A combination of the harmonic-oscillator deviation from equilibrium and this semi-empirical theory would probably be quite useful.

We have elected to pursue a completely different method of calculating the rate constant, involving a more explicit determination of vibrational collisional cross sections, in the hope that this will provide an alternative point of view from those outlined above.

Section 3. The SSH Theory.

This theory was developed to account for vibrational relaxation times in shock-heated gases. It has had fair success in reproducing experimental results, takes into account the quantum numbers of the initial and final states

and the energy difference between them, and treats collisional exchange between different vibrational modes. Also, very importantly, the computations are quite simple. For these reasons, it provides a suitable basis for what must be regarded as an exploratory calculation.

For later discussion, we proceed to give a brief resume of the theory, which stems from an earlier paper by Jackson and Mott (1932), on collisions of atoms with solids.

The coordinates used to describe an inelastic collision of an atom and a diatomic molecule are the inter- and intra-molecular distances r and X. As discussed in Chapter I, the electronic wave functions may be factored out of the total wave function. The remainder, which we denote by Ψ, is then expanded as a linear combination of the products of the vibrational wave functions of the diatomic molecule, ψ_i, and Legendre polynomials, $P_\ell(\cos\theta)$, where θ is the angle subtended by the oncoming atom onto a fixed axis:

$$\Psi(r,X) = \sum_{i}\sum_{\ell} \zeta_{i\ell}(r)\ P_\ell(\cos\theta)\ \psi_i(X) \qquad \text{(IV.4)}$$

The expansion coefficients are denoted by ζ. This is a three-dimensional model, because of the angular dependence. The final cross section is summed over all partial waves ℓ. which is equivalent to integrating over all impact parameters (related to the initial angle of approach). The cross section is determined by imposing suitable boundary conditions on ζ.

It is then assumed that the intermolecular potential $V(r,X,\theta)$ is spherically symmetrical, i.e., independent of θ. This is usually justified by assuming that the diatomic molecule rotates very rapidly compared with the duration of a collision, although this assumption is rather questionable (Takayanagi 1963, p.85). The expansion (4) is then substituted into the Schrodinger equation for the atom/diatomic molecule system:

$$[H - \frac{\hbar^2}{2m}\nabla_r^2 + V(r,X) - E]\Psi = 0$$

Here H is the Hamiltonian of the isolated molecule, m the reduced mass of the colliding partners, and E their energy. After multiplying this equation by $P_\ell(\cos\theta)\,\psi_j$ and integrating over X and θ, a series of coupled second-order differential equations is obtained:

$$[d^2/dr^2 + k_i^2 - \ell(\ell+1)/r^2]\,\zeta_{i\ell}(r) = \frac{2m}{\hbar^2}\sum_j \zeta_{j\ell}(r)\,V_{ij}(r) \qquad (IV.5)$$

Here i and j refer to vibrational states, and ℓ to the partial wave, $V_{ij}(r)$ is the matrix element of the intermolecular potential $V(r,X)$ with respect to the vibrational wave functions $\psi_i(X)$ and $\psi_j(X)$, and $k^2 = 2mE/\hbar^2$. Thus the problem is reduced to determining the correct form of $V(r,X)$ and to solving the set of coupled equations (5).

SSH find an approximate solution to these equations from the distorted wave approximation (DWA), which ignores all

coupling between the equations except the matrix elements between the initial and final states. This reduces the problem to two coupled equations for each partial wave ℓ. They then assume that the solution for the ℓ^{th} partial wave can be expressed in terms of the solution for the s-wave (i.e., when $\ell = 0$).

The potential V(r,X) is assumed to have the form:

$$V(r,X) = V_o \exp[\ -(r + X)/L\ ] \qquad \text{(IV.6)}$$

The parameters V_o and L (the latter is called α by SSH) are determined by fitting the exponential function to a Lennard-Jones (LJ) potential (determined from viscosity data or from virial coefficients), such that the two potentials have the same value and slope at the classical turning point corresponding to the collisional energy E. The $V_{ij}(r)$ may then be written:

$$V_{ij}(r) \equiv V_o\ e^{-r/L} \langle \psi_i | e^{-X/L} | \psi_j \rangle$$

$$\equiv V_o\ e^{-r/L}\ V'_{ij} \qquad \text{(IV.7)}$$

If it is assumed that ψ_i and ψ_j are the wave functions for an harmonic oscillator, then V'_{ij} may be evaluated analytically (see, for example, Marriott 1964a). The formula for V'_{ij} depends on the parameters of the harmonic oscillator, including the reduced mass of the diatomic molecule. We return to this point later.

With these assumptions, the coupled differential equations may be solved to find the cross section, which is then converted to the collision rate by integrating over a Boltzmann distribution of the collision energy E. SSH then proceeded to find an approximate analytical form for this integral, but this has since been found to be an inaccurate approximation (see, for example, Steinfeld 1967a). The final form now usually used to determine the SSH collision rate is the integral over a Boltzmann distribution, which is evaluated numerically. The formula now used is that quoted by Stretton (1965); this is actually in the form of a "probability of transition per collision", but this is easily converted to a collision rate formula, namely

$$P\,A_{ij} = \frac{16N^\circ\pi^3\sigma^2m^2E_{ij}^2e^{\varepsilon/kT}(V'_{ji})^2d_i}{3\,kT\,\hbar^4}\int_{\Delta E}^{\infty}\frac{L^4\,e^W}{(1-e^W)^2}\left(\frac{2E}{m}\right)^{\frac{1}{2}}e^{-E/kT}\,dE \qquad (IV.8)$$

where N° is the number of inert gas molecules per unit volume, ε and σ are the LJ parameters, $E_{ij} = |E_i - E_j|$ is the absolute magnitude of the energy difference between the two states, d_i is the degeneracy, ΔE is the minimum energy for the collision (either zero or E_{ij} - see eq. II.12), and

$$W = 2\pi L\sqrt{2Em}\;\{1 - (1+E_{ij}/E)^{\frac{1}{2}}\}/\hbar \qquad (IV.9)$$

(In Stretton's formula, we have put $r_c/r_o = 1$ and used the conventional steric factor of 1/3).

The formula for L, the intermolecular potential parameter, is

$$L = \frac{(2\eta - 1)}{24\eta^{7/6}(1 - 1/n_a)}$$

where n_a is the number of atoms in the molecule, and

$$\eta = \tfrac{1}{2}[1 + (1 + E/\varepsilon)^{\frac{1}{2}}]$$

(Marriott 1964a). Note that L is dependent on the collision energy E, although this dependence is very slight over the energy range of interest in the integral (8). In some treatments, L is used as an adjustable parameter. Strictly speaking the matrix element V'_{ij} also depends on the collision energy, but this dependence is only very slight, and so V'_{ij} may be evaluated for a particular energy and taken outside the integral. Since all the quantities in (8) except V'_{ij} depend only on the energy difference E_{ij} between the states i and j, and are otherwise independent of these quantum numbers, we may write

$$A_{ij} = (V'_{ji})^2 f(E_{ij}) \qquad \text{(IV.10)}$$

where the function $f(E_{ij})$ is defined by (8). We plot this function for a range of temperatures in Figure (13), for both upward and downward transitions. The LJ parameters are those corresponding to N_2O/Ar collisions (see below).

ıction $f(E_{ij})$ (Equations IV.8, IV.10),

$_{j})^2$, determining that part of the collision

ding only on the energy difference between

l and final states, at various temperatures.

so indicated kT. $f(E_{ij})$ is in $sec^{-1}cm^3mole^{-1}$.

ters used in Equation IV.8 correspond to

between Ar and N_2O.

(a) Upward transitions

(b) Downward transitions

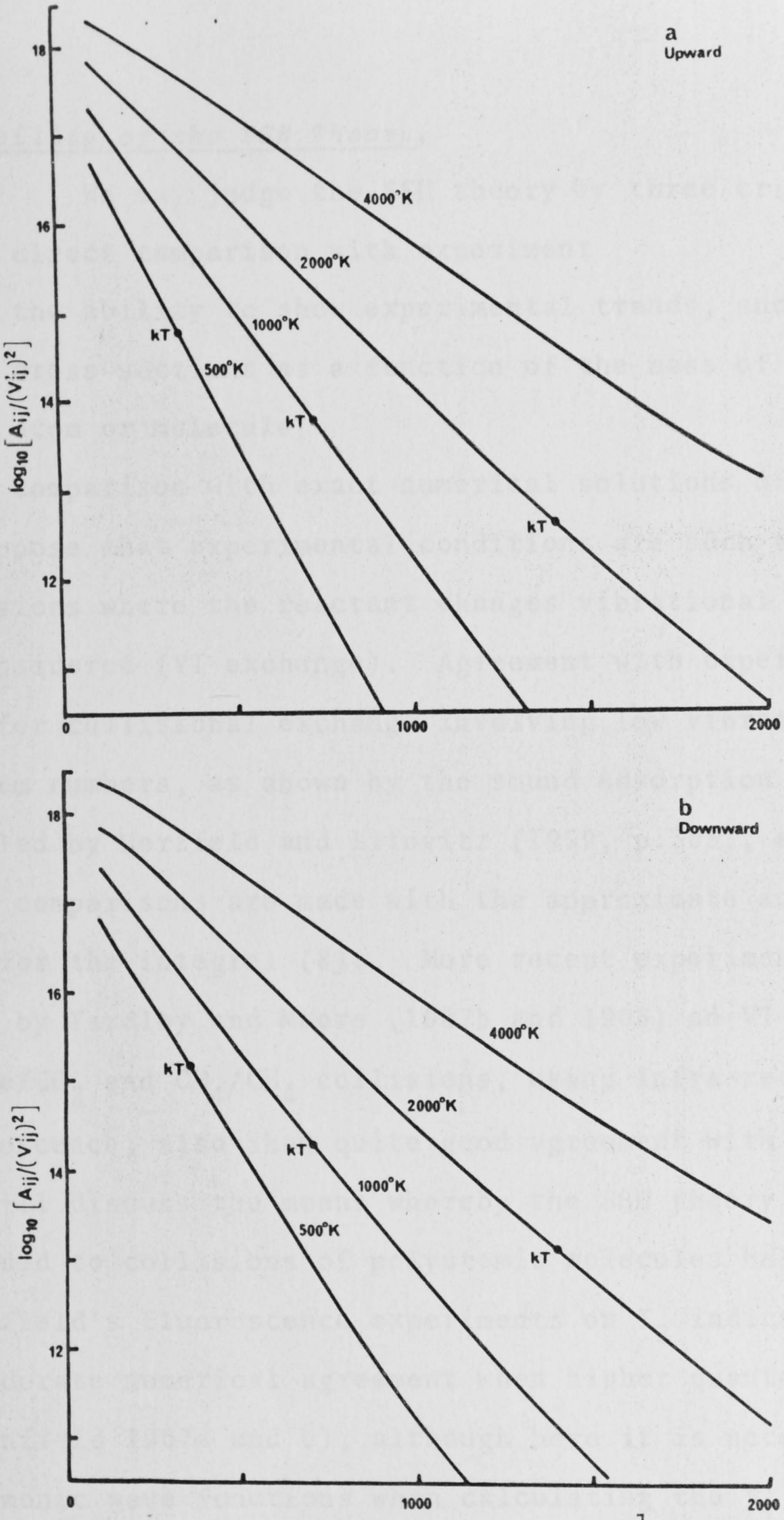
a
Upward
18
16
14
12
$\log_{10}[A_{ij}/(V'_{ij})^2]$
4000°K
2000°K
1000°K
500°K
kT
kT
kT
0
1000
2000
b
Downward
18
16
14
12
$\log_{10}[A_{ij}/(V'_{ij})^2]$
4000°K
2000°K
1000°K
500°K
kT
kT
kT
0
1000
2000
Energy difference E_{ij} (cm^{-1})

Reliability of the SSH Theory.

We may judge the SSH theory by three criteria:

(i) direct comparison with experiment

(ii) the ability to show experimental trends, such as relative cross sections as a function of the mass of the incident atom or molecule

(iii) comparison with exact numerical solutions of (5).

We suppose that experimental conditions are such that only collisions where the reactant changes vibrational state need be considered (VT exchange). Agreement with experiment is fair for collisional exchange involving low vibrational quantum numbers, as shown by the sound adsorption data compiled by Herzfeld and Litovitz (1959, p.303), although their comparisons are made with the approximate analytical form for the integral (8). More recent experiments such as those by Yardley and Moore (1967b and 1968) on VT transitions in He/CO_2 and CH_4/CH_4 collisions, using infra-red fluorescence, also show quite good agreement with the theory (we will discuss the means whereby the SSH theory can be extended to collisions of polyatomic molecules below). Steinfield's fluorescence experiments on I_2 indicate that there is moderate numerical agreement when higher quanta are involved (Steinfield 1967a and b), although here it is necessary to use anharmonic wave functions when calculating the V'_{ij}. One method of obtaining numerical agreement is to adjust the

parameter L, as did Yardley and Moore (1968) when comparing VT and VV transitions in CH_4. However the collision rate is not strongly dependent on L.

The I_2 experiments also show that the variation of the relative collision rate with the mass of the colliding partner is quite well reproduced by the SSH theory. Steinfeld also compares theoretical and experimental results for multiple quantum jumps, in the form of the ratio of collision rates for $\Delta v = 1$ and 2. However, this comparison is based on the rather suspect assumption that the relative rate is determined by the ratio of the square of the matrix elements, $(V'_{ij})^2$, and that the effect of the different energy gaps between the two transitions is unimportant, because these energy gaps are $\sim kT$. By reference to Figure (13b), we feel that this assumption is unjustified.

The only accurate numerical calculations involving vibrational exchange in three-dimensional collisions are those of Marriott (1964 a and b). His figures agree quite well with those calculated from (8). Coupling between states other than the initial and final states, which is ignored in the DWA, has a definite effect on the cross section, but does not change its values by more than a factor of two or three.

Within the last few years several workers have devised elaborate numerical treatments of the one-dimensional collisional problem, i.e., for a collinear collision (for a

review, see Rapp and Kassal 1969). At present, these methods have not been extended to three-dimensional vibrational collisions. The one-dimensional computations show that the mathematical approximations used in the SSH theory are not very accurate. However, recently Roberts (1968) has shown that the SSH version of the DWA can be improved without a large increase increase in computational labour; however this refinement has not been included in our own calculations. Because collinear collisions are presumably rather rare events, one hopes that these calculations can be extended to three dimensions, to supplement the work of Marriott.

Extension to Polyatomics.

The SSH theory was derived for a collision of a structureless particle with a vibrating diatomic molecule. Here we are not concerned with the case where the colliding atom can have an internal structure. The theory may be extended to a collision of a structureless atom with a polyatomic molecule by assuming that the intermolecular potential function has the form:

$$V(r,X_1,X_2,\ldots) = V_o \exp[\ -(r + X_1 + X_2 + \ldots)/L] \qquad \text{(IV.11)}$$

where $X_1, X_2, \ldots$ are the normal coordinates of the polyatomic molecule. Equations (7) and (8) then remain unchanged, except that V'_{ij} becomes the product of matrix elements of the type

$V'_{i_1 j_1} V'_{i_2 j_2} \ldots$, corresponding to each normal mode. However, it is then necessary to define the oscillator reduced mass corresponding to each vibration to replace the reduced mass of a diatomic molecule used in the original theory. Tanczos (1958) and Stretton (1965) suggested that only the "surface atoms" (for example H and Cl in CH_3Cl) are involved in the collision because the assumption of a spherically symmetrical potential requires a rapidly rotating molecule (breathing sphere model). Stretton then derived a method of defining the reduced mass corresponding to each normal coordinate in terms of the Wilson G and S matrices (Wilson *et al* 1955, p.307), appropriately modified to include only surface atoms. With this method, he obtained quite reasonable agreement with experiment for the vibrational relaxation times of a number of molecules. More recently, Yardley and Moore (1968) have also obtained quite good agreement for CH_4 collision rates, from their IR fluorescence experiments. Fluorescence studies on a larger molecule such as benzene (either in the IR or UV) could eventually provide data for a more extensive test of the breathing-sphere model.

However, we feel that this method is not suitable for N_2O, where it would appear unsafe to ignore the central N atom. In theoretical studies on vibrational relaxation in CO_2 (Witteman 1961, Marriott 1964), the reduced masses were

derived by treating the molecule as a quasi-diatomic (Marriott 1968). For example, the in-phase stretch is considered to be equivalent to a carbon atom vibrating against two rigidly linked oxygen atoms, and so on. Since the mass asymmetry of NNO is small, and the force constants for the NN and NO bonds similar, we have applied this reasoning here. Specifically, the oscillator masses we have used for N_2O are $m_N m_O/(m_N+m_O)$ for the out-of-phase stretch, and $m_N(m_N+m_O)/(2m_N+m_O)$ for the other two modes. However it should be observed that the collision rate is not strongly dependent on this parameter.

The Lennard-Jones parameters ε and σ for N_2O/Ar were evaluated using the semi-empirical method described in Hirschfelder, Curtiss and Bird (1964, p.567):

$$\sigma_{N_2O/Ar} = \tfrac{1}{2}(\sigma_{N_2O} + \sigma_{Ar}) \qquad \varepsilon_{N_2O/Ar} = (\varepsilon_{N_2O}\,\varepsilon_{Ar})^{\frac{1}{2}}$$

Strictly speaking, we should also include dipole/induced dipole corrections (see, for example, Marriott 1966), but as NNO has a very small dipole moment, these are negligible.

In Table 4 we show the matrix elements V'_{ij} for the bending and in-phase stretching modes of N_2O. From this table and from Figure (13) it can be seen that there will be a high cross section for such processes as exchange between (0 0 1) and ($0\,1^2\,0$), where the energy gap is comparatively small. Thus an important prediction of the SSH theory,

Table 4. The absolute values of the matrix element.

$$V'_{ij} = \int \psi_i(X)\ e^{-X/L}\ {}_j(X)\ dX$$

appearing the the SSH theory (equations IV.7, IV.8) for the bending and in-phase stretching vibrations. ψ_i and ψ_j are taken to be harmonic oscillator wave functions. The parameters used correspond to N_2O/Ar collisions. As the matrix is symmetric, we only show the lower triangular part.

ν_2(bending) vibration

j \ i	0	1	2	3	4
0	$1x10^{0}$				
1	$2x10^{-1}$	$1x10^{0}$			
2	$6x10^{-2}$	$2x10^{-1}$	$1x10^{0}$		
3	$1x10^{-2}$	$4x10^{-2}$	$3x10^{-1}$	$1x10^{0}$	
4	$3x10^{-3}$	$4x10^{-3}$	$5x10^{-2}$	$3x10^{-1}$	$1x10^{0}$

ν_3(in-phase stretching) vibrations

j \ i	0	1	2	3	4
0	$1x10^{0}$				
1	$1x10^{-1}$	$1x10^{0}$			
2	$1x10^{-2}$	$1x10^{-1}$	$1x10^{0}$		
3	$2x10^{-3}$	$9x10^{-3}$	$1x10^{-1}$	$1x10^{0}$	
4	$2x10^{-4}$	$5x10^{-4}$	$1x10^{-2}$	$2x10^{-1}$	$1x10^{0}$

and one borne out by experiment (e.g., Yardley and Moore 1967a), is that there is a high probability for collisional exchange between what we might perhaps term "reactive" and "unreactive" vibrational modes, such as between the bending and stretching modes in our models in Chapter III. Therefore it is inadequate to treat energising collisions as only involving those modes which belong to the reaction coordinate.

The great difficulty in comparing even an accurate numerical solution with experiment is the form of the intermolecular potential function, particularly the dependence on the internal coordinates X_i. Mies (1965) has criticised the exponential function (equation 6) which has been used in most assaults on the problem so far, on the basis of a calculation on the He/H_2 potential (Kraus and Mies 1965). However this potential is obtained from a single determinant Hartree-Fock wave function, and it is well known that this treatment is unreliable. It is to be hoped that some information on the potential will be forthcoming from molecular beam or infra-red fluorescence experiments. Until then, both crude and sophisticated procedures are equally likely to be unrelated to experiment. In view of the moderate successes of the SSH theory, we have adopted it here.

Section 4. The Pseudo-level Approximation.

There are about 10^4 vibrational levels in N_2O between the zero-point level and the experimental activation energy. To construct and diagonalise the complete transport matrix J is clearly impractical, and we have devised a graining technique to reduce the computation. A related method has been used by Tardy and Rabinovitch (1966), who however do not give any details.

If two levels have similar energies, then the cross section for collisional exchange between them will be high. Thus they might be approximated as a single, doubly degenerate level. Suppose that the J matrix of equation II.3 is grouped into rectangular blocks, and the population vector x grouped correspondingly. We define a condensed population vector x^s, where each element is equal to the sum of the elements in a block of x, so that population is conserved. The corresponding condensed levels we term "pseudo-levels". We suppose that this procedure gives rise to a condensed transport matrix J^s, such that

$$\frac{dx}{dt} = Jx \text{ implies } \frac{dx^s}{dt} = J^s x^s \qquad \text{(IV.12)}$$

where each element of J^s corresponds to an entire block of elements in J. Because the condensation procedure conserves population, the formal properties of J^s are the same as those

of J, provided that the degeneracy of each pseudo-level is included.

We can provide a mathematical rationalisation of this procedure as follows. Relation (12) will be true if in each block of J, the sums of the columns are equal, and the corresponding element of J^s is equal to the total sum of all the elements in the block. The proof of this statement is quite straightforward. For simplicity, suppose that we are condensing a 6x6 matrix in the following way:

$$\begin{array}{cccccc}
J_{11} & J_{12} & J_{13} & J_{14} & J_{15} & J_{16} \\
J_{21} & J_{22} & J_{23} & J_{24} & J_{25} & J_{26} \\
J_{31} & J_{32} & J_{33} & J_{34} & J_{35} & J_{36} \\
J_{41} & J_{42} & J_{43} & J_{44} & J_{45} & J_{46} \\
J_{51} & J_{52} & J_{53} & J_{54} & J_{55} & J_{56} \\
J_{61} & J_{62} & J_{63} & J_{64} & J_{65} & J_{66}
\end{array}$$

We then have

$$x_1^s = x_1 + x_2 + x_3$$

$$\frac{dx_1^s}{dt} = \frac{dx_1}{dt} + \frac{dx_2}{dt} + \frac{dx_3}{dt}$$

$$= \sum J_{1j}x_j + \sum J_{2j}x_j + \sum J_{3j}x_j$$

Then, if

$$J_{11}+J_{21}+J_{31} = J_{12}+J_{22}+J_{32} = J_{31}+J_{32}+J_{33} = \frac{1}{3}J^{s}_{11}$$

and so on, we have

$$\frac{dx^{s}_{1}}{dt} = J^{s}_{11}x_{1}{}^{s} + J^{s}_{12}x^{s}_{2} + J^{s}_{13}x^{s}_{3}$$

etc., which proves the result.

Now, we could proceed to generate all the elements of J, and test our assumption that the sums of the elements in each column of a block of J being condensed to a particular J^{s}_{ij} are equal. However, considering the accuracy of present methods of evaluating vibrational collisional cross sections (especially since anharmonicity will be very pronounced when the levels are closely spaced) such a calculation would be not only time consuming but also would bear little resemblance to nature. We have therefore assumed that the order of magnitude of the collision rates between pseudo-levels can be found by treating them as single levels, of appropriate degeneracy, having quantum numbers and energies equal to the *average* quantum numbers and energies of the component levels. We assume that the collision rate between two pseudo-levels is the same as the rate between two levels with the average quantum numbers and energies of the pseudo-levels, divided by the degeneracy of the final level. Using this scheme,

the J^s matrix would become the complete J matrix in the limit of one level per pseudo-level. The consistency of the method can be tested by seeing if the rate constants converge as the grain size is reduced. The calculation of the following section indicate that this indeed occurs.

Table 5 shows average quantum numbers, energies and degeneracies

Table 5. Average quantum numbers and energies of the pseudo-levels of N_2O, calculated with a grain size of 1000 cm^{-1}.

Average quantum numbers			Degeneracy	Average Energy above zero-point level (cm^{-1})
ν_1	ν_2	ν_3		
0	0	0	3	393
0	1	0	10	1564
0	2	0	18	2626
0	2	1	30	3542
0	2	1	53	4524
0	3	1	87	5580
1	3	1	101	6547
1	4	1	167	7519
1	4	2	208	8537
1	4	2	273	9521
1	5	2	342	10495
1	5	2	472	11521
1	6	2	526	12532
1	6	3	662	13508
1	7	3	800	14508
2	7	3	961	15516
2	7	3	1091	16506
2	8	3	1352	17511
2	8	4	1494	18519
2	9	4	1719	19503
2	9	4	2026	20503
2	10	4	2273	21510
2	10	4	2574	22511
2	10	5	2896	23510
3	11	5	3234	24509

of the pseudo-levels in N_2O, using a grain size of 1000 cm^{-1}. No account has been taken of anharmonicity.

We then proceed to calculate collision rates between pseudo-levels using the SSH theory. Because of the nature of the pseudo-level scheme, it seems pointless to include anharmonicity in the cross section calculation.

Since the collision rates are the products of an energy-dependent term, $f(E_{ij})$, and the required matrix element $(V'_{ij})^2$ (equation 16), it can be seen by reference to Figure 13 that, for a sufficiently coarse grain size (i.e., a large number of levels per pseudo-level), all except nearest-neighbour transitions could be ignored. This justifies the approximate formula for the low pressure activation energy derived in Chapter II, Section 7, when the complete collision matrix was replaced by a tridiagonal matrix.

With our pseudo-level procedure, it is not immediately obvious where to truncate the collision matrix A when calculating the low pressure rate constant. If the calculation considered each level individually, then the levels could be indexed so that all active levels are placed above all inactive ones. Under our condensation procedure, however, a single "level" contains many individual levels with a wide range of quantum numbers, and the levels are best ordered by average energy. Now, consideration of microscopic rate/energy plots such as Figures 8 and 12 shows that a pseudo-

level with energy which is greater than D_e, the minimum energy for reaction, but less than the energy at which the sharp rise characteristic of most of these plots occurs, will contain mainly inactive levels, together with a few active levels with small microscopic rates. It would appear unreasonable to label this whole pseudo-level as active. Similarly, pseudo-levels with energy above the energy of the sharp rise cannot really be described as inactive. It would seem a fair assumption to truncate the condensed collision matrix at this sharp rise. This will include some active levels in the highest inactive pseudo-level, and *vice versa*, but hopefully these errors will be self-cancelling. The onset of reaction (i.e., the transition from negligible to appreciable microscopic rates) occurs over only a few kcal/mole, and so no great uncertainty is involved in this choice. We will examine the case where there is no sudden onset of reaction in a later section.

Section 5. Computational Procedure.

The calculation of the rate constant requires the evaluation of the largest (i.e., closest to zero) eigenvalue of the condensed matrix J^s (intermediate pressure) or A^s (low pressure limit). Alternatively, an approximate value for the population vector g may be substituted into (1)(we pointed

out above that the steady state approximation leads to a large error in the low pressure region). Determining the eigenvalue requires storage of the entire J^S or A^S matrix, whereas if the eigenvector is known, the only storage required is this eigenvector and the A'_{ii} of equation (2).

Valance and Schlag (1966) have derived an iterative solution of the problem: the many-shot expansion. Their method does not require simultaneous storage of the complete matrix. However, in view of the approximate nature of the SSH theory and of the pseudo-level technique, we feel that in the present calculation there is no advantage to be gained by having 100 instead of 500 levels in a pseudo-level, and we have restricted our calculations to comparatively coarse grain size (our finest graining was a spacing of 175 cm^{-1} between pseudo-levels). It is then possible to store the entire matrix within the computer available to us, and we have used the simple power method to determine the eigenvalue [see, e.g., Perlis (1952,p.208)]. As this method finds that eigenvalue which is largest in absolute value, and as the rate constant is the eigenvalue which is closest to zero, and so smallest in magnitude, the matrix must first be inverted. Eigenvalue and inversion procedures are notoriously susceptible to roundoff errors, and so we checked our method by comparing the eigenvalue obtained from a tridiagonal matrix with the eigenvalue calculated from the quotient-difference algorithm

(Bennet *et al* 1960), which does not require inversion. We found that to obtain a fair accuracy (0.1%) it was necessary to use double precision arithmetic, and to first normalise the matrix so that the absolute value of its largest element is unity.

Section 6. Low Pressure Rate Constants and Activation Energy.

Figure 14 shows the calculated low pressure rate constant as a function of temperature, for various grain sizes. The experimental values collated by Troe and Wagner are also shown.

It appears that the rate constant converges to a limit as the grain size is reduced, indicating the internal consistency of the pseudo-level technique for a given method of calculating collision rates. Considering the approximations involved in the calculation, the agreement with experiment is as good as could be expected.

We find that at 2000°K, the error in the rate constant if the complete A^S matrix is replaced by a tridiagonal matrix is less than 1% compared with the complete calculation, for a spacing of 500 cm^{-1} or greater between pseudo-levels.

In Figure 15 we show the ratio of the exact population g_i of each pseudo-level to the equilibrium population b_i, for a grain size of 500 cm^{-1}. The populations of the

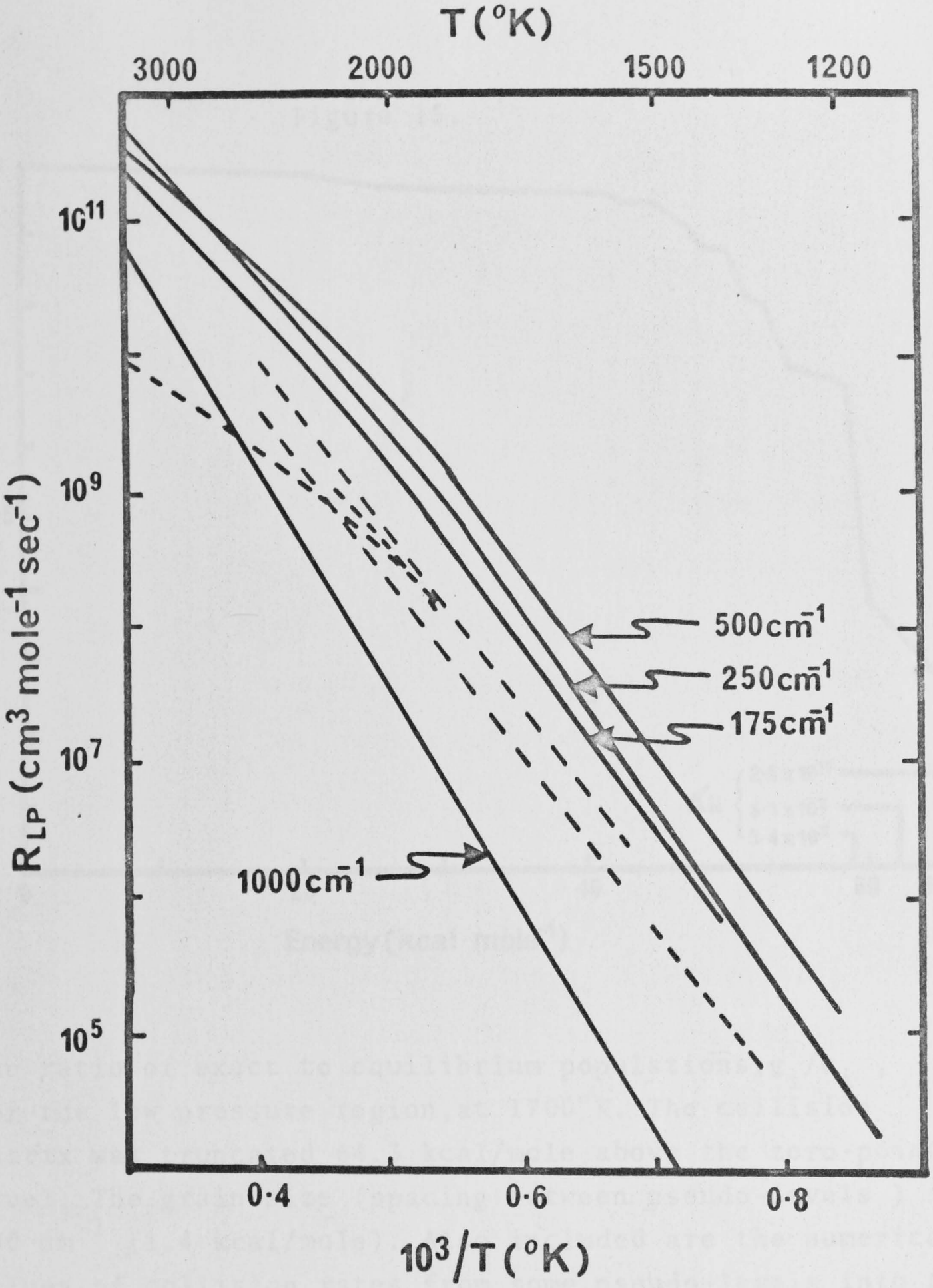

Figure 14.

Low pressure rate constants, R_{LP}. Full lines: calculated values for various grain sizes, as indicated. Broken lines: experimental results of various workers, as collated by Troe and Wagner (1967).

Figure 15.

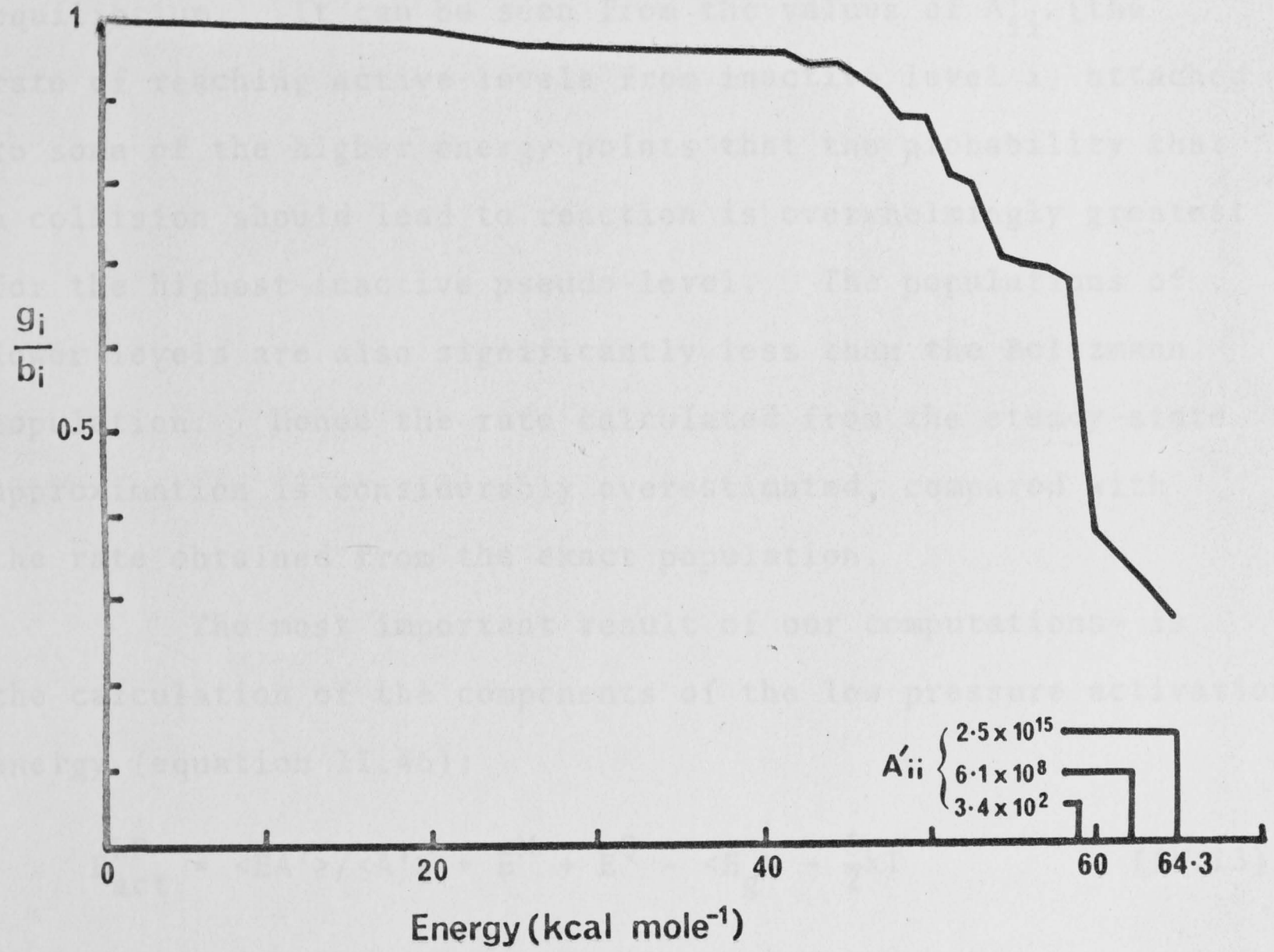

The ratio of exact to equilibrium populations, g_i/b_i , for the low pressure region, at 1700°K. The collision matrix was truncated 64.3 kcal/mole above the zero-point level. The grain size (spacing between pseudo-levels) is 500 cm^{-1} (1.4 kcal/mole). Also included are the numerical values of collision rates from some pseudo-levels into the active region, namely the A'_{ii} of equation IV.2

highest inactive levels show a pronounced deviation from equilibrium. It can be seen from the values of A'_{ii} (the rate of reaching active levels from inactive level i) attached to some of the higher energy points that the probability that a collision should lead to reaction is overwhelmingly greatest for the highest inactive pseudo-level. The populations of lower levels are also significantly less than the Boltzmann population. Hence the rate calculated from the steady-state approximation is considerably overestimated, compared with the rate obtained from the exact population.

The most important result of our computations is the calculation of the components of the low pressure activation energy (equation II.46):

$$E_{act}^{LP} = \langle EA' \rangle / \langle A' \rangle + E^{M} + E^{Q} - \langle E_g \rangle - \frac{3}{2}kT \qquad (IV.13)$$

Our aim is to determine the importance of the various terms: $\langle EA' \rangle / \langle A' \rangle$, which may be visualised as the average energy of those inactive levels with a high probability of collisional excitation to active levels; E^{M}, which is zero if the population is a Boltzmann distribution, and which may therefore be regarded as a measure of the inadequacy of the steady state approximation (both of the above terms arise from microscopic reversibility); E^{Q}, derived from the matrix elements A_{ij}, which are functions of the energy-dependent cross section,

$Q_{ji}(E)$; and the average thermal energy terms $\langle E_g \rangle$ and $\frac{3}{2}kT$.

The cross sections were calculated from the SSH theory. Now the final form for the collision rate, equation 8, is slightly different from a thermal average of Q, equation II.12, which was used to derive (13). We therefore make a minor alteration in the expression for E^Q (equation II.47), by adding a term $k(\frac{1}{2}T-\varepsilon)$, where ε is the Lennard-Jones parameter, to the A_{ij} calculated from the differential of (8) with respect to temperature. This brings the activation energy expression to the same form as (13).

We also wish to compare the exact expression for the low pressure activation energy with that obtained from the steady state approximation (equation II.50):

$$E_{act}^{LP} \simeq \sum b_i A'_{ii} E_i \; / \; \sum b_i A'_{ii} \; - \; \frac{3}{2}kT \; - \; \langle E \rangle \qquad \text{(IV.14)}$$

where the population is approximated by a Boltzmann distribution, and the E^Q term is ignored. The exact and steady state rate constants and activation energies are compared in Table 6, for a grain size of 500 cm^{-1}; essentially similar results are obtained for different grain sizes.

It can be seen that the activation energy indeed approximates the energy of the first reacting level. In fact, this energy is also close to the sum of the "microscopic reversibility" terms $\langle EA' \rangle / \langle A' \rangle + E^M$. This is because the cross section dependent term, E^Q, approximately cancels the

average thermal energy terms $\langle E_g \rangle + \frac{3}{2}kT$, for the temperatures at which the N_2O reaction has been studied.

Table 6. Calculated low Pressure rate constants and activation energies for the thermal decomposition of N_2O.[a]

	Complete expression			Steady state approximation		
	900°K	1700°K	2000°K	900°K	1700°K	2000°K
	Rate Constants ($sec^{-1} cm^3 mole^{-1}$)					
	9.1×10^1	1.6×10^9	2.0×10^{10}	1.4×10^2	5.9×10^9	1.1×10^{11}
	Activation energy components (kcal/mole)					
E^M	21.05	41.79	43.31			
$\langle EA' \rangle / \langle A' \rangle$	45.47	18.71	12.76			
E^Q	6.81	12.73	15.20			
$-\langle E_g \rangle$	-4.36	-9.15	-10.92			
$-\langle E \rangle$				-4.36	-9.20	-11.29
$-\frac{3}{2}kT$	-2.68	-5.07	-5.96	-2.68	-5.07	-5.96
$\frac{\sum b_i E_i A'_{ii}}{\sum b_i A'_{ii}}$				66.22	66.20	66.20
	Total activation energy (kcal/mole)[b]					
	66.29	59.01	54.39	59.18	51.93	48.95

[a] The collision matrix was truncated at 64.3 kcal/mole above the zero-point level. The grain-size (energy difference between pseudo-levels) is 500 cm^{-1} (1.4 kcal/mole)

[b] The activation energy calculated from pairs of rate constants (obtained from the complete expression) are 63.49 and 56.71 kcal/mole for the intervals 900 - 1700°K and 1700 - 2000°K respectively.

Note that in the steady state approximation, the principal term in the activation energy, $\sum b_i E_i A'_{ii} / \sum b_i A'_{ii}$, is also very close to the energy of the first reacting level; however as this approach does not include the E^Q term, the activation energy predicted by this approximation is in serious error. Furthermore, the rate constant calculated from the steady state approximation is much greater than that calculated from the exact population.

We find that the E^Q term decreases with decreasing temperature, and that below 1000°K it is relatively unimportant. Thus at low temperatures the steady state approximation predicts the activation energy quite adequately, although for the wrong reason.

Our calculations indicate that the deviation of the actual population from equilibrium increases with increasing temperature. In our approximate formula for the low pressure activation energy, equation II.51 (derived for a tridiagonal matrix), the leading term is $E_{N+1} g_{N-1} / b_{N-1}$. Therefore we would expect that the sum of the E^M and $\langle EA' \rangle / \langle A' \rangle$ terms would decrease at high temperatures; the results of Table 6 show that this is indeed so. This has the effect of reducing the activation energy at higher temperatures, in addition to the reduction caused by the increase in the thermal energy terms $\langle E_g \rangle$ and $\frac{3}{2}kT$; in fact the increase in these last terms is approximately cancelled by the corresponding increase in E^Q.

The experimental results for N_2O (Figure 14) appear to indicate a decrease in the activation energy about 2500°K, although these results must be viewed with caution.

This reduction in the activation energy at high temperatures is considerably more pronounced than that predicted by the steady state approximation, which is due to the increase in the thermal energy terms alone. Thus at high temperatures, our calculations indicate that it is quite incorrect to associate the experimentally observed low pressure activation energy with a barrier height, because of the reduction of the activation energy at high temperatures caused by the increased deviation of the actual population from equilibrium. This effect is significant above 1000°K; such temperatures are now routinely used to study high temperature reactions in shock tubes.

The Low Pressure Activation Energy of the CO_2 Decomposition.

Experiments on the thermal decomposition of CO_2:

$$CO_2 \rightarrow CO + O$$

indicate that the low pressure activation energy (74±6 kcal/mole) at 4000°K) is much less than the minimum energy for reaction (ΔH° = 126.5 kcal/mole) (Clark *et al* 1969, and references therein to earlier work). One postulated explanation for this peculiar behaviour is the influence of side reactions, another is the many sources of error associated with temperature

measurement in shock tubes at these high temperatures. Now, in view of our above discussion on the effect of the increased deviation from equilibrium at high temperatures, it is possible that our present theory can provide a partial explanation of this anomaly. We therefore carried out a model calculation to determine the low pressure activation energy of the CO_2 decomposition.

Our main interest here is the reduction in the low pressure activation energy at high temperatures. Rather than carry out a complete calculation to determine the energy at which to truncate the collision matrix, as in our N_2O calculation, we simply assumed that this truncation energy was a few kcal/mole above the minimum energy for reaction, namely at 129 kcal/mole. We then calculate an activation energy of 114 kcal/mole at 4000°K, using a grain size of 500 cm^{-1}. Although this is indeed below $\Delta H°$, it is insufficient to account quantitatively for the experimentally observed value. Nevertheless, the reduction in the calculated activation energy below the least possible barrier height is striking, and would be further reduced at higher temperatures.

The E^Q Term.

We have been unable to gain any simple understanding of the nature of the E^Q term. Examining numerical values for the various terms in II.47:

$$E^Q = \frac{\sum \frac{g_i^2}{b_i} \sum_{j>N} \mathcal{A}_{ij} \frac{b_j}{b_i} + \sum \frac{g_i}{b_i} \sum_{j=i+1}^{N} \mathcal{A}_{ij}(g_i b_j / b_i - 2g_j) + \sum_{j>i} g_i \mathcal{A}_{ji}}{\sum\sum g_i g_j A_{ij}/b_i}$$

we find that the summations are dominated by the contributions from the lowest energy level, i.e., when i=1. This term is large and negative, because the $\sum_{j<i} g_i \mathcal{A}_{ji}$ term is zero. All the remaining terms in the sum, however, are positive, and their total is very close to the value of the first term. Thus in the end it appears to be the contribution from the highest inactive level which determines the value of E^Q. It is possible that further formal manipulation of the above expression could explain this behaviour. A more reliable estimate of E^Q requires further information on the $\mathcal{A}_{ij}$; this must await an improved expression for the energy dependence of vibrational cross sections.

Section 7. Intermediate Pressure Rate Constant.

The rate constants at intermediate pressure were evaluated from the largest eigenvalue of the complete matrix $J^S = PA^S - K^S$. To test the ability of the theory to predict the pressure dependence of the rate constant, we rescaled the A^S and K^S matrices to reproduce exactly the experimentally observed low and high pressure rate constants.

In setting out to make this comparison with experiment, we suffer from the embarrassment that the simple Lindemann-Hinshelwood (LH) formula fits the observed data quite satisfactorily, at the two temperatures where the complete pressure range has been studied. Now, the LH expression is in fact the limiting form of our graining technique, i.e., when the graining is so coarse that only two pseudo-levels, one active and one inactive, remain. In this case, as Buff and Wilson (1960) have pointed out, the 2x2 eigenvalue problem can be easily solved, and after neglecting small terms, the rate constant becomes

$$R = \frac{P\ K_{22}^{S}\ A_{21}^{S}}{P\ A_{12}^{S} + K_{22}^{S}} \qquad \text{(IV.15)}$$

which is the LH expression. As this formula fits the experimental results quite well if the two parameters $(A_{12}^{S}/K_{22}^{S}A_{21}^{S})$ and A_{21}^{S} are chosen to reproduce the high and low pressure limits, our multilevel formula will be hard put to improve on what may perhaps be a fortuitous agreement. Nevertheless, our calculations give quite good results. Furthermore, they indicate that the exothermic reaction of Chapter III, Section 6, which because of tunnelling exhibited an anomalous dependence of the high pressure activation energy and frequency factor on temperature, should also show a distinctive pressure dependence of the rate constant. This would not be

predicted by a simple two-level theory.

To carry out the calculations requires a method of constructing the condensed K matrix K^s, i.e., of determining the microscopic rates for the pseudo-levels. Our chosen method was to use Figures 8 or 12 as follows (both one- and two-dimensional calculations give similar results). From the average energy of each pseudo-level, we read off the corresponding rate constant; K^s_{ii} then taken to be this rate constant divided by the degeneracy of the pseudo-level.

In keeping with our discussion in the previous section on the truncation energy for the condensed collision matrix, microscopic rates below the sharp rise characteristic of the N_2O rate/energy plot were ignored. Hence all the K^s_{ii} will be of similar magnitude. We also wished to determine the pressure dependence of the rate constant when the rate/energy plot does not show a sudden transition from negligible to significant microscopic rates, as in the exothermic decomposition of Figure 10. We therefore carried out the N_2O calculation including some K^s_{ii} below the sharp cutoff, having values several orders of magnitude below those of the other microscopic rates. In Figure 16 we compare the pressure dependence of the rate constants derived from the two different sets of K^s_{ii} with that obtained from the LH formula, and with the experimental results of Olschewski *et al* (1966). The LH formula and the multilevel rate constant with K^s_{ii} all of

Figure 16

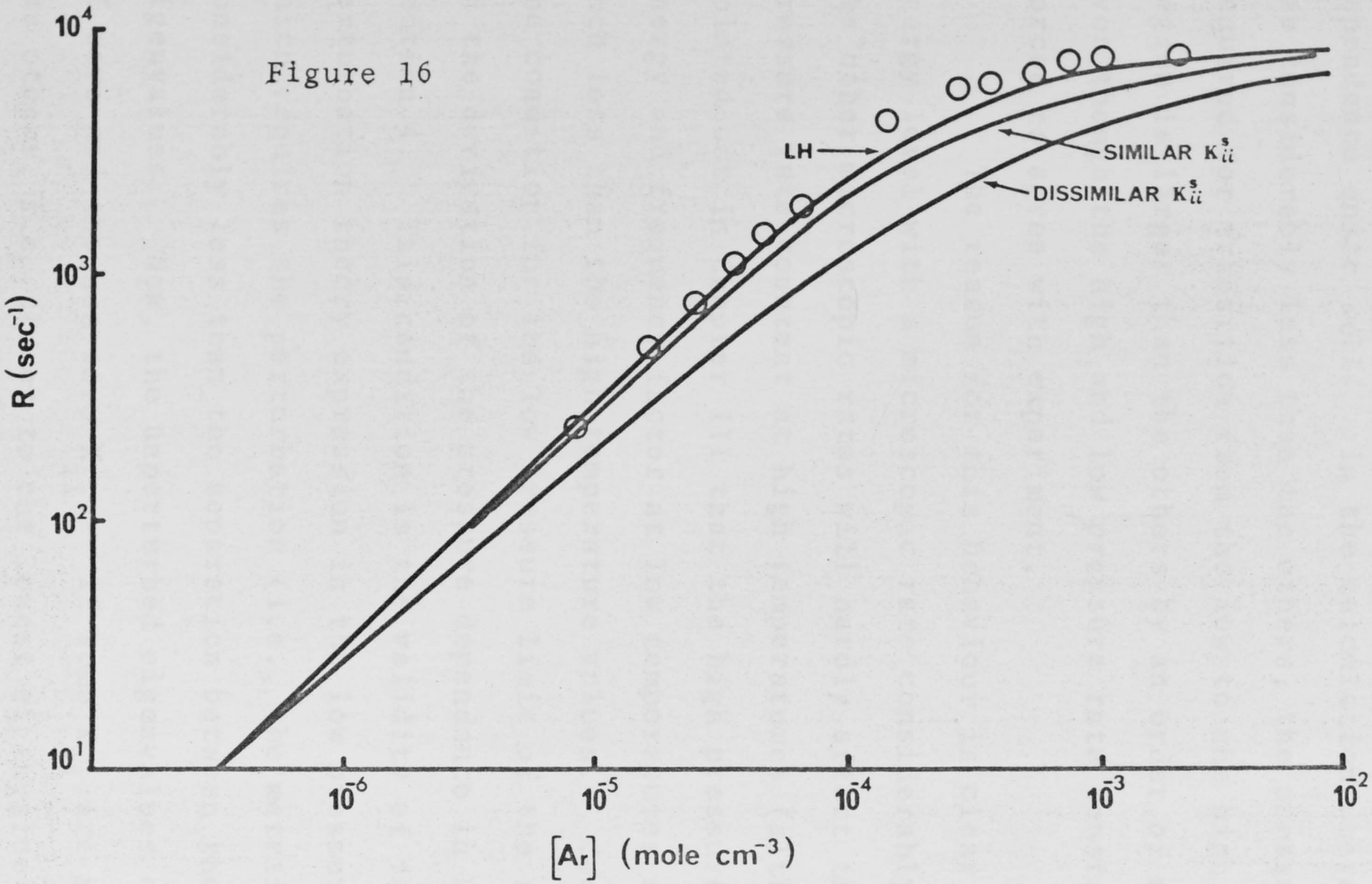

Rate constants as a function of pressure at 1700°K.
o - experimental points (Olschewski *et al.*, 1966)
solid lines : Lindemann-Hinshelwood expression (LH)
: present theory, microscopic rates for active pseudo-levels all of similar magnitude
: present theory, microscopic rates for some active pseudo-levels considerably less than others.

similar magnitude both reproduce the experimental pressure dependence quite well. In the calculation where some K^s_{ii} are considerably less than the others, the pressure range required for transition from the low to the high pressure region is larger than the others by an order of magnitude, even though the high and low pressure rate constants are forced to agree with experiment.

The reason for this behaviour is clear enough. An energy level with a microscopic rate considerably less than the other microscopic rates will hardly affect the high pressure rate constant at high temperatures (although we pointed out in Chapter III that the high pressure activation energy and frequency factor at low temperatures should be much less than the high temperature values. Consider, however, the condition for the low pressure limit of the rate constant in the derivation of the pressure dependence in Chapter II, Section 4. This condition is the validity of the first-order perturbation theory expression in the low pressure limit, which requires the perturbation (i.e., the matrix PA) to be considerably less than the separation between the unperturbed eigenvalues. Now, the unperturbed eigenvalues of K consist of zero and the non-zero K_{ii}. If some K_{ii} are much less than the others, i.e. closer to the lowest eigenvalue (zero), then a much lower pressure will be required for this condition to be met.

Unfortunately, this result gives some cause for alarm concerning the good agreement with experiment that we obtained for the pressure dependence of the N_2O rate constant, which required ignoring all the K^s_{ii} below the sharp onset of reaction. For very fine graining, the arguments we invoked in the previous section to enable us to ignore these small microscopic rates will no longer be valid. Thus for fine graining, we would predict a considerably slower approach to the low pressure limit than is apparently observed experimentally, because there will be a few K^s_{ii} with values much closer to zero. This effect is swamped in the coarse graining which we use in these calculations. We have thought of two ways of circumventing this difficulty. In the first, we take refuge in the empirical nature of the product potential function which we used to calculate microscopic rates, and hope that the actual potential is such that the transition from zero to high values of K_{ii} is practically infinitely sharp. In the second, it is possible that indeed the transition to true second order kinetics actually occurs at considerably lower pressures than is thought at present, although because there will only be a few small microscopic rates, the deviation from second order kinetics will be slight at higher pressures. Professor H.M. Frey (1970) has remarked to us that there is indeed some experimental evidence that this is so. The experimental difficulties at very low pressures are of course

considerable. Apart from technical considerations, there is the problem that at low pressures, as the pressure of inert gas is reduced, the effect of reactant/reactant collisions can no longer be ignored (Valance and Schlag 1967).

The fact that small microscopic rates would cause a slow transition from first to second order kinetics has also been pointed out by Wilson (1960), who however ascribed the existence of such low K_{ii} to anharmonicity (or more specifically, to anharmonicity which mixes "reactive" and "unreactive" modes). The inclusion of such anharmonicity in the present theory would also result in low microscopic rates, but unless there was also extensive tunnelling this effect would only occur for levels with energies comparable to the energy of the crossing point. Thus, although this would result in a slow transition from first to second order kinetics, the distinctive temperature dependence of the high pressure activation energy and frequency factor would not be observed unless there was also significant reaction below the potential barrier.

We therefore feel that the observation of a unimolecular reaction which exhibits both an abnormally slow transition from the low to the high pressure region, and a high pressure activation energy and frequency factor which show a significant rise over a large enough temperature range, would provide convincing evidence that it is insufficient to describe a unimolecular reaction purely in terms of classical

or semi-classical theories.

CONCLUSION

Section 1. Summary

In Chapter I we discussed the quantum mechanical description of a unimolecular reaction, and argued that the process could be described either in terms of a potential barrier between reactant and product, which is the basis of most unimolecular theories, or in terms of separated reactant and product surfaces. The latter method offers many computational advantages, but the requirement that the perturbation which induces transitions between the crossing surfaces should be small restricts the choice of separated potentials. If the perturbation is sufficiently small, the microscopic rate of conversion from reactant to product may be calculated from "Fermi's Golden Rule."

The population of reactant levels varies in time because of reaction and collisional exchange between other levels. These complex kinetics may be conveniently expressed in terms of matrix algebra. The rate constant then becomes the largest eigenvalue of a matrix $J = PA - K$, where P is the pressure, A the matrix of collision rates and K the (diagonal) matrix of microscopic rates of conversion to product. In Chapter II we derived the pressure and temperature dependence of the rate constant from the properties of A and K inherent in the quantum mechanical formulation of Chapter I. We derived

a general expression for the activation energy of all pressures, making no assumptions as to the populations of reactant levels, and derived the high and low pressure limits of this expression. In the high pressure limit, this expression reduces to a well-known formula which can be traced back to Tolman. In the low pressure limit, however, one of the main components of the activation energy is a term which depends on the deviation from equilibrium of the population of inactive levels; another important term involves the energy-dependent cross-sections. We found that although under certain conditions the high and low pressure activation energies correspond approximately to the height of the potential barrier between reactant and product, this was by no means an invariable rule. In the calculations of Chapters III and IV we have given examples where both high and low pressure activation energies were considerably below the height of the point of intersection of reactant and product potential surfaces.

We calculated the low, intermediate and high pressure rate constants for the thermal decomposition of nitrous oxide. Because of lack of information on wave functions and potential surfaces, we were forced to use approximations to make the calculations feasible. These simplifications involve the introduction of adjustable parameters, and so the moderately good agreement with experiment which we obtain gives no especial

cause for congratulation. Rather, the benefit of the calculations comes from the results which precede this final comparison, and from the results of calculations based on potential functions which serve as models of other types of unimolecular reactions.

We found that a plot of microscopic rates of conversion to product as a function of energy usually exhibits a sharp change from negligible to significant values at the crossing point, and a maximum slightly above this. Nevertheless, the microscopic rates below this point are significant, because of tunnelling. The main component of the high pressure activation energy, namely the average energy of active levels, usually corresponds with the maximum in rate/energy curves. If, however, these curves do not exhibit a sharp onset of reaction, then this term, and hence the activation energy and frequency factor, are strongly temperature dependent. An example of such behaviour was found in a hypothetical exothermic unimolecular decomposition. Our intermediate pressure calculations showed that another characteristic of such reactions would be a very slow transition from first to second order kinetics.

In numerical studies of our expression for the low pressure activation energy, we found that at low temperatures this parameter indeed approximates the energy at which conversion to product becomes most effective. This result is

also given by the steady-state approximation, which however at low pressures can give very inaccurate values for the rate constant itself. At high temperatures, we found that the deviation of the actual population from equilibrium caused a marked decrease in the low pressure activation energy. At temperatures which are now commonly used to study reactions in shock tubes, this can cause the low pressure activation energy actually to be below the minimum energy for reaction.

Section 2. Extensions

The reaction which forms the focus of this study, the thermal decomposition of nitrous oxide, is particularly suited to the theory discussed here. As reactant and product have different spins, the perturbation may be unambiguously assigned to spin-orbit coupling, and is sufficiently small for first-order time-dependent theory to be quite adequate. Here also the very convenient Condon approximation is almost certainly valid. Since the reaction is a predissociation, no difficulties arise from having to describe discrete product states in terms of a quasi-continuum, with the problems that this would entail in determining a quantum-mechanical expression for the microscopic rates. Even for this simple molecule, some drastic approximations are involved. In the high-pressure limit, potential functions are the main difficulty

but here *ab initio* calculations could eventually make some inroads. To improve on our rather crude treatment of the low and intermediate pressure regions, much further work is needed on calculating vibrational collisional cross sections, and for this a better knowledge of the intermolecular potential function is the most important requirement for bringing computation into touch with reality. If sufficiently accurate cross sections were available, the use of techniques such as the many-shot expansion of Valance and Schlag (1966) would perhaps obviate the need for our pseudo-level approximation, which no doubt obscures much interesting physics. This would bring better understanding of the intransigient E^Q term in the low pressure activation energy.

The perturbation treatment of unimolecular reaction should be extensible to reactions other than the decomposition of N_2O. An immediate application would be the decomposition of a molecule such as SO_2 (Troe and Wagner 1967 and references therein), although at present the experimental data for this reaction is only available in the low pressure region. This reaction, like the N_2O decomposition, is a predissociation, but it is not spin-forbidden. The calculation of the perturbation matrix element would therefore give rise to some very informative difficulties, which would test some of the techniques discussed in Chapter I.

In view of our discussion on the effect of tunnelling

on the temperature dependence of the activation energy and frequency factor, and on the pressure dependence of the rate constant, a study of exothermic decompositions would be of particular interest. Possible examples of such reactions are the decompositions of F_2O_2 (Schumacher and Frisch 1937), N_2O_4 (Carrington and Davidson 1953) and formyl fluoride (Fischer and Buchanan 1964), although considerably more experimental work is needed on these reactions to see if they are indeed as simple as has been proposed. The formyl fluoride reaction appears an especially enticing prospect, because of the anomalously low frequency factor, which is predicted by our theory. As Fischer and Buchanan's investigations were carried out using traditional techniques, shock tube studies of the decomposition in a large excess of inert gas would no doubt prove most informative.

The perturbation treatment should also be applicable to unimolecular isomerisations, such as the rearrangement of methyl isocycanide (Rabinovitch *et al* 1965, and references therein). Microscopic rates would then have to be calculated from discrete/quasi-continuum formulae such as that developed by Bixon and Jortner (1968).

It is clear from the difficulties which we encountered that even a very approximate quantum mechanical treatment is limited to very small molecules. After this, semi-classical treatments such as the RRKM or transition state theories must

be used. We feel that the theory which we have examined here furnishes a necessary complement to the older theories, in providing a firmer quantum mechanical basis, and an extended insight into the details of the unimolecular process.

REFERENCES

Bennett, J.M., Ross, I.G. and Wells, E.J., J.Mol.Spec. 4, 342 (1960).

Berman, M. and Schoenfeld, R., J.App.Phys. 27, 1361 (1956).

Berry, R.S. and Nielsen, S.E., J.Chem.Phys., to be published.

Bixon, M. and Jortner, J., J.Chem.Phys. 48, 715 (1968).

Bixon, M., Jortner,J. and Dothan, Y., Mol.Phys. 17, 109 (1969).

Born, M. and Huang, K., "Dynamical theory of crystal lattices", Oxford University Press, (1954).

Buckingham, R.D., in "Quantum Theory", Vol.I, (ed.D.R. Bates), Academic Press, NY, (1961).

Buff, F.P. and Wilson, D.J., J.Chem.Phys. 32, 677 (1960).

Byrne, J.P., McCoy, E.F. and Ross, I.G., Aust.J.Chem. 18, 1589 (1965).

Carrington, T. and Davidson, N., J.Phys.Chem. 57, 418 (1953).

Carrington, T., Disc.Far.Soc. 33, 44 (1962).

Condon, E.U., Phys.Rev. 32, 858 (1928).

Condon, E.U., Astrophys. J. 79, 217 (1934).

Clark, T.C., Garnett, S.H. and Kistiakowsky, G.B., J.Chem.Phys. 51, 2885 (1969).

Coolidge, A., James, H. and Present, R., J.Chem.Phys. 4, 193 (1936).

Coulson, C.A. and Zalewski, K., Proc.Roy.Soc. A268, 437 (1962).

Davidson, E., J.Chem.Phys. 35, 1189 (1961).

Drummond, L.J. and Hiscock, S.W., Aust.J.Chem. 20, 815 (1967).

Eyring, H., J.Chem.Phys. 3, 107, (1935).

Eyring, H., Walter, J. and Kimball, G., "Quantum Chemistry" John Wiley, NY (1944).

Eyring, H. and Zwolinski, B., J.Am.Chem.Soc. 69, 2702 (1947).

Felenbok, P. and Lefebvre-Brion, H., Can.J.Phys. 44, 1677 (1966).

Fischer, G. and Buchanan, A.S., Trans.Far.Soc. 60, 378 (1964).

Forst, W., J.Chem.Phys. 48, 3665 (1968).

Frey, H.M., Private Communication (1970).

Frey, R. and Thiele, E., J.Chem.Phys. 48, 3240 (1968).

Gill, E.K. and Laidler, K., Canad.J.Chem. 36, 1570 (1958).

Glasstone, S., Laidler, K. and Eyring, H., "The Theory of Rate Processes", McGraw-Hill, NY, (1941).

Goldberger, M.L. and Watson, K.M., "Collision Theory", John Wiley, NY, (1964).

Gutman, D., Belford, R., Hay, A. and Pancirov, R., J.Phys. Chem. 70, 1793 (1966).

Hall, G.G. and Levine, R.D., J.Chem.Phys. 44, 1567 (1966).

Harris, R.A., J.Chem.Phys. 39, 978 (1963).

Herzberg, G., Ann.Physik, 15, 677 (1932).

Herzberg, G. and Teller, E., Z.Physik.Chem. B21, 410 (1933).

Herzberg, G., "Spectra of Diatomic Molecules", van Nostrand, Princeton (1950).

Herzfeld, K. and Litovitz, T., "Absorption and Dispersion of Ultrasonic Waves", Academic Press, NY, (1959).

Hirschfelder, J.O., Curtiss, C.F. and Bird, R.B., "Molecular theory of gases and liquids", John Wiley, NY, (1964).

Hofacker, G.L., J.Chem.Phys. 43, S208 (1965).

Hougen, J.T. and Lewis, J.K., J.Chem.Phys. 48, 5329 (1968).

International Business Machines Corporation, "Scientific Subroutine Package, Version III", White Plains, NY, (1968).

Jackson, J. and Mott, N.F., Proc.Roy.Soc., A137, 708 (1932).

Jortner, J., "Electronic Relaxation in large molecules" - preprint, (1969).

Jortner, J. and Bixon, M., Isr.J.Chem. 7, 189 (1969).

Kassel, L.S., J.Phys.Chem. 32, 225, 1065 (1928).

Kaufmann, F., J.Chem.Phys. 46, 2449 (1967).

Kim, S.K., J.Chem.Phys. 28, 1057 (1958).

Kolos, W. and Wolniewicz, L., Rev.Mod.Phys. 35, 473 (1963).

Kolos, W. and Wolniewicz, L., J.Chem.Phys. 50, 3228 (1969).

Krauss, M. and Mies, F.H., J.Chem.Phys. 42, 2703 (1965).

Labhardt, H., Chem.Phys.Letters 1, 263 (1967).

Lagerqvist, A. and Miescher, E., Helv.Phys.Acta 31, 221 (1958).

Lagerqvist, A. and Miescher, E., Can.J.Phys. 44, 1525 (1966).

Landau, L., Physik.Zeit.Sowietunion 2, 46 (1932).

Landau, L. and Teller, E., Physik.Zeit.Sowietunion 10, 34 (1936).

Langer, R.M., Phys. Rev. 34, 92 (1929).

Lefebvre-Brion, H. and Guerin, F., J.Chem.Phys. 49, 1446 (1968).

Lefebvre-Brion, H., Can.J.Phys. 47, 541 (1969).

Levine, R.D., Chem.Soc.Special Publication 20, 297 (1966).

Levine, R.D., J.Chem.Phys. 44, 2029, 3597 (1966).

Levine, R.D., J.Chem.Phys. 48, 4556 (1968).

Lin, S.H., J.Chem.Phys. 44, 3759 (1966).

Lindemann, F.A., Trans.Far.Soc. 17, 599 (1922).

Longuet-Higgins, H.C., Advances Spect. 2, 429 (1961).

Löwdin, P-O., J.Mol.Spec. 3, 46 (1959).

Löwdin, P-O., Rev.Mod.Physics 34, 520 (1962).

Marcus, R.A., Chemische Elementarprozesse, ed Heydtmann, Springer-Verlag, Berlin,(1968).

Marriott, R., Proc.Phys.Soc. 83, 159 (1964a).

Marriott, R., Proc.Phys.Soc. 84, 877 (1964b).

Marriott, R., Proc.Phys.Soc. 88, 83 (1966).

Marriott, R., Private communication, (1968).

McLean, A.D. and Yoshimine, M., "Tables of Linear Molecule Wave Functions", International Business Machines Corporation, San Jose, California (1967).

Menzinger, M. and Wolfgang, R., Angew.Chem.internat.Edn. 8, 438 (1969).

Messiah, A., "Quantum Mechanics", Vol. I & II. North Holland, Amsterdam (1964).

Mies, F.H. and Krauss, M., J.Chem.Phys. 45, 4455 (1966).

Mies, F.H., J.Chem.Phys. 42, 2709 (1965).

Mies, F.H., J.Chem.Phys. 51, 787 (1969).

Mirsky, L., "Introduction to linear algebra", Oxford, Clarendon Press, (1955).

Montroll, E. and Shuler, K., Adv.Chem.Phys. 1, 361 (1958).

Mott, N.F. and Massey, H.S.W., "The theory of atomic collisions", Clarendon Press, Oxford (1965).

Murrell, J.N. and Taylor, J.N., Mol. Phys. 16, 609 (1969).

Nikitin, E.E., "Theory of thermally induced gas phase reactions", Indiana University Press, NY, (1966).

Olschewski, H.A., Troe, J. and Wagner, H.Gg., Ber. Bunsengesellschaft Physik.Chem. 70, 450 (1966).

Penny, W. and Sutherland, G., Proc.Roy.Soc. London 156, 654 (1936).

Perlis, S., "Theory of matrices", Addison-Wesley, Reading, Mass. (1952).

Peyerimhoff, S.D. and Buenker, R.J., J.Chem.Phys. 49, 2473, (1968).

Rabinovitch, B.S., Gilderson, P.W. and Schneider, F.W., J.Am.Chem.Soc. 87, 158 (1965).

Rapp, D. and Kassal, T., Chem.Rev. 69, 61 (1969).

Rice, O.K. and Ramsberger, H.C., J.Am.Chem.Soc. 49, 1617 (1927).

Rice, O.K., Phys. Rev. 34, 1451 (1929).

Richardson, W.S. and Wilson, E.B., J.Chem.Phys. 18, 694 (1950).

Roberts, R., J.Chem.Phys. 49, 2880 (1968).

Roginsky, S. and Rosenkevitch, L., Z. Physik Chem. 10B, 47 (1930).

Rosen, N., J.Chem.Phys. 1, 319 (1933).

Schlag, E.W. and Valance W.G., J.Chem.Phys. 49, 605 (1968).

Schlag, E. and Weyssenhoff, J.Chem.Phys. 51, 2508 (1969).

Schumacher, H.J. and Frisch, P., Z. Physik Chem. B37, 1, 18 (1937).

Schwartz, R. and Herzfeld, K., J.Chem.Phys. 22, 767 (1954).

Slater, N.B., "Theory of Unimolecular Reactions", Cornell University Press, Ithaca, NY, (1959).

Slawsky, Z., Schwartz, R. and Herzfeld, K., J.Chem.Phys. 20, 1591(1952).

Sponer, H. and Bonner, L.G., J.Chem.Phys. 8, 33 (1940).

Stearn, A.E. and Eyring, H., J.Chem.Phys. 3, 778 (1935).

Steinfeld, J.I., J.Chim.Physique 64, 17 (1967a).
J.Chem.Phys. 46, 4550 (1967b).

Stretton, K., Trans.Far.Soc. 61, 1053 (1965).

Suzuki, I., J.Mol.Spec. 32, 54 (1969).

Takayanagi, K., Supp.Prog.Theoretical Physics (Japan) 25, 1 (1963).

Tanczos, F., J.Chem.Phys. 25, 439 (1958).

Tardy, D.C. and Rabinovitch, B.S., J.Chem.Phys. 45, 3720 (1966) and refs. therein.

Teller, E., Isr.J.Chem. 7, 227 (1969).

Thompson, S., J.Chem.Phys. 49, 3410 (1968).

Tolman, R.C., "Statistical Mechanics with applications to Physics and Chemistry", NY, Chemical Catalog. Co. (1927).

Troe, J. and Wagner, H. Ber.Bunsengesellschaft Physik.Chem. 71, 937 (1967).

Valance, W. and Schlag, E., J.Chem.Phys. 45, 216 (1966).

Valance, W. and Schlag, E., J.Chem.Phys. 47, 3276 (1967).

Walsh, A.D., J.Chem.Soc. 2260 (1953).

Wieder, G.M. and Marcus, R.A., J.Chem.Phys. 37, 1835 (1962).

Wigner, E and Pelzer, H., Z Physik. Chemie B15, 445 (1931-2).

Wilson, D.J., J.Phys.Chem. 64, 323 (1960).

Wilson, E.B., Decius, J.C. and Cross, P.C., "Molecular Vibrations", McGraw-Hill, NY, (1955).

Witteman, W.J., J.Chem.Phys. 35, 1 (1961).

Yardley, J.T. and Bradley-Moore, C., J.Chem.Phys. 46, 4491 (1967a).

Yardley, J.T. and Bradley-Moore, C., J.Chem.Phys. 46, 1191 (1967b).

Yardley, J.T. and Bradley-Moore, C., J.Chem.Phys. 49, 1111 (1968).

Young, J.M., J.Chem.Phys. 51, 4061 (1969).

Zelikoff, M., Watanabe, K. and Inn, E., J.Chem.Phys. 21, 1643 (1953).

Zener, C., Proc.Roy.Soc. A137, 696 (1932).

GLOSSARY OF SYMBOLS

A		matrix of collision rates (Chap.II,Sect.2)
A_{ij}		element of A matrix
$A!_{ii}$		total rate of reaching active levels from inactive level i (eq.II.29).
A^s		Condensed collision matrix (Chap.IV, Sect. 4).
$\bar{A}_{ij}$		integral of EQ_{ji} over thermal energy distribution (eq. II.38).
a_{ij}		expansion coefficient (Chap.III, Sect. 8).
B		symmetrised transport matrix (Chap.II,Sect.3)
B°		matrix B truncated at highest inactive level(eq.II.27)
$\|B\rangle$		a bound state (Chap. III,Sect.8).
b		vector of Boltzmann populations (Chap.II.Sect.3)
b_i		element of b (eq. II.15)
b_B		symmetrised Boltzmann vector (eq. II.21)
c	(i)	total concentration of reactant (Chap.I,Sect.2)
	(ii)	symmetrised population vector (Chap.II, Sect.3.)
	(iii)	parameter in dissociative product potential (Chap.III)
D_o		thermochemical dissociation energy (Chap.III,Sect.4).
D_e		minimum energy for reaction (Chap.III,Sect.4)
d_i		degeneracy of level i.
E	(i)	energy of isolated molecule (Chaps. I & III).
	(ii)	collision energy (Chaps.II & IV).
E_{act}		activation energy (eq.II.30).
$E_{act}^{LP}, E_{act}^{HP}$		low and high pressure limits of activation energy (Chap.II,Sect.6).
E_C		energy of continuum part of product wave function (Chap. III,Sect.8)
E_{ij}		absolute value of energy difference between two product levels (Chap.IV, Sect.3)
E^M		term in low pressure activation energy, containing difference between exact and equilibrium populations (eq. II.49)
E^Q		cross section dependent term in low pressure activation energy (eq. II.47).

$\langle EA' \rangle / \langle A' \rangle$	energy of active levels, weighted by probability of collisional activation to an active level, averaged over low pressure population - a term in low pressure activation energy (eq.II.48).
$\langle E \rangle$	Boltzmann average of internal energy (eq.II.44)
$\langle E_g \rangle$	average of internal energy over low pressure population (eq.II.50).
$\langle EK \rangle / \langle K \rangle$	average energy of active levels, weighted by the probability of reaction (eq.II.44).
$\tilde{E}^M$	microscopic reversibility energy matrix (eqs. II.36,37).
F (i)	Wilson F matrix (Chap. II, Sect. 8).
(ii)	a parameter in the square well wave function (Chap. III, Sect. 7)
F^*, F	partition functions of activated complex and reactant in transition state theory (Chap.II,Sect.9)
f	a general function (Chap.II,Sect. 2)
$f(\omega)$	a function in the theory of time-dependent transitions (eq. III.28)
$f(E_{ij})$	a function in the SSH theory, determining the collision rate between initial and final states as a function of the energy difference between them (eq. IV.10).
G	Wilson G matrix (Chap. III, Sect.8, Chap. IV,Sect.3)
g	population vector, eigenvalue of J matrix corresponding to the rate constant (Chap. II).
H	total Hamiltonian of the isolated molecule.
H_o	zero-order Hamiltonian of isolated molecule, wherein reactant and product are clearly separable (Chap.I, Sect. 2).
H_o^{el}	zero-order electronic Hamiltonian (Chap.I,Sect.3)
I	unit matrix (eq.II.58)
I_o	moment of inertia of reactant (Chap.III,Sect.3).
I_a	moment of inertia of active levels (Chap.III,Sect.3)
I_*	moment of inertia of activated complex (transition state theory).
J	the transport matrix, = PA - K (Chap.II,Sect.2)
J^s	condensed transport matrix (Chap.IV,Sect.4)
J	rotational quantum number (Chap.III,Sect.3)

K		diagonal matrix of microscopic rates K_{ii} (Chap.II,Sect.2)
K_{ii}		microscopic rate of conversion to product from level i of reactant (eq.I.5), an element of K
K^s		condensed K matrix (Chap.IV,Sect.4)
$K_{iq}(z)$		Bessel function K of imaginary order (Chap.III.Sect.4)
k	(i)	the Boltzmann constant
	(ii)	parameter in a continuum wave function (Chaps.III and IV).
k'_{NN}, k_{NO}		force constants for NN and NO bonds
k_J		a unit vector, an eigenvector of K
L		parameter in the SSH intermolecular potential function (Chap. IV, Sect. 3).
ℓ	(i)	partial wave (Chap.IV., Sect.3)
	(ii)	parameter to subdivide a grained collision matrix (Chap.II, Sect. 8).
m	(i)	reduced mass of two colliding molecules (Chaps. II and IV.)
	(ii)	the reduced mass of the atom pair NO (Chap. III).
m_N, m_O		mass of nitrogen and oxygen atoms
N		the index of the highest inactive level (Chap.II, Sect.2)
N°		number of inert gas molecules per unit volume
n	(i)	index of level with largest microscopic rate (Chap.II,Sect.9)
	(ii)	NN vibrational quantum number in the product state for two-dimensional model (Chapter III, Sect. 8)
n_a		the number of atoms in a colliding molecule (Chap. IV, Sect.3)
$\mathcal{O}$		a projection operator
P		pressure
$P_\ell(\cos\theta)$		a Legendre polynomial
$\mathcal{P}$		matrix of "probabilities of transition per collision" (Chap.II, Sect. 3)
p		subscript referring to electronic state of product.
$Q_{ij}(E)$		the energy-dependent cross section for collisional transition from level i to level j (Chap.II,Sect.3).
q		parameter in the wave function for an exponential potential (Eq. II.9)

R		rate constant.
R^{HP}		high pressure rate constant (Chap.II,Sect.4).
R^{LP}		second-order low pressure rate constant (Chap. II, Sect. 4).
R_{NN}		the displacement from the NN equilibrium distance.
R°_{NN}		N_2 equilibrium distance in two-dimensional model (Chap. III, Sect. 8).
R_{NO}		the displacement from the NO equilibrium distance.
R°_{NO}		classical turning point along NO bond corresponding to a given energy.
R'		parameter in the square well wave function (eq.III.19)
r	(i)	subscript referring to electronic state of reactant
	(ii)	intermolecular distance.
S	(i)	similarity transformation which symmetrises J (Chap. II).
	(ii)	Wilson S matrix (Chap. IV, Sect. 3).
s		number of degenerate oscillators in extension of the harmonic oscillator model for collision rates (Chap. II, Sect. 8).
T		absolute temperature.
t		time
$U(t)$		evolution operator (Chap. III, Sect. 8).
$U^{sq}(E)$		upper part of square well potential (Eq. III.18).
U'		potential function of product (Chap. III).
U''		potential function of reactant (Chap. III).
V		perturbation separating reactant and product.
V(r,X)		intermolecular potential function.
VT		vibrational-translational (collisional exchange)
VV		vibrational-vibrational (collisional exchange)
V_o		parameter in the SSH intermolecular potential function (Eq. IV.6).
$V_{ij}(r)$		matrix element of V(r,X) with respect to vibrational wave functions i and j (Eq. IV.5).
V'_{ij}		matrix element of the part of $V_{ij}(r)$ which depends only on i and j, the internal wave functions (Eq. IV.7).

$V_{rp}(X)$		electronic perturbation matrix connecting reactant and product.
v	(i)	maximum quantum number for the NN vibration in the product state in the two-dimensional model (Chap. III, Sect. 8).
	(ii)	vibrational quantum number (Chap. IV, Sect. 3).
	(iii)	velocity of colliding particles (Chap. II, Sect. 3).
W(t)		time-dependent transition probability (Eq.III.24).
W		a function in the SSH theory (Eq.IV.9).
X		internuclear coordinate
X_c		internuclear coordinate at crossing point.
x	(i)	electronic coordinate (Chap. I).
	(ii)	population vector (Chap. II, Sect. 2).
x_i		population of level i, an element of x.
x^s		condensed population vector (Chap. IV, Sect. 4).
Z		largest diagonal element of the collision matrix (Eq. II.58).
z		parameter in the wave function for an exponential potential (Eq. III.9).
α		ratio of Boltzmann factors of neighbouring levels in the harmonic oscillator treatment of collision rates (Eq. II.56).
β		parameter in the wave function for an exponential potential (Eq. III.9).
Γ, Γ_{ij}		matrix describing time-dependent perturbation (Chap. I, Sect. 4).
γ_{ij}		rate of collision + induced transitions from level i to level j (Chap. II, Sect. 2).
γ		adjustable parameter in treatment of Olschewski *et al* of the low pressure rate constant (Chap. IV, Sect. 2)
Δ_X		Laplacian operator with respect to X.
ΔE	(i)	minimum energy for a collisional transition (Eq. II.12).
	(ii)	energy difference between neighbouring levels in the harmonic oscillator treatment of collision rates (Chap. II, Sect. 8).
δ		Dirac dela-function or Kronecker delta.

ε		Lennard-Jones parameter.
$\zeta_{i\ell}$		coefficient in the expansion of total wave function of a collision in terms of isolated molecule wave function and Legendre polynomials (Chap.IV,Sect.3).
θ	(i)	intermolecular angle (Chap.I,Sect.2, Chap.IV.Sect.3).
	(ii)	parameter in square well wave function (Eq.III.9).
η		a parameter in the SSH theory (Chap.IV, Sect.3).
κ		transition state theory transmission coefficient (Chap. II, Sect. 9).
λ_1, λ_3		parameters in normal coordinate potential function (Chap. III, Sect. 8).
λ		spin-orbit coupling (Chap. III).
λ_o		largest eigenvalue of transport matrix (Chap. II).
λ_i		an eigenvalue of the transport matrix (Chap. II, Sect. 2).
ν_{max}		maximum in UV absorption spectrum of N_2O corresponding to product state $^3\Sigma^+$.
$\nu_{NO}, \nu_{NN}, \nu_{bend}$.		frequencies of NO, NN and bending vibrations in N_2O (Chap. III).
ξ_1, ξ_3		normal coordinates (Chap. III, Sect. 8).
$\rho(E)$		energy density of product (Eq. 1.5).
σ		Lennard-Jones potential parameter.
τ		mean first passage time (Eq. II.10).
ϕ	(i)	intermolecular angle (Chap. I, Sect. 2).
	(ii)	electronic wave function (Chap. I, Sect. 1).
χ	(i)	constant in harmonic oscillator treatment of collision rates (Eq. II.55).
	(ii)	parameter in square well wave function (Eq.III.19).
Ψ		total wave function describing a collision, with electronic wave functions factored out (Chaps. I and IV).
Ψ_1, Ψ_2		vibrational wave function (ψ_1) and slope (ψ_2) for numerical solution of Schrödinger equation (Chap. III, Sect. 5).
ψ		vibrational wave function.
ω	(i)	collision frequency (Chap. II, Sect. 3).
	(ii)	a frequency (Eq. III.27).